

DECKBLATT

Philipps



Universität

Marburg

A genetic analysis to elucidate the function of the *Plasmodium falciparum* parasitophorous vacuole protein, PfPV1.

DISSERTATION
zur Erlangung des Doktorgrades
der Naturwissenschaften
(Dr. rer. nat.)

dem
Fachbereich Biologie
der Philipps-Universität Marburg
vorgelegt von

Trang T.T. Chu
aus Bac Ninh, Viet Nam

Marburg/ Lahn 2009

Vom Fachbereich Biologie der Philipps-Universität Marburg als Dissertation am
angenommen.

Erstgutachter: Prof. Dr. Klaus Lingelbach

Zweitgutachter: Prof. Dr. Uwe G. Maier

Tag der mündlichen Prüfung am:

To my Parents

TABLE OF CONTENTS

List of Figures.....	v
List of Tables	vi
Abbreviations	vii
1. Introduction.....	1
1.1. The life cycle of <i>Plasmodium falciparum</i>	1
1.2. The parasite compartments	6
1.3. The parasite induces alterations of the human erythrocyte.....	8
1.3.1. Structural alterations	8
1.3.1.1. Parasitophorous vacuole	8
1.3.1.2. The Maurer’s Clefts	9
1.3.1.3. The tubulovesicular network.....	9
1.3.1.4. Knobs	9
1.3.2. Biochemical/ physiological alterations	10
1.4. The parasitophorous vacuole- form and function.....	10
1.4.1. Invasion of erythrocytes and the PV formation	10
1.4.2. The PV – a transit compartment.....	12
1.4.3. The PV – nutrition acquisition and regulation of the ionic environment.	13
1.4.4. The PV – preparation of merozoite egress	14
1.5. Genetic manipulation of <i>P. falciparum</i>.....	16
1.5.1. Difficulties with <i>P. falciparum</i> transfection.....	17
1.5.2. Functional analysis by integrative transfection.....	18
1.5.2.1. Gene targeting by single-crossover.....	18
1.5.2.2. Gene targeting by double-crossover homologous recombination using negative selection marker.....	19
1.5.3. Other gene technique advances in <i>P. falciparum</i>	23
1.6. PfPV1 – a novel parasitophorous vacuole protein	24
1.7. Objective	25
2. Materials and Methods.....	28
2.1. Materials	28
2.1.1. Equipment	28
2.1.2. Chemicals	29

2.1.3.	Antibodies and working concentration	31
2.1.4.	Enzymes	31
2.1.5.	Molecular biological kits and reagents	32
2.1.6.	Cell culture materials	32
2.1.7.	Cells and organisms	32
2.1.8.	Media and solutions	33
2.1.8.1.	Solutions for protein-based experiments	33
2.1.8.2.	Solutions for DNA-based experiments	35
2.1.8.3.	Bacteriological media	38
2.1.8.4.	Media and solutions for parasite culture and transfection	39
2.1.9.	Plasmids	41
2.1.10.	Synthetic oligonucleotides	42
2.2.	Methods.....	44
2.2.1	Bioinformatics methods	44
2.2.2	Transfection of plasmid constructs	44
2.2.2.1	pHTK- Δ PV1	44
2.2.2.2	pARL-DHFR-PV1g	45
2.2.2.3	pARL-BSD-PV1g	45
2.2.2.4	pARL- Δ PV1g.....	46
2.2.2.5	pARL-mutPV1	46
2.2.3	Parasite	50
2.2.3.1	Parasite culture.....	50
2.2.3.2	Parasite transfection	50
2.2.3.3	Drug selection of integrated plasmid containing parasites	51
2.2.3.4	Parasite cloning by limiting dilution.....	52
2.2.4	Monitoring transfectants: genetic analysis.....	52
2.2.4.1	PCR analysis	52
2.2.4.2	Southern blot analysis	53
2.2.4.3	Pulsed field gel analysis (PFGE)	54
2.2.5	Preparation of nucleic acid materials	54
2.2.5.1	Preparation of transfection plasmids.....	54
2.2.5.2	Preparation of <i>P. falciparum</i> genomic DNA	54
2.2.5.3	Preparation of <i>P. falciparum</i> RNA	55

2.2.5.4	Preparation of <i>P. falciparum</i> chromosome blocks.....	55
2.2.6	Methods on parasite proteins	56
2.2.6.1	Fractionation of infected erythrocytes by SLO.....	56
2.2.6.2	Labelling the newly synthesised parasite proteins with [³⁵ S]L-methionine	56
2.2.6.3	Fluorescence microscopy.....	56
2.2.7	Immunoblotting analysis	57
2.2.8	Expression and purification of recombinant proteins	57
2.2.8.1	Constructing the expression vector	57
2.2.8.2	Over-expression and solubility test of recombinant proteins in <i>E. coli</i>	58
2.2.8.3	Purification of GST fusion protein from <i>E. coli</i>	58
2.2.9	GST pull-down assay	59
3.	Results	60
3.1.	PV1 identification, orthologs and bioinformatics analysis.....	60
3.2.	Strategy one: Gene targeting by double cross-over homologous recombination using a negative selection system	65
3.2.1.	Double cross-over integration of pHTKΔPV1 under the selection of ganciclovir still required WR99210 cycling	65
3.2.2.	pHTKΔPV1 integrated into chromosome but not in a simple double cross-over or a 5' or 3' single cross-over.....	69
3.2.3.	The TK encoding sequence might still exist in the integrant but appears not to be active	74
3.2.4.	Analysis of transfectants with the DHFR probe	75
3.2.5.	The PfPV1 appears to be essential for asexual stage development of <i>P. falciparum</i>	78
3.3.	Strategy two: episomal expression of PV1-GFP followed by integration into the endogenous PV1 coding region.....	80
3.3.1.	The episomal pHTKΔPV1 in the double transfected parasites only disappears after negative selection with ganciclovir.....	80
3.3.2.	The <i>PfPVI</i> gene might act as selectable marker itself to maintain the pARL-BSD-PV1g vector when blasticidin S was removed	83

3.3.3.	Single clones from double transfected parasites possess different genotypes.....	84
3.4.	Identification of interaction partners of PfPV1 by GST pull-down assay	89
3.4.1.	Purification of the recombinant PfPV1-GST protein.....	89
3.4.2.	GST pull-down assay was not able to detect any interaction.....	90
4.	Discussion	92
4.1.	PfPV1 knock-out studies	92
4.2.	A possible genetic re-arrangement by integrated parasites to inactivate TK activity	95
4.3.	Blasticidin S resistance	97
4.4.	Identifying interaction partners	99
4.5.	Conclusion: PfPV1 – a conserved, unique protein with unknown but essential function	101
	References	103
	Summary	116
	Zusammenfassung	118
	Acknowledgement	120
	Curriculum Vitae	121
	Erklärung	122

List of Figures

Figure 1.1. Current distribution of indigenous malaria and the control status of the disease-----	3
Figure 1.2. Life cycle of <i>P. falciparum</i> -----	4
Figure 1.3. The trophozoite stage of <i>P. falciparum</i> -infected RBC -----	5
Figure 1.4: Schematic representation of single and double crossover homologous recombination in <i>P. falciparum</i> .-----	22
Figure 1.5: PfPV1, conserved hypothetical protein encoded by PF11_0302 -----	27
Figure 2.1: Vector maps for <i>P. falciparum</i> transfection plasmids -----	47
Figure 3.1 Structure, feature and conservation of PfPV1 -----	61
Figure 3.2. The PfPV1 locus cannot be targeted by simple negative selection -----	66
Figure 3.3. The episomal pHTK Δ PV1 only disappeared after adding ganciclovir to rounds of WR99210 cycling-----	68
Figure 3.4. pHTK Δ PV1 integrated into chromosome but not in a simple double cross-over or a 5' or 3' single cross-over -----	70
Figure 3.5. Schematic representation of possible integration event of pHTK Δ PV1 into <i>PV1</i> locus-----	72
Figure 3.6. Inability to amplify the specific TK fragment from pHTK Δ PV1-integrated parasite clones -----	75
Figure 3.7 Analysis of the integrated pTK Δ PV1 into <i>P. falciparum</i> by the hDHFR probe -----	77
Figure 3.8. Protein PfPV1 still expresses in pHTK Δ PV1-integrated clones. -----	78
Figure 3.9. Quantitative Southern blot confirm the single copy of endogenous <i>PfPV1</i> locus after the integration -----	79
Figure 3.10 Genotypic analysis of double transfected parasites with pHTK Δ PV1 and pARL-BSD-PV1g vector -----	82
Figure 3.11. Not all clones from the double transfected parasites can co-express both PV1 and PV1GFP fusion protein -----	85
Figure 3.12 Single clones from double transfected parasites display different genotypes -----	88

Figure 3.13 Purification of PfPV1-GST fusion protein -----	89
Figure 3.14 GST pull-down assay of PfPV1-GST fusion protein and parasite extract from SLO pellet did not detect any interacting proteins-----	90
Figure 4.1 Expression profile of PfPV1 and CRT protein -----	95
Figure 4.2 Y2H interactions of PfPV1 -----	100

List of Tables

Table 1. List of Plasmids used in this study-----	41
Table 2. List of PCR primers used in this study -----	42
Table 3. Mini motifs predicted in PfPV1 -----	63
Table 4. Expression profiles similarity to PfPV1 -----	102

Abbreviations

µg	microgram
µl	microliter
µM	micromolar
3' UTR	Three prime untranslated region
5' UTR	Five prime untranslated region
AP	Alkaline Phosphatase
bp	base pair
BSD	Blasticidine S deaminase
CAM	Calmodulin
CRT	chloroquine resistance transporter
DAPI	4',6-Diamidino-2-phenylindole dihydrochloride
DHFR/TS	Dihydrofolate reductase/thymilidate synthase
DHPS	Dihydropteroate synthase
ER	Endoplasmic reticulum
EXP1	Exported protein 1
EXP2	Exported protein 2
gan	Ganciclovir
gDNA	Genomic DNA
GFP	Green Fluorescent Protein
GST	Glutathione S-Transferase
hDHFR	Human dihydrofolate reductase
h	hour
hrp2/3	histidine rich protein 2/3
HSP	Heat shock protein
IPTG	Isopropyl-1-thio-D-galactopyranoside
iRBC	Infected erythrocyte
KAHRP	Knob associated histidine rich protein
kb	kilobases
kDa	Kilodalton
l	liter
LB medium	Luria-Bertani medium
MALDI	Matrix assisted laser desorption ionization
MC	Maurer's Clefts
min	Minute
mg	milligram
ml	milliliter
mM	millimolar
MS	Mass spectrometry
Mw	Molecular weight
Neo	Neomycin phosphotransferase II
nM	nanomolar
NPP	novel permeation pathway
OD	Optical density
Pb	<i>Plasmodium berghei</i>
PBS	Phosphate buffered saline
PCR	Polymerase chain reaction
PEXEL	<i>Plasmodium</i> export element

Pf	<i>Plasmodium falciparum</i>
PFGE	Pulse field gel electrophoresis
PIC	Protease inhibitor cocktail
PMSF	Phenylmethylsulphonyl fluoride
PV	Parasitophorous vacuole
PVM	Parasitophorous vacuolar membrane
RBC	Red blood cell
RBCM	Red blood cell membrane
rpm	Revolutions per minute
RPS medium	supplemented RPMI medium
RT	Room temperature
SDS-PAGE	Sodium dodecyl sulfate polyacrylamide gel electrophoresis
SERA/SERP	Serine rich antigen/serine rich protein
SLO	Streptolysin O
SLO-MF	SLO membrane fraction
SLO-SF	SLO soluble fraction
SSC	Standard saline citrate
TAE	Tris-Acetate containing EDTA
Tg	<i>Toxoplasma gondii</i>
TK	Thymidine kinase
Tris	2-Amino-2-hydroxymethyl-propane-1,3-diol
TVN	Tubovesicular network
WR	WR99210
WT	Wild-type
Y2H	Yeast two-hybrid

1. Introduction

Despite more than a century of efforts to control malaria, the disease remains a major global problem, one of the most severe in public health worldwide. Data from 2006 suggest that about 3.3 billion people - half of the world's population – are living in areas at risk of malaria, an estimated 250 million cases, leading to nearly a million deaths (WHO, 2008a), (Figure 1.1). Malaria is a serious problem in Africa, where one in every five (20%) childhood deaths is due to the effects of the disease, and every 30 seconds a child dies from malaria (WHO, 2008a).

Human malaria is caused by infection with intracellular parasites of the genus *Plasmodium* that are transmitted by *Anopheles* mosquitoes. There are four species causing human malaria, *Plasmodium falciparum*, *Plasmodium vivax*, *Plasmodium malariae* and *Plasmodium ovale*. The simian malaria *Plasmodium knowlesi* has recently been recognized as the fifth species of *Plasmodium* causing malaria in human populations (Cox-Singh and Singh, 2008). *P. falciparum* and *P. vivax* are the most common causative agents and *P. falciparum* is the most lethal form. In 2004, *P. falciparum* was among the leading causes of death worldwide from a single infectious agent (WHO, 2008b).

1.1. The life cycle of *Plasmodium falciparum*

The human malaria *Plasmodium spp* have a complicated life cycle involving two hosts, and cycles between an asexual stage in the vertebrate host and a sexual phase in an insect vector (Figure 1.2). Sporozoites are initially transmitted to the human host through the bite of the female *Anopheles* mosquito. The parasites migrate to the liver, and penetrate hepatocytes where they undergo asexual division (exo-erythrocytic schizogony) to produce thousands of merozoites. *P. vivax* and *P. ovale*, at this stage can remain dormant as a hypnozoite form that can reactivate after symptomless intervals of up to several years after infection. The merozoites enter the blood stream, and quickly invade red blood cells. The asexual reproduction of parasites in erythrocytes (schizogony) and the release of merozoites from infected red blood cells are responsible for the pathogenesis of the disease. *P. falciparum* develops approximately 48 hours inside the red blood cells, from ring stage (0-10 h post invasion) to the trophozoite (10 – 36 h post invasion) and the schizont stage (36 – 48 h post invasion) (Figure 2). During the erythrocytic schizogony, the parasite starts

Introduction

several rounds of asexual division, resulting in mature schizonts (segmenters), each containing 16–32 daughter merozoites. Approximately 48 hours post invasion, infected erythrocytes rupture and free merozoites then can invade other red blood cells and continue the cycle of parasite multiplication, with extensive red blood cell destruction. In some case, the merozoites penetrate the red blood cell but do not divide, instead they differentiate into male and female gametocytes, which can live quiescently in the blood stream for weeks and be taken up by the mosquito. Once drawn into the mosquito, the gametocytes rapidly activate, fertilise to form the diploid zygote. After 18 to 24 hours, the motionless zygote becomes an elongated and motile ookinete. The short-lived ookinete moves between or through the midgut wall, and lies beneath the basement membrane, develops into oocyst. Through asexually multiplication, a large number of haploid sporozoites are formed. Eventually the oocyst ruptures and the sporozoites migrate to the salivary glands, ready for the next transmission cycle into the human host (Figure 1.2) (Dluzewski *et al.*, 2008; Miller *et al.*, 2002a).

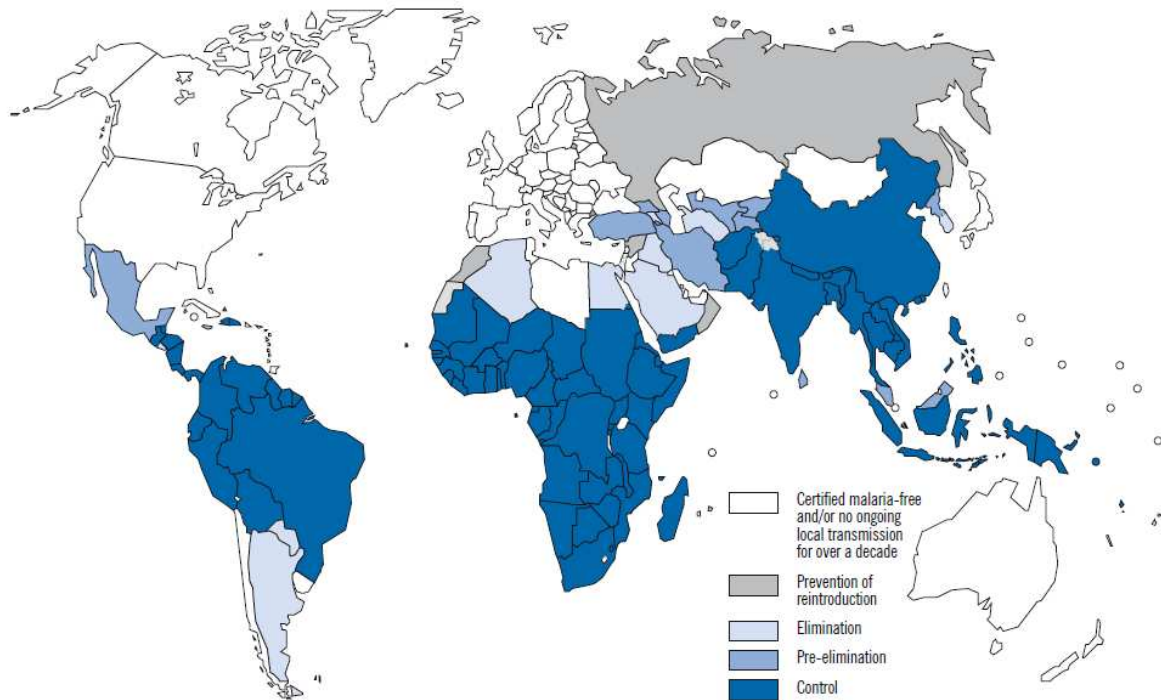


Figure 1.1. Current distribution of indigenous malaria and the control status of the disease (WHO, 2008a). White area, malaria-free countries and/or no ongoing local transmission for over a decade. Gray area, malaria-endemic countries in phase of prevention of reintroduction. Alice blue area, malaria-endemic countries in phase of elimination. Light blue area, malaria-endemic countries in phase of pre-elimination. Dark blue area, malaria-endemic countries in control program.

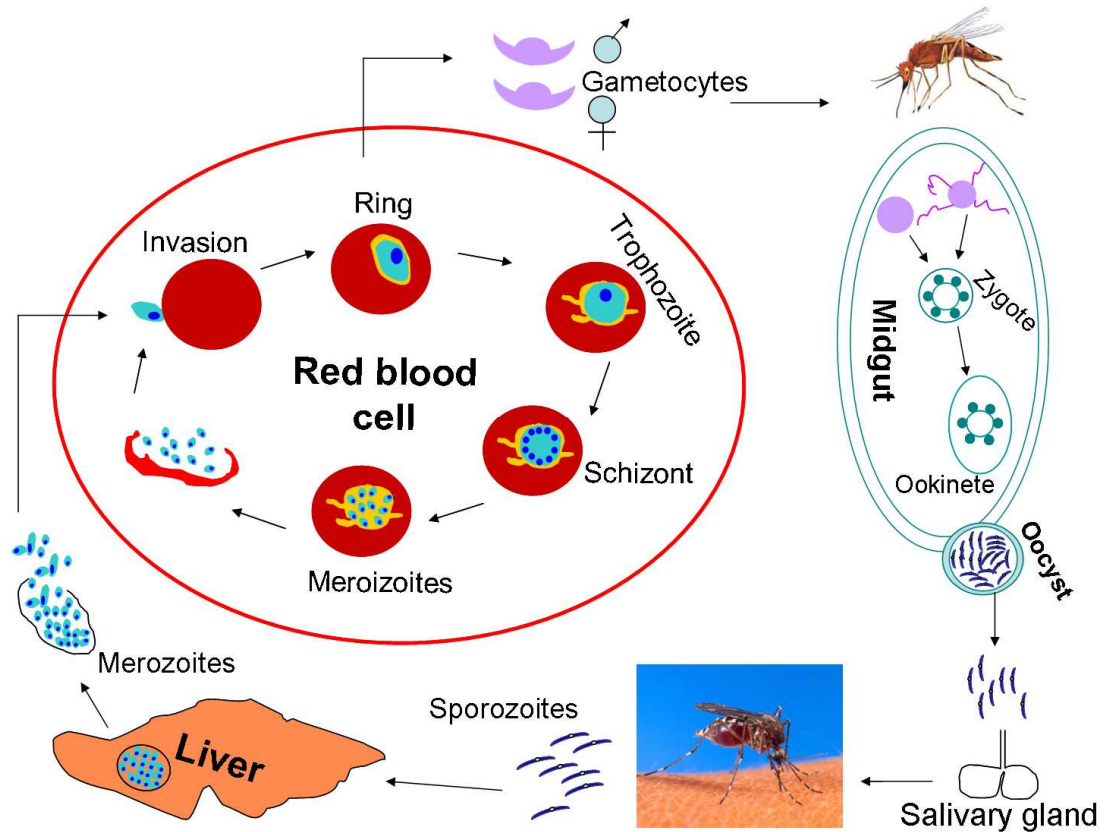


Figure 1.2. Life cycle of *P. falciparum* [adapted from (Winzeler, 2008)]. The infective sporozoites are dispensed from salivary gland of a female *Anopheles* mosquito into the human host. The sporozoites undergo schizogony in hepatocytes to produce thousands of merozoites which are released into the blood stream where they invade erythrocytes. The erythrocytic asexual cycles periodically complete and rupture the hosts to invade fresh red blood cells. Some merozoites differentiate into sexual gametocytes which, when ingested by the mosquito, initiate sexual development in the midgut, involving ookinetes and oocysts. The sporozoites inside the oocysts eventually migrate to the salivary gland, await transfer to the next vertebrate host.

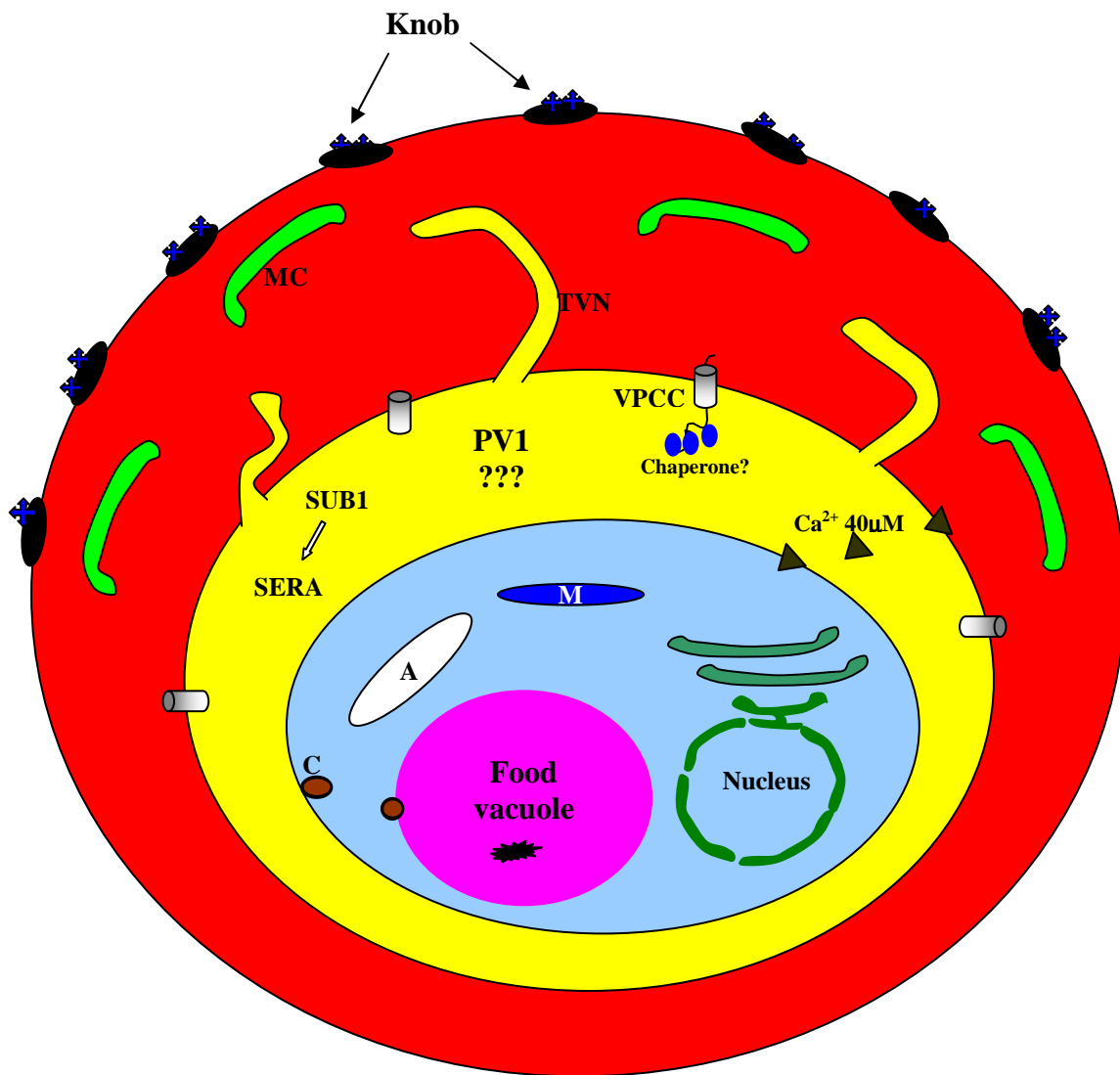


Figure 1.3. The trophozoite stage of *P. falciparum*-infected RBC [adapted from (Tilley *et al.*, 2008)]. Red compartment: RBC cytosol; yellow compartment: PV lumen; sky blue compartment: parasite. MC: Maurer's cleft structure, TVN: tubulovesicular network, C: cytosome, A: Apicoplast, M: Mitochondrion. Some proteins inside the PV lumen are presented: PV1, SERA, PfSUB1 and some chaperones. VPCC: putative vacuolar protein-conducting channel within the PVM. $\text{Ca}^{2+} 40\mu\text{M}$: Ca^{2+} concentration in the vacuolar space. See text (1.4) for more details.

1.2. The parasite compartments

Plasmodium belongs to the phylum Apicomplexa, a diverse group of unicellular protozoan parasites characterised by the presence of specialised secretory organelles at the anterior end of their invasive forms. These protozoa are pathogens of medical, veterinary and economic importance. The Apicomplexa phylum includes intracellular parasites of humans (*Plasmodium*, *Toxoplasma*, *Cryptosporidium*, *Cyclospora*, *Isospora*, *Babesia*), cattle (*Theileria*, *Babesia*, *Neospora*, *Sarcocystis*) and poultry (*Eimeria*).

The merozoite: All apicomplexan parasites share features including presence of a specialised apical complex (after which the group is named), which is central to the invasion process. The erythrocytic invasive forms of *Plasmodium* – the merozoite, as well as other invasive forms, the sporozoite and insect ookinete, are highly polarized cells containing the apical complex at the apical end of the parasite (Bannister *et al.*, 2000). These organelles consist of the rhoptries, the micronemes, the apical polar ring, and the conoid [review in (Blackman and Bannister, 2001)]. The club-shaped rhoptries and the small, elongated micronemes are unique secretory organelles. They contain products required for motility, adhesion to host cells, invasion of host cells, and establishment of the parasitophorous vacuole (PV). The third secretory organelle, the spherical dense granules, present in all parts of the cytoplasm, are likely to be involved in the maturation of the PV [(review in (Mercier *et al.*, 2005)]. In addition to the apical complex, apicomplexa have other exclusive structures, such as the apicoplast [(Köhler *et al.*, 1997; McFadden *et al.*, 1996; Wilson *et al.*, 1996)], which may play an essential role in the synthesis of lipids, heme and isoprenoids (Waller and McFadden, 2005). Another unique feature of Apicomplexa is the pellicle, a composite structure consisting of the plasma membrane and the closely apposed inner membrane complex (IMC) (Lobo *et al.*, 1999b). The pellicle is intimately associated with a number of cytoskeletal elements, including actin, myosin, microtubules, and a network of intermediate filament-like proteins [review in (Morrissette and Sibley, 2002)].

In the human blood stream, the parasite grows through different stages to gain nutrients and modify the host cell before escaping and invading new RBC. The

Introduction

parasite undergoes numerous morphological changes throughout the life cycle [review in (Bannister *et al.*, 2005)].

The ring stage: After invasion, the parasite deforms into a thin biconcave disc (Langreth *et al.*, 1978), thicker at the cytoplasm regions around the organelles nucleus, mitochondria, plastid, most of the ribosomes and endoplasmic reticulum (ER) while the center region is thinner because of less structures, giving the ring shape in Giemsa staining blood smear. The parasite resides inside the newly formed PV within the RBC, start feeding itself with haemoglobin catabolism through the cytostome structure (Francis *et al.*, 1997; Goldberg *et al.*, 1990; Lobo *et al.*, 1999b) as well as taking up other nutrients transported in from the plasma. As the ring stage enlarges, it begins to synthesise molecules specific to this stage (Spielmann and Beck, 2000) and to extend the surrounding PV membrane (PVM) (Atkinson and Aikawa, 1990; Elford *et al.*, 1995). The ring eventually grows into the rounder trophozoite stage.

The trophozoite: The difference between the ring and trophozoite stages depends on cell size and shape rather than any fundamental internal difference, and indeed the ring is more properly called the ring form of the trophozoite stage (Bannister *et al.*, 2005). This is the period of most active feeding, growth and red blood cell (RBC) modification by exporting various parasite proteins into the host cytoplasm. In Giemsa slides, trophozoites are characterised by its large, rounded shape and dots in the RBC cytosol, defined as Maurer's clefts (Langreth *et al.*, 1978; Wickert and Krohne, 2007a). There are also small knobs on the surface of the RBC (Atkinson and Aikawa, 1990). The membranous intracellular organelles also increase the size and the activity during growth (Bannister *et al.*, 2005). The parasite continues feeding on haemoglobin, and the haem products of haemoglobin digestion are accumulated into a dark pigment, haemozoin, scattered within a large food (pigment) vacuole (Egan *et al.*, 2002; Francis *et al.*, 1997).

The schizont: The parasite synthesises and assembles components that are needed for the next cycle of RBC invasion (Florent *et al.*, 2004). About 16 nuclei are generated (the number may vary from 8 to 32 in a single schizont) (Margos *et al.*, 2004) and these move into merozoite buds formed around the schizont's periphery (Bannister *et al.*, 2005). The merozoites are not completely mature until short before the release

from the RBC. Finally, the merozoites are released in a protease-dependent process [(Yeoh *et al.*, 2007), review in (Blackman, 2008)] and the free merozoites are ready for the next cycle.

1.3. The parasite induces alterations of the human erythrocyte

The mature human erythrocyte lacks a nucleus and other intracellular organelles, is devoid of *de novo* protein/lipid synthesis. Thus, as the parasite grows and replicates within the vacuole, it drastically remodels the host cell to the favour of its adaptation. These changes involve a range of morphological and physiological modifications of the erythrocyte, both to facilitate accessing to nutrients and causing adhesion of the infected RBC to the vascular endothelium [review in (Lingelbach *et al.*, 2004; Plattner and Soldati-Favre, 2008)]. Structures unique to *P. falciparum* infected erythrocytes have been detected by detail via electron microscopy analyses, these include electron dense protein-containing structures on the surface of RBCs (the knobs) and several membranous structures – the Maurer’s clefts (MC) and the tubulovesicular network (TVN).

1.3.1. Structural alterations

1.3.1.1. Parasitophorous vacuole

Many intracellular parasites reside and develop within vacuoles. The *Leishmania* passively enters their host cells via the phagocytic pathway and replicate within the phagolysosomes. In contrast, apicomplexan parasites such as *Toxoplasma* and *Plasmodium* actively invade the host cell. As a result, they reside within a parasitophorous vacuole (PV) which maintains a neutral pH [review in (Lingelbach and Joiner, 1998; Nyalwidhe *et al.*, 2003)]. Such a safe niche confers resistance to some host cell defenses but significantly cuts the parasites off from host metabolites. These parasites have adopted different tactics to circumvent the problem, remodeling their vacuole to make it permissive to vital substances (Plattner and Soldati-Favre, 2008). In case of the malaria parasite, the PVM forms a barrier between the infected RBC (iRBC) cell cytosol and the parasite surface. The vacuolar space represents a proteome which is clearly distinct from the erythrocyte cytosol and from the parasite cytosol (Nyalwidhe and Lingelbach, 2006).

1.3.1.2. The Maurer's Clefts

The membrane-bound compartment MC are the other major structural features seen in the cytoplasm of infected RBCs [review in (Wickert and Krohne, 2007b)]. Among proteins associated with the MCs are the skeleton-binding protein 1 [SBP-1, (Blisnick *et al.*, 2000)], the membrane-associated histidine-rich protein [MAHRP, (Spycher *et al.*, 2003)], the ring-exported proteins REX-1 (Hawthorne *et al.*, 2004) and REX- 2 (Spielmann *et al.*, 2006), the repetitive interspersed family (RIFINS) (Petter *et al.*, 2007) and the subtelomeric variable open reading frame [STEVOR, (Przyborski *et al.*, 2005)]. The MCs play a role as a parasite-induced intermediate 'sorting' compartment for proteins destined to the erythrocyte membrane [review in (Lanzer *et al.*, 2006; Przyborski, 2008; Wickert and Krohne, 2007b)].

1.3.1.3. The tubulovesicular network

The TVN projecting from the PVM to the red cell have been imaged by fluorescence microscopy (Behari and Haldar, 1994; Elmendorf and Haldar, 1993; Haldar *et al.*, 1989) and these studies suggest that the PVM and TVN are all interconnected compartments with other intraerythrocytic structures such as the Maurers clefts. The enlargement of the membrane most likely is due to metabolic processes by the parasite since mammalian erythrocytes do not synthesise lipids or proteins *de novo* (Lingelbach and Joiner, 1998).

1.3.1.4. Knobs

An important aspect in virulence of *P. falciparum* is the ability of infected erythrocytes to sequester in and obstruct the microvasculature of different organs (MacPherson *et al.*, 1985). Cytoadhesion is mediated by the antigenically variant *P. falciparum* erythrocyte membrane protein-1 (PfEMP1) (Baruch *et al.*, 1995; Hay *et al.*, 2009; Kilejian, 1979; Su *et al.*, 1995). PfEMP1 is concentrated on electron-dense elevations of the membrane termed as knobs (Luse and Miller, 1971; Trager *et al.*, 1966). The knob provides a platform for adherence under physiologic flow conditions (Crabb *et al.*, 1997; Deitsch and Wellems, 1996). The other main component of knobs is the knob-associated histidine-rich protein (KAHRP) (Kilejian, 1979), and it contributes to altered mechanical properties of parasite-infected erythrocytes (Rug *et al.*, 2006).

1.3.2. Biochemical/ physiological alterations

In addition to morphological and structural changes to the infected erythrocyte, the parasite alters the permeability of the RBC membrane (RBCM) to allow the uptake of nutrients, the removal of “waste” and volume and ion regulation of the infected cell (Ginsburg *et al.*, 1983; Kirk, 2001). The increase of RBC permeability is attributable to the appearance in the membrane of 'New Permeation Pathways' (NPP) (Kirk, 2001), thought to be one or more types of channels. Recently, the involvement of parasite encoded proteins in the generation of the pathways was reported, either as components of the pathways themselves or as auxiliary factors (Baumeister *et al.*, 2006).

1.4. The parasitophorous vacuole- form and function

1.4.1. Invasion of erythrocytes and the PV formation

The invasion of erythrocytes by merozoites occurs rapidly (Cowman and Crabb, 2006; Maier *et al.*, 2006). The entire process of erythrocyte invasion takes about 30 s to 60 s and only about another 10 to 20 min to transform into an intracellular ring-stage parasite (Dvorak *et al.*, 1975; Mitchell and Bannister, 1988). Upon contact with an erythrocyte, the merozoite attaches and orients its anterior end towards the erythrocyte. The initial contact between the merozoite and erythrocyte is a crucial step, probably a random collision and presumably involves reversible interactions between proteins on the merozoite surface and the host erythrocyte (Bannister and Dluzewski, 1990). Primary attachment of the polar merozoite appears to occur at any point on the surface of this parasite stage. Several merozoite surface coat proteins have been described in this primary contact (Maier *et al.*, 2006), largely comprised of glycosylphosphatidylinositol (GPI) anchored membrane proteins. The best characterised protein is the merozoite surface protein-1 (MSP-1), the most abundant protein on the merozoite surface. MSP-1 is essential for parasite survival, and is one of the major vaccine candidates (Holder *et al.*, 1999; O'Donnell *et al.*, 2000).

The reorientation then occurs so that the apical end of the parasite is facing the erythrocyte membrane. A close association known as tight moving junction is formed between the merozoite and the host cell membrane, and the microneme contents are released at the same time (Aikawa *et al.*, 1978; Aikawa *et al.*, 1981; Bannister and Mitchell, 1989; Bannister and Dluzewski, 1990). The apical membrane antigen-1

Introduction

(AMA-1) has been implicated to establish a key link between the weak initial contact involving MSPs and irreversible tight associations formed with microneme proteins (Alexander *et al.*, 2006; Mital *et al.*, 2005; Triglia, 2000). Two protein families, the Duffy binding-like (DBL) protein family (Camus and Hadley, 1985; Miller *et al.*, 2002a) and *P. falciparum* reticulocyte binding protein homolog (PfRh or PfRBL) are prime candidates for the adhesins in junction formation (Maier *et al.*, 2006; Triglia *et al.*, 2005). The motor factor(s) in *Plasmodium* merozoites have not been specifically identified, but in sporozoites that invade liver cells, thrombospondin-related anonymous protein (TRAP) appears to provide the crucial link (Morahan *et al.*, 2009; Sultan *et al.*, 1997).

The entry phase of merozoite invasion into erythrocyte is an active process by the parasite since the mature RBC is not capable of either phagocytosis or receptor-mediated endocytosis. Ultrastructural studies show that upon the forming of the junction, the merozoite moves toward the apical end and a membrane-lined invasion pit, the PV, begins to form beyond the boundaries of the junctional bands and the roptery constituents are discharged into the PV (Aikawa *et al.*, 1978; Aikawa *et al.*, 1981; Bannister and Mitchell, 1989; Sam-Yellowe *et al.*, 1988). These ultrastructural observations, together with proteomic data (Sam-Yellowe *et al.*, 2004) indicate that the roptery components participate in formation of the PVM and the PV [review in (Galinski *et al.*, 2005; Lingelbach and Joiner, 1998)].

Invasion ends with a sequence of further changes. First, the PV is sealed off by the fusion of the RBC membrane across the mouth of the pit, and the PVM also seals and detaches from the RBC surface. Second, the dense granules (DG) move to the merozoite surface and fuse with it to release their contents into the PV, causing the further expansion of the PVM (Aikawa *et al.*, 1978; Bannister and Dlugowski, 1990). Ring-infected erythrocyte surface antigen (RESA), the first identified dense granule protein (Aikawa *et al.*, 1990), was detected to release from merozoite DG after erythrocyte invasion (Culvenor *et al.*, 1991).

The biochemical composition and molecular process of the PVM formation remain unclear, but recent studies of both *Plasmodium* and *Toxoplasma* are opening some answers. Whatever the mechanism, it is clear that the RBC membrane is modified at

the point of invasion, and that secretion from the merozoite rhoptries is largely if not wholly responsible for the changes. For the lipid part of the PVM, host cell membrane lipids are substantially involved in PVM formation (Hakansson *et al.*, 2001; Haldar and Uyetake, 1992; Pouvelle *et al.*, 1994; Ward *et al.*, 1993). But the composition is somewhat unexpected when Phosphatidylinositol - 4,5 - biphosphate, a major phosphoinositide in erythrocyte membranes, was found excluded from the PV (Murphy *et al.*, 2007), thus providing the first evidence for erythrocyte phospholipid remodeling by the parasite. Analysis of detergent resistant microdomains (DRM) obtained from a total membrane fraction of infected erythrocytes (iRBC) also revealed several host proteins in the PVM, including flotillins-1 and -2, aquaporin-1, scramblase (Murphy *et al.*, 2004) and most recently, aquaporin-3 (Bietz *et al.*, 2009). However, whereas a host cell DRM-associated stomatin, band 7, is excluded from the PVM, a parasite stomatin in rhoptry DRM rafts and the parasite RhopH proteins enter the vacuole (Hiller *et al.*, 2003). The mechanism of these events clearly requires the participation of both host- and parasite-derived factors.

1.4.2. The PV – a transit compartment

Mature erythrocytes are devoid of trafficking machinery or organelles and, therefore, the parasites must set up and regulate protein transport within the erythrocyte cytoplasm to mediate the uptake of nutrients from the host bloodstream, in addition to displaying parasite-encoded proteins on the erythrocyte surface (Charpian and Przyborski, 2008; Cooke *et al.*, 2004). To reach the host cell cytosol or surface, parasite proteins must passage across both the parasite plasma membrane (PPM) and the PVM.

Trafficking of proteins to the PV is similar to the classical pathway of higher eukaryotes, with proteins entering the endoplasmic reticulum (ER), based on an N-terminal ER targeting signal (Adisa *et al.*, 2003; Benting *et al.*, 1994; Wickham *et al.*, 2001). Some proteins, such as the serine-rich antigen (SERA) family, remain in the vacuolar lumen (Delplace *et al.*, 1988; Knapp *et al.*, 1989), whereas other proteins, such as KAHRP are directed outwards across the PVM (Wickham *et al.*, 2001). Earlier studies evidenced that soluble parasite proteins destined for the host erythrocyte pass transiently through the lumen of the PV before being secreted into the red blood cell (Ansorge *et al.*, 1996; Baumeister *et al.*, 2001). Later publications

reported that those exported parasite proteins require a conserved motif (RxLxE/Q/D), termed the *Plasmodium* export element (PEXEL) or Host Cell Targeting (HCT)/Vacuolar Targeting Sequence (VTS), for targeting beyond the PVM into the host cell (Hiller *et al.*, 2004; Marti *et al.*, 2004). PEXEL appears to be cleaved within the parasite's ER. The “new” n-terminus of the protein is then acetylated (Boddey *et al.*, 2009; Chang *et al.*, 2008). The machinery involved in protein transport across the PVM is poorly understood. It has previously been reported that PEXEL-containing chimaeras within the PV have the appearance of a necklace of beads that are resistant to recovery after photobleaching, suggesting the presence of subcompartments within the vacuole (Adisa *et al.*, 2003; Wickham *et al.*, 2001). These compartments may house factor(s) that identify and translocate proteins trafficked there. Latest evidence reported that soluble proteins must cross the PVM into the erythrocyte cytoplasm in an unfolded state, strongly supporting the existence of a vacuolar protein-conducting channel (VPCC) within the PVM (Gehde *et al.*, 2009).

1.4.3. The PV – nutrition acquisition and regulation of the ionic environment

Apart from being a protein sorting compartment, the PV is also postulated to play a role in nutrient acquisition (Lingelbach and Joiner, 1998). *Plasmodium* ingests approximately 80% of the host cell haemoglobin for its amino acid supply and to provide “space” for the growing parasite cell (Lew *et al.*, 2003). The cytostome structure (see 1.2 above) constantly phagocytoses the PVM including haemoglobin and transport to the food vacuole where the haemoglobin is digested. Those poorly represented amino acids (cysteine, methionine, and glutamine) or absent (isoleucine) in human haemoglobin or other essential nutritive materials must be uptaken from the external environment. The proposed mechanisms of acquisition might be from the NPP (Kirk and Saliba, 2007)(see 1.3 above). Electrophysiological and biochemical studies have shown that the PVM contains nonselective pores that allow passive bidirectional movement of small molecules up to 2000 Da (Desai and Rosenberg, 1997; Kirk, 2001; Nyalwidhe *et al.*, 2002).

From the molecular sieve feature of the PVM, the ionic composition of the PV is expected to be very similar, if not identical, to the cytoplasm of the erythrocyte. However, if the vacuolar space contains the same ionic environment as RBC cytosol, the parasite faces critical survival problems. In common with other mammalian cells, the erythrocyte cytoplasm maintains high K⁺ concentration (140 mM) and very low

Introduction

Ca^{2+} (100 nM), clearly in contrast to that of regular extracellular medium in most cells (Alleva and Kirk, 2001). Regarding Ca^{2+} , eukaryotic cells normally need an extracellular Ca^{2+} concentration close to millimolar range. *Plasmodium* parasite cleverly overcomes the problem by the maintenance of a high Ca^{2+} concentration within the PV (Gazarini *et al.*, 2003). The $[\text{Ca}^{2+}]$ within this compartment was found to be around 40 μM , sufficiently high to be compatible with a normal loading of the *Plasmodia* intracellular Ca^{2+} stores (100 – 1,000-fold higher than that in the parasite and RBC cytoplasm respectively). The authors also demonstrated experimentally that, if the Ca^{2+} concentration in the PV was reduced, the maturation of the parasites was impaired, and eventually is incompatible with the survival of the *Plasmodia* within the RBC. The sequencing of the *Plasmodium* genome (Gardner *et al.*, 2002) and several recent studies have identified in this parasite a number of signaling molecules related to those of vertebrate cells, including many proteins concerned with Ca^{2+} handling and signaling [review in (Garcia *et al.*, 2008)]. The key question addressed here is to identify factors involving in the Ca^{2+} homeostasis and the Ca^{2+} -based signaling mechanisms, with the PV as a Ca^{2+} reservoir outside of the parasite plasma membrane.

1.4.4. The PV – preparation of merozoite egress

To invade the host cell, the parasite must firstly initiate egress from its infected cell, and this process involves disruption the PVM and the host cell membrane. It was observed that egress is a rapid, and therefore, by inference, highly regulated event [review in (Blackman, 2008)]. The mechanism and the temporal sequence of PVM and host cell membrane rupture are not well understood. Live microscopy and selective inhibitor studies have revealed that *P. falciparum* merozoite egress is a two-step process, but whether the PVM or the host cell membrane ruptures first is still much on debate (Glushakova *et al.*, 2005; Soni *et al.*, 2005; Wickham *et al.*, 2003). Recent work by Heussler and colleagues in liver stage merozoites has revealed some important parallels with the blood stage egress. The observation, very clearly detectable in these relatively large cells, has agreed with the work from Wickham *et al.* in which the PVM breakdown precedes RBC membrane rupture (Sturm *et al.*, 2006; Sturm and Heussler, 2007; Wickham *et al.*, 2003).

Introduction

Whatever the sequence of membrane rupture is, various publications evidenced that the egress requires protease activity. Treatment of the cultures of *P. falciparum* asexual blood stages parasites with a range of protease inhibitors, such as a mixture of leupeptin, chymostatin, antipain (a serine and cysteine protease inhibitor), E64 (cysteine protease inhibitor), pepstatin (an aspartic protease inhibitor) resulted in the blocking of merozoite egress [review in (Blackman, 2008)]. Nevertheless, at least three common conclusions can be drawn from the accumulated data: that breakdown of the PVM and host cell membrane is differentially regulated; that both events are protease-dependent; and that PVM rupture is an E64-sensitive process. Given the high specificity of E64 for cysteine proteases, this strongly implicates the involvement of one or more cysteine proteases in PVM rupture, and at least one additional distinct activity in host cell membrane rupture. Members of the SERA, a family of nine genes in *P. falciparum*, are one of the best potential mediators of egress.

The SERA proteins are most highly expressed at schizont stage and localize to the PV lumen (Delplace *et al.*, 1987; Delplace *et al.*, 1988; Knapp *et al.*, 1989; Knapp *et al.*, 1991; Miller *et al.*, 2002b), putting them in the right place and at the right time to take part in egress. All the SERA gene products share a central relatively conserved papain-like domain as well as N- and C-terminal regions that contain a number of conserved Cys residues (Miller *et al.*, 2002b). SERA5 and SERA 6 are most abundantly transcribed and translated. Early studies also marked a close temporal association between the proteolytic processing of SERA5 and blood-stage egress (Delplace *et al.*, 1987; Delplace *et al.*, 1988). The processing of SERA5 was shown to be mediated by a subtilisin-like serine protease called PfSUB1 (Blackman *et al.*, 1998; Sajid *et al.*, 2000; Yeoh *et al.*, 2007). Using a transgenic parasite line expressing epitope-tagged PfSUB1, Yeoh and colleagues showed that PfSUB1 was expressed in an unusual set of dense granule-like organelles (exonemes) from which it is released, in a fully soluble form, into the PV space just prior to egress (Yeoh *et al.*, 2007). A selective PfSUB1 inhibitor prevented egress and also blocked SERA5 processing, suggesting a link between these events. Moreover, upon its release into the PV, PfSUB1 directly mediates the primary proteolytic processing of three major proteins on the merozoite surface, MSP1, MSP6 and MSP7 (Koussis *et al.*, 2009). Thus the PV contain factor(s), so far PfSUB1, which regulate both egress and

proteolytic remodelling of the developing merozoite in preparation for its release from the infected cell.

In addition to parasite-derived proteases activity in parasite egress, the latest work on *P. falciparum* and *Toxoplasma* reveals that both parasites hijack host cell calcium-regulated calpain protease to facilitate their escape from infected cells (Chandramohanadas *et al.*, 2009). The authors suggest a model involving calcium signal triggered late in the development stages. Once again, it raises the question of how the parasite regulates Ca²⁺-based signaling mechanisms (see 1.4.3 above). As a distinct compartment from both the parasite and the host cell cytosol, the PV resident proteins would have unique features and functions, waiting for further research.

Generally, the function of gene products can be explored by experimental approaches that involve in the knocking-out of individual or several genes. A major limitation in determining the function of genes in *Plasmodium* has been the inability to genetically manipulate this parasite with ease. Also, classical genetics studies in *P. falciparum* are limited due to the difficulties in creating genetic crosses (Walliker *et al.*, 1987). Nevertheless, the generation of knock-out *P. falciparum* parasites has been successfully applied and enabled researchers to study phenotypic changes.

1.5. Genetic manipulation of *P. falciparum*

The malaria parasite represents a unique challenge for transfection because the introduced DNA must cross multiple membranes before it can enter the parasite nucleus, including those of the RBC, the parasitophorous vacuole, the parasite and the nucleus itself. Therefore, although the *in vitro* culture system of *P. falciparum* has been used widely for many years (Trager and Jensen, 1976), transfection of the parasites remained elusive despite intensive efforts. Transfection of malaria parasites was first performed transiently in the sexual stages of the bird malaria parasite *P. gallinaceum* (Goonewardene *et al.*, 1993). It was not until 1995 that Wu and colleagues performed the transient transfection in the human malaria parasite *P. falciparum* (Wu *et al.*, 1995) and van Dijk first reported the stable transfection in *Plasmodium*, using the model organism of rodent malaria *P. berghei* (van Dijk *et al.*, 1995). Soon after, the similar system demonstrated at last that *P. falciparum* within erythrocyte can be successfully modified by integrative transfection (Crabb and Cowman, 1996; Wu *et al.*, 1996). Despite the low efficiency of the *P. falciparum*

Introduction

transfection, these crucial breakthroughs shed new light to malaria research, widened studies of many aspects for understanding *Plasmodium* biology and malaria pathogenesis in molecular terms.

1.5.1. Difficulties with *P. falciparum* transfection

Unlike many other systems, including the rodent malaria parasite *P. berghei*, *P. falciparum* can only take up the circular plasmid DNA, with a very low efficiency in the range of 10^{-6} (O'Donnell *et al.*, 2002), compare to the efficiency of *P. berghei* ($\sim 10^3 - 10^4$). The low competence is primarily related to the requirement of performing the transfection at the intracellular ring stage of the blood stage cycle. Hence, the exogenous DNA must cross the four layers of membranes before reaching the nucleus. The transfection efficiency in *P. berghei* is, however, much higher due to the transfection directly into the freely extracellular merozoites, avoiding the multilayers. *P. falciparum* extracellular merozoites have a short half-life and to date, there is no method to prepare sufficient viable *P. falciparum* merozoites alone, not to mention for use in transfection.

Another major obstacle is the extremely rich A/T content of *P. falciparum* DNA sequences, which leads to difficulties in cloning steps in *Escherichia coli*. The AT composition of the extragenic region of *P. falciparum* genes can be higher than 90%. For most of stable transfections, vector constructs are quite large, containing both the ampicillin resistance marker for selection in *E. coli* and selectable marker cassette in *Plasmodium*, as well as the targeting sequence. The plasmid constructs are highly unstable and poorly yield, often end up in extensive recombination state. The cloning steps might take several months and are labor consuming with a need to screen large numbers of *E. coli* colonies to identify those that contain the correct plasmids in an unrearranged state.

Another complication of *P. falciparum* transfection is their ability to maintain transfected plasmids as stable episomal replication form (SRFs) under the pressure of drug selection (Kadekoppala *et al.*, 2001; O'Donnell *et al.*, 2001). These SRFs are large concatamers of the parental plasmids, comprising at least nine plasmids in a head-to-tail array. Subsequently, the plasmid integration into a specific chromosomal locus is achievable in *P. falciparum* but the methods are slow and laborious [reviewed

in (Crabb *et al.*, 2004)]. This problem can be circumvented by double homologous recombination and removal of episome-containing parasites, using negative selection system of marker thymidine kinase (*TK*) (Duraisingh *et al.*, 2002) (Figure 1.4).

The stable transfection in *Plasmodium* is also restricted by the limited number of positive selectable markers. The two most commonly used selectable markers are a modified *Toxoplasma gondii* dihydrofolate reductase-thymidylate synthase gene (*DHFR-TS*) (Wilson *et al.*, 1996), confers resistance to pyrimethamine and the human *DHFR* gene (*hDHFR*) which resists to the experimental antimalarial drug WR99210 (Fidock and Wellems, 1997). Three other positive selectable markers have been successfully used in *P. falciparum* selections, including blasticidin S deaminase (*BSD*) (Mamoun *et al.*, 1999), neomycin phosphotransferase II (*NEO*) (Mamoun *et al.*, 1999) and puromycin-*N*-acetyltransferase (*PAC*) (de Koning-Ward *et al.*, 2001), encode resistance to blasticidin, geneticin (G418) and puromycin, respectively.

1.5.2. Functional analysis by integrative transfection

At the moment applying the RNAi technique might not be possible in *Plasmodium*, mostly due to the absence of RNAi pathway ortholog in any of the available *Plasmodium* databases [review (Militello *et al.*, 2008)], thus, genetic studies of gene characterisation in this parasite mainly depend on introducing exogenous DNAs by transfection techniques, either by transient or stable transfection.

1.5.2.1. Gene targeting by single-crossover

The advancement of stable transfection and homologous recombination in *Plasmodium* has allowed direct studies on malaria protein function. In *T. gondii*, integration into the genome occurs preferring non-homologous over homologous recombination, leading to efficient insertional mutagenesis (Roos *et al.*, 1997). However, if the length of the homologous sequence is sufficient (2-3 kb), double cross-over in *T. gondii* is favourable (Wilson *et al.*, 1996). In contrast, integration in the *Plasmodium* system is almost exclusively homologous, and as little as 250 – 300 bp of targeting sequence is effective enough for the integration (Lobo *et al.*, 1999a). The *Plasmodium* genome is haploid and integration of transfected DNA into the *Plasmodium* genome occurs by homologous recombination (Crabb and Cowman,

1996). This has provided a capable system for manipulating the *Plasmodium* genome by gene disruption or allelic replacement.

1.5.2.2. Gene targeting by double-crossover homologous recombination using negative selection marker

Despite the ability to disrupt many genes, there are at least two big disadvantages to knockout by single-crossover integration. First, after integration, the plasmid backbone is still maintained at the site of the gene locus, making it challenging to knock out a second gene, using a different selectable marker, as the second integration event would be favored the first integrated plasmid backbone over the desired locus (Cowman and Crabb, 2005). The existence of the plasmid backbone can also lead to a potential reversion event by looping the plasmid back out from the genome, generating plasmids that could segregate during schizogony. Although it is rare, reversion has been previously reported in *P. berghei* (de Koning-Ward *et al.*, 2000; Sultan *et al.*, 1997). Furthermore, the single-crossover recombination can result in truncated proteins with a potential dominant negative effect as demonstrated with PfEMP3 (Waterkeyn *et al.*, 2000). Secondly, the time required to obtain integrants by single-crossover incident is prolonged due to the persistence of the circular episomal plasmids. It takes 2 to 3 weeks for the integration of linear DNA into *P. berghei* chromosomes but at least 3 months to select the integration of circular plasmid DNA in *P. falciparum* (Crabb *et al.*, 1997; Crabb *et al.*, 2004). The parasites containing integrated plasmid have to compete with the parasites with episomal form. The episomal plasmid containing parasites possibly grow faster, limiting the selection of homologous recombination parasites. In some cases it is impossible to isolate parasites with gene disruptions that result in decreased growth rates. To isolate integrated parasites, a growth on and off drug cycling can be applied. Episomal plasmids are segregated non-evenly into daughter merozoites (O'Donnell *et al.*, 2001; van Dijk *et al.*, 1995), resulted in some cells obtaining many plasmid copies whereas others are plasmid deficient. In contrast, integrated plasmids will be equally distributed into daughter merozoites. Removal of drug selection will rapidly lead to the loss of episomal plasmids, and re-introduction of drug pressure after a period would select for parasites with integrated events (Cowman and Crabb, 2005). Thus, the strategy of on-and-off drug cycling, however time consuming, has still been the

Introduction

conventional method for selecting parasites with single-crossover homologous recombination.

To overcome the disadvantages of single-crossover strategy, the rare double-crossover event has been recovered by use of a negative selection marker (Duraisingh *et al.*, 2002). Negative selection relies on the expression of a foreign gene in a cell that converts a normally harmless drug into a toxic one. The thymidine kinase (*TK*) gene from *Herpes simplex* virus is an enzyme that activates nucleoside analogues such as ganciclovir into a toxic metabolite which inhibits the *de novo* pyrimidine biosynthesis pathway and DNA synthesis directly. The *TK* gene was used together with the positive selectable marker *hDHFR* to create positive/negative selection systems. The positive selectable marker was flanked by the two homologous regions of target sequence. Under the pressure of positive and negative selection, parasites containing episomal plasmids are resistant to WR99210 but susceptible to ganciclovir. The only survival parasites were those with integration by double-crossover recombination, deleting the negative selection cassette as well as the plasmid backbone, and incorporating the positive selectable marker into the locus of interest on the chromosome, generating the knockout line. Duraisingh *et al.* had also tested the ability of using the *E. coli* cytosine deaminase (CD) enzyme in negative selection. CD converts the prodrug 5-fluorocytosine (5-FC) into the 5-fluorouracil (5-FU) toxic form, inhibits RNA synthesis as well as the thymidylate synthase. However, at the time of experiment, the *E. coli* CD system was not successful as it resulted in mutant *P. falciparum* parasites resistant to the effect of the 5-FC metabolite.

While the double-crossover recombination by negative selection strategy using the TK enzyme has now become the main approach to knockout genes in *P. falciparum*, the system itself has been reported not potent enough. In some cases, parasites with a single copy of the plasmid integrated via single-crossover recombination could still survive in high concentration of ganciclovir (Duraisingh *et al.*, 2003b; Maier *et al.*, 2003). The possible reason was the lack of sufficient TK expression from one copy of the gene, allowing some parasites to survive. A more potent negative selection system is required. The yeast fusion protein yCDUP from *Saccharomyces cerevisiae* CD (ScCD) and uracil phosphoribosyl transferase (ScUPRT) were recently successfully applied for positive-negative selection in *P. falciparum* (Maier *et al.*, 2006) and shown to be very effective for double-crossover. However, the concentration of the

Introduction

prodrug 5-FC must be in control because no parasites were obtained after selection with more than 1 μ M of 5-FC. This was likely because of the “bystander effect”, where ScCDUP expressing parasites metabolise the prodrug 5-FC to the toxic metabolite 5-FU which could diffuse into the non-ScCDUP containing parasites, resulting in growth inhibition and killing them. In the TK or *E. coli* CD negative selection system, this “bystander effect” was also observed (Duraisingh *et al.*, 2002).

Despite the shortcomings of the TK-negative selection vector, the system has been very useful in knockout studies in *P. falciparum*, including those genes which were not able to be disrupted previously by single-crossover strategy (McCoubrie *et al.*, 2007). The application of gene disruption by double-crossover recombination was taken to a new level by a large scale gene knockout approach with functional characterisation of 83 parasite proteins that are potentially exported out of the PV into the host erythrocyte (Maier *et al.*, 2008). The work was initially started with pHTK vector (Duraisingh *et al.*, 2002), and further improved by ScCDUP system (Maier *et al.*, 2006). In the study they were able to disrupt 53 of 83 genes by double-crossover homologous recombination. For the rest 30 genes, the transfection was successful but not the integration. While the inability to select the integrated form for some genes is not a convincing proof that they are essential under laboratory conditions, it is consistent with the suggestion that they might play important functions in growth of the erythrocyte stage parasites. This study significantly extends our understanding of the role of exported proteins in host/parasite interactions being essential for survival of *P. falciparum in vivo* and defines a group of potentially novel therapeutic targets.

While gene disruption is an important technique to address protein function, there are essential genes which are impossible to knockout; gene targeting for allelic replacement via single-crossover recombination has become an important tool. This technique is particularly useful in studying the role of mutations in drug resistance; especially when targets are essential genes and the modification of amino acids would not disrupt the sequence and function of proteins. Allelic replacement has also been applied to address the role of antibodies in immunity or to identify polymorphisms [for review see (Cowman, 2005)].

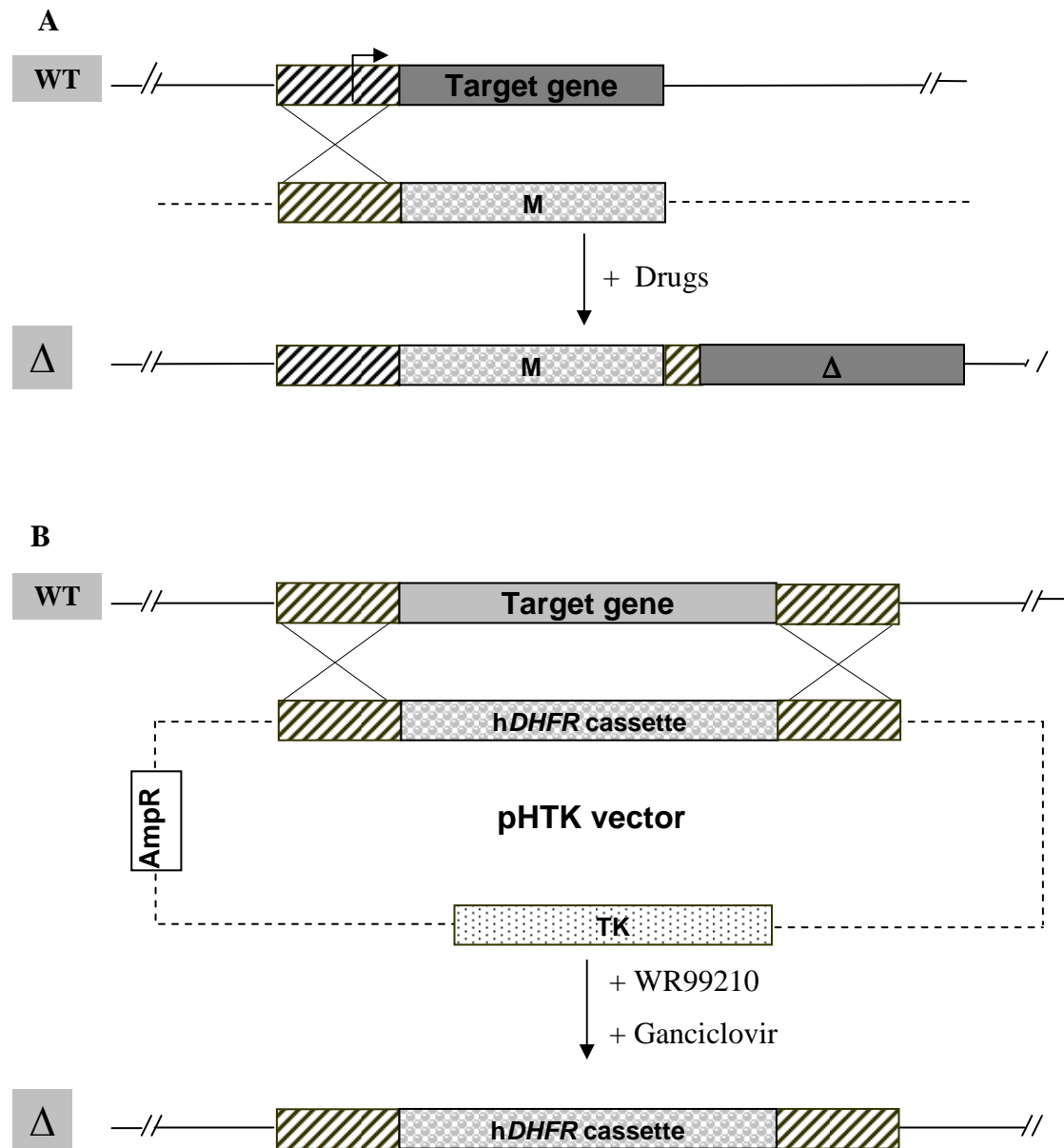


Figure 1.4: Schematic representation of single (A) and double (B) crossover homologous recombination in *P. falciparum*. (A) The insertion construct contains a selection cassette (sphere box, M) and a fragment of the targeting sequence (wide upward diagonal box). The targeting sequence could either be at the 5' or 3' end of the target gene (solid box), here is shown the scheme of the 5'-end single crossover. (B) Double crossover with the pHTK vector. The *hDHFR* cassette is flanked by the two homologous regions of the targeting sequence. The plasmid backbone (dashed line) also contains the *Thymidine kinase* cassette (TK, dot box) for negative selection. See text for more details. **WT**: target locus of wild-type parasite, **Δ** prediction of the integrated locus.

1.5.3. Other gene technique advances in *P. falciparum*

Although insight into malaria protein function has been achieved through the gene disruption by homologous recombination, the technique cannot be applied in essential genes. The only way to control the expression of essential genes, in the haploid organism *P. falciparum*, is to regulate the gene expression system, which has not been described until recently. The first conditional expression system in *P. falciparum* was based on the Anhydrotetracycline (ATc)- inducible system (Meissner *et al.*, 2005). However, because of its complicated system and the time-consuming procedure, the method has not been widely applied.

Most recently several methods have been developed, including the ribozyme-based system (Agop-Nersesian *et al.*, 2008). The ribozyme was placed at the translational start region of the gene of interest, leading to cleavage of mRNA and its degradation. RNA self-cleavage can be controlled by specific inhibitors of ribozyme activity, keeping the mRNA stable and hence, its translation. In principle, embedding this regulation system into any locus allows placing the gene of interest under the control of its endogenous promoter to ensure the right timing of expression. The method is still a newborn technique and in the process of finding specific and harmless ribozyme inhibitors to prevent the cells from toxic effects.

Another strategy is the post-translational regulation by a destabilization domain technology (Armstrong and Goldberg, 2007). This method prevents proteins from degradation by adding Shield-1, a permeable small molecule ligand of the human rapamycin-binding protein FKPB12. The ‘destabilization domain’ of FKPB12 is fused to the N- or C-terminus of the target protein, thereby facilitating its degradation. However, the destabilization domain technology has not been developed for secreted proteins yet. The latest advancement is the co-regulated transgene and *bsd* selectable marker by a bidirectional promoter (Epp *et al.*, 2008).

In *P. berghei*, tool for functional analyses of essential genes have been achieved by the Flp/FRT site-specific recombination (Carvalho *et al.*, 2004). A site-specific recombination system has also been developed in *P. falciparum*, using the mycobacteriophage Bxb1 integrase (Nkrumah *et al.*, 2006). The Bxb1 system offers a method to complement gene function but currently the system is of no advantage for available gene knockout lines as these do not contain the required site-specific *attB* and *attP* site.

With more than 60% of the genome coding for hypothetical proteins (Gardner *et al.*, 2002), the conventional one-by-one knockout procedure is not strong enough for the study of protein function. Tools to identify essential genes in malaria parasites require high-throughput screening selection. Only until recently have the transposon based mutagenesis been developed, allowing functional genomic studies to be performed proficiently. In *P. berghei* that was the shuttle transposon mutagenesis system, using a mini Tn5 transposon derivative (Sakamoto *et al.*, 2005). In *P. falciparum*, it was developed by Balu *et al.*, using the piggyback transposable elements (Balu *et al.*, 2005). This is the first system that allows widespread, random and direct integration with high efficiency into the *P. falciparum* genome. Currently the system has only been tested the transiently expressed transposase therefore a large scale screening has not achieved (Balu *et al.*, 2005).

1.6. PfPV1 – a novel parasitophorous vacuole protein

In order to identify and characterise the vacuolar proteins that are involved in various processes, we have begun to analyse the PV's proteome (Nyalwidhe *et al.*, 2002; Nyalwidhe and Lingelbach, 2006). Proteins of the PV fall into the following main classes: chaperones, proteases, and metabolic enzymes, consistent with the expected functions of the vacuole (Nyalwidhe and Lingelbach, 2006). From the proteomic data, we identified a protein which was named PfPV1 for which no functional annotations are available. The encoding gene PF11_0302 on chromosome 11 contains no intron and expresses a product of 452 amino acids. PfPV1 has a theoretical pI of 4.97 and molecular mass of 51951.49 Dalton [from PlasmoDB, (Aurrecochea *et al.*, 2009)]. The protein is predicted to have an N-terminal signal sequence and the cleavage site is between position 21 and 22: IYG- NV (Bendtsen *et al.*, 2004). The *PfPV1* gene had been evidenced to be expressed at all stages of the intraerythrocytic development (Bozdech *et al.*, 2003b; Le Roch *et al.*, 2003). The latest update from PlasmoDB has also reported peptide sequences of PfPV1 found in purified merozoite proteomics [PlasmoDB, (Aurrecochea *et al.*, 2009)] and gametocyte and ookinete stages (Aurrecochea *et al.*, 2009).

Introduction

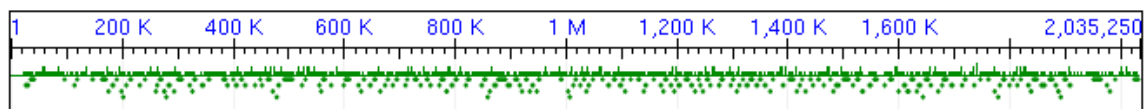
1.7. Objective

While it is reasonable to speculate that vacuolar membrane shelters the parasite in a potentially hostile environment, there are much more to the biological function of this particular compartment. The aim of this study is to characterise PfPV1 protein by reverse genetic approaches. The generation of knock-out parasites will enable us to test whether the respective gene is essential and, if their deletion results in viable parasites, it will enable us to study phenotypic changes. The recombinant protein fused to GST or 6x His-tag expressed in *E. coli* is also studied to further proceed in pull down assays to identify interacting patterns.

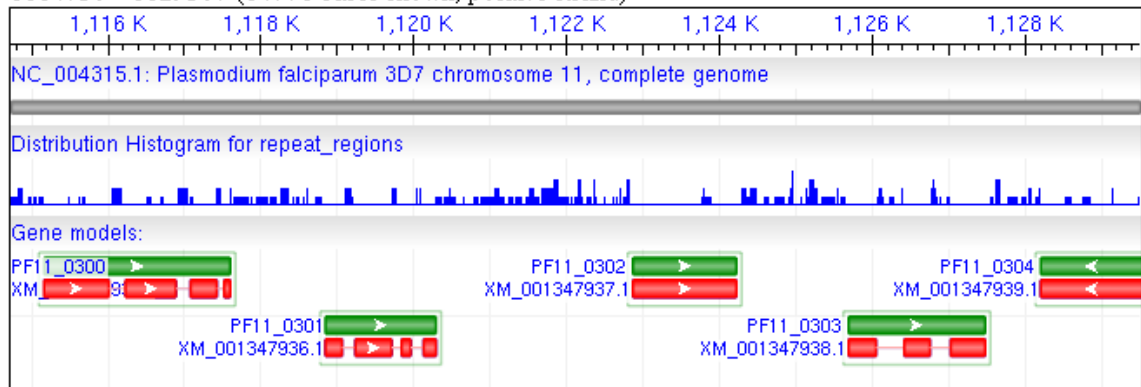
A

Plasmodium falciparum 3D7 chromosome 11, complete genome

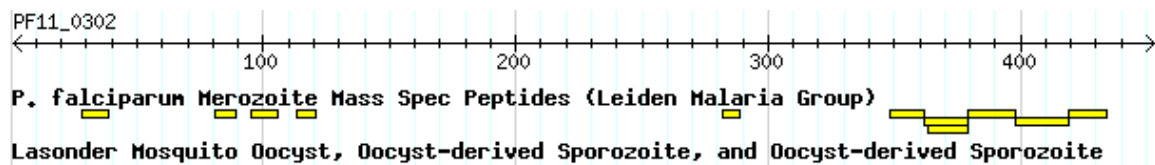
23508210



1114736 - 1129507 (14771 bases shown, positive strand)

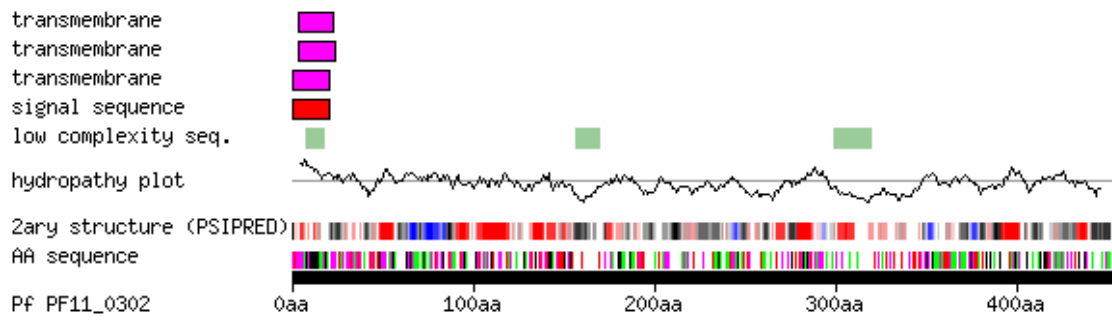


B

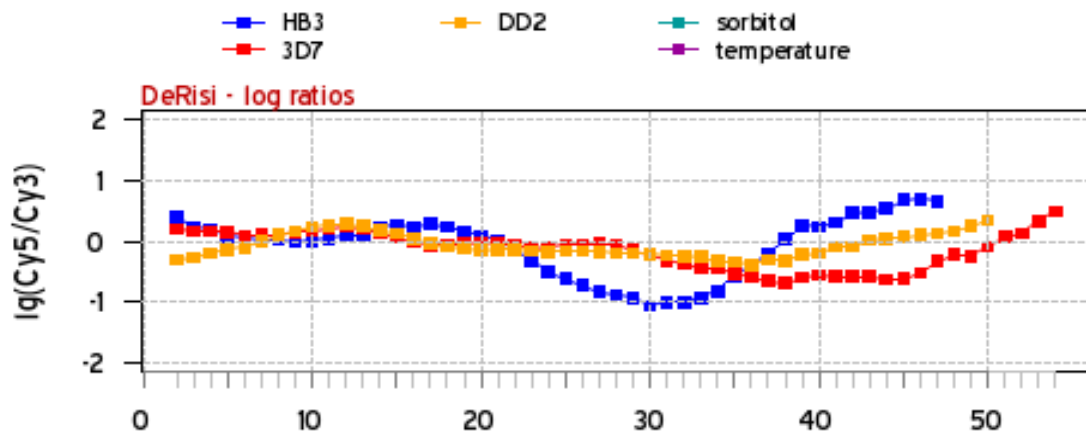


Introduction

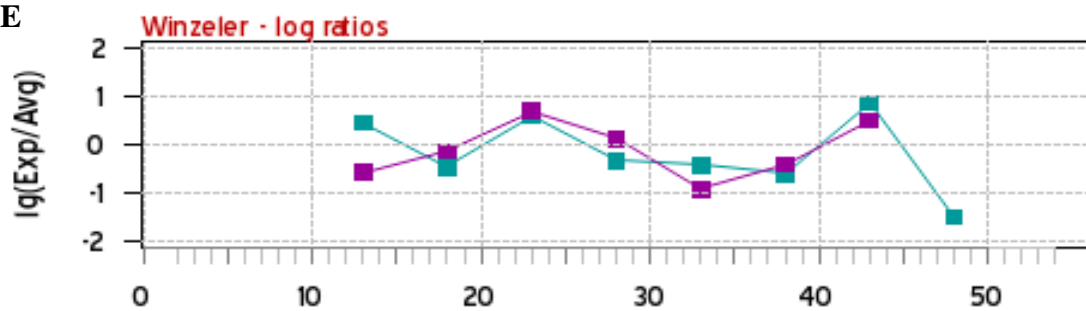
C



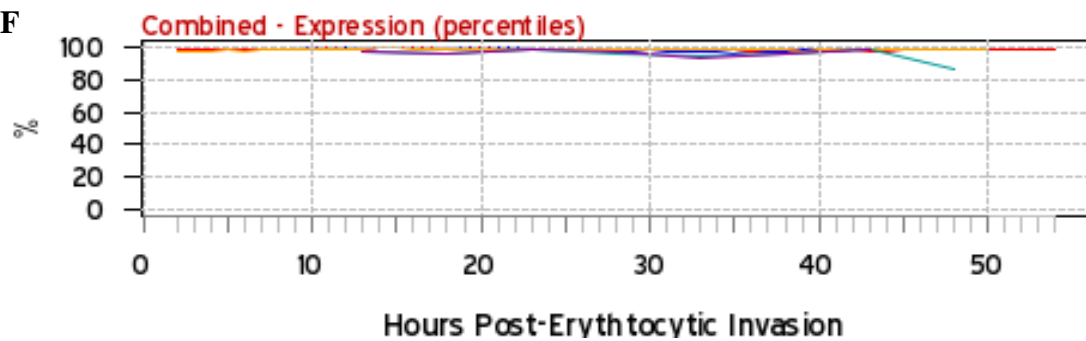
D



E



F



G

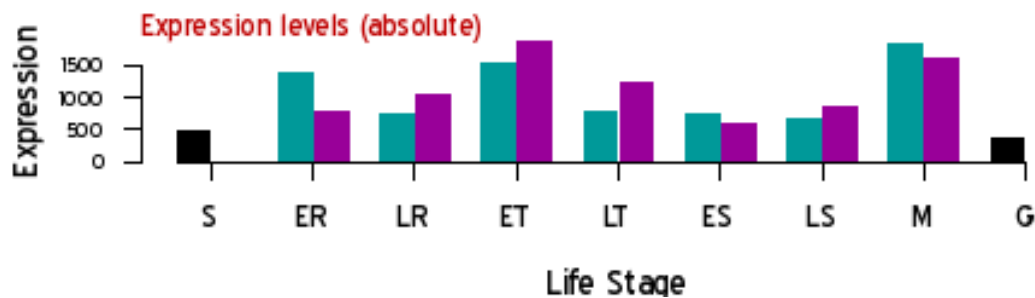


Figure 1.5: PfPV1, a conserved hypothetical protein encoded by PF11_0302. (A), Genome browser of PF11_0302 gene (GenBank: XM_001347937) on chromosome 11 (graphic from NCBI). The neighbouring genes PF11_0300, PF11_0301 and PF11_0303, PF11_0304 were also displayed on the map. (B), Peptides of PfPV1 were detected from mass spectrometry data of free merozoites (Aurrecochea *et al.*, 2009). (C), Protein features of PfPV1, graphic from PlasmoDB 4.4. (D), Expression profile of PF11_0302 gene, data from glass slide oligo array (Bozdech *et al.*, 2003a) on 3 different *P. falciparum* strain: HB3, 3D7 and Dd2, color specific for each strain as depicted on the graphic; y-axis, averaged smoothed normalized log (base 2) of cy5/cy3 for PF11_0302. (E), Expression profile of PF11_0302 based on data from photolithographic oligo array (Le Roch *et al.*, 2003), color specific for studies on Sorbitol- or Temperature-synchronized 3D7 strain parasites as depicted on the graphic; y-axis, log (base 2) ratio of Affymetrix MOID expression value (normalized by experiment) to average MOID value for all time points for a gene. (F), Expression intensity percentile, the y-axis gives the percentile of PF11_0302 gene expression intensity in the spectrum of all other genes' expression intensities for that time point. For all (D), (E) and (F), x-axis is time in hours post invasion. (G), Expression value of PF11_0302 normalized by Affymetrix MOID experiment (Le Roch *et al.*, 2003). Graphs of (D) – (G) were from PlasmoDB 5.5 (Aurrecochea *et al.*, 2009).

2. Materials and Methods

2.1. Materials

2.1.1. Equipment

Agarose gel chambers	Gibco BRL, Neu-Isenburg
Autoclave 3870ELV	Tuttnauer
Biofuge fresco	Heraeus, Hanau
Biofuge pico	Heraeus, Hanau
Blotting apparatus	Phase, Lübeck
BD Falcon™ centrifuge tube	Sarstedt, Nümbrecht
Centrifuge 5804R	Eppendorf, Hamburg
Centrifuge mikro 22R	Hettich Zentrifugen,
Digital camera EDAAS 120	Kodak, Japan
Drying machine	Heraeus, Hanau
Eppendorf reaction tubes	Eppendorf, Hamburg
Erlenmeyer flask	Kobe, Marburg
Exposition cassettes	Rego, Augsburg
Flow Hera safe	Heraeus, Hanau
Gene-Pulser II	BIO-RAD, UK
Glass slides	IDL, Nidderau
Hybridization oven 6/12	UniEquip, Leipzig
Ice machine AF-20	Scotsman
Incubator shaker G25	New Brunswick Scientific, USA
Macintosh power PC 7500/100	Apple Macintosh, USA
Magnetic bubbler Combimag RCH	IKA, Staufen
Medical X-Ray film	Fuji, Japan
Nitrocellulose membrane	Schleicher & Schuell, Dassel
Nylon hybridisation membrane, Hybond-N+	GE Healthcare, UK
Pasteur pipettes	COPAN, Italy
PCR reaction tubes	Sarstedt, Nümbrecht
Personal cycler	Biometra, Göttingen
pH-meter 766	Calimatic, Mering
Pipette tips	Greiner, Frickenhausen
Plastic petri dishes	Greiner, Frickenhausen

Materials and Methods

Plastic pipettes	Greiner, Frickenhausen
Power supply 2103 LKB	Biochrom, USA
Printer stylus photo 700	Epson
Uno-Thermoblock	Biometra, Göttingen
Vortexer Reax 2000	Heidolph, Schwabach
Waterbath	Köttermann, Uetze/Hänigsen
Weighing machine 1205 MP	Sartorius, Göttingen
Weighing machine P1200	Mettler, Gießen
Whatman-paper	Schleicher & Schuell, Dassel

2.1.2. Chemicals

Agarose low EEO	Roth, Karlsruhe
Ampicillin	Roth, Karlsruhe
Ammoniumpersulfat (APS)	Roth, Karlsruhe
Albumax	Invitrogen, Groningen
Bromophenol blue	Merck, Darmstadt
Calcium chloride	Roth, Karlsruhe
Carbenicillin	Roth, Karlsruhe
Chloroform	Merck, Darmstadt
Cresol red	Sigma, Taufkirchen
[alpha-P ³²]Deoxyadenosine 5'-triphosphate ([alpha-P ³²]dATP)	Hartmann Analytic, Braunschweig
DNA labeling kit, HexaLabel Plus	Fermentas, Germany
Deoxyribonucleic acid type III	Sigma-Aldrich, Schnelldorf
Diethyl pyrocarbonate (DEPC)	Fluka, Neu-Ulm
Dimethyl sulphoxide (DMSO)	Fluka, Neu-Ulm
1,4-dithio-DL-threitol (DTT)	Fluka, Neu-Ulm
Di-potassium phosphate	Roth, Karlsruhe
Ethanol p.a. (EtOH)	Applichem, Darmstadt
Ethidiumbromid (EtBr)	Sigma, Taufkirchen
Ethylendiamintetra-acetic acid (EDTA)	Sigma, Taufkirchen
Ethylene glycol-bis-(beta-aminoethylether)	
N,N,N',N'-tetra acetic acid (EGTA)	Roth, Karlsruhe

Materials and Methods

Glucose	Merck, Darmstadt
Guanidine hydrochloride	Roth, Karlsruhe
Glycine	Roth, Karlsruhe
Glycerol	Applichem, Darmstadt
Hydrogen peroxide	Fluka, Neu-Ulm
Hydrochloric acid	Roth, Karlsruhe
Hydroquinone	Roth, Karlsruhe
1 kb+ DNA ladder	Invitrogen, Groningen
Isopropanol	Roth, Karlsruhe
LB-agar (Lennox)	Roth, Karlsruhe
Magnesium chloride	Roth, Karlsruhe
Manganese chloride	Fluka, Neu-Ulm
Methanol	Merck, Darmstadt
[S ³⁵] L-Methionine	Hartmann Analytic, Braunschweig
Mono-potassium phosphate	Roth, Karlsruhe
Milk powder	Serva, Heidelberg
NNN'-N-tetra methylene ethylene diamine (TEMED)	Fluka, Neu-Ulm
Nutrient-broth	Roth, Karlsruhe
Pepton	Roth, Karlsruhe
Phenol/chloroform/isoamyl alcohol (25/24/1)	Roth, Karlsruhe
p-coumaric acid	Sigma, Taufkirchen
Ponceau S	Serva, Heidelberg
Potassium acetate	Applichem, Darmstadt
Potassium bromide	Applichem, Darmstadt
Potassium chloride	Merck, Darmstadt
RostisolV®HPLC Gradient Grade Water	Roth, Karlsruhe
Rotiphorese®Gel 30	Roth, Karlsruhe
Saponin	Roth, Karlsruhe
SDS-PAGE standard high range	Bio-Rad, München
SDS-PAGE standard low range	Bio-Rad, München
Sodium carbonate	Roth, Karlsruhe
Sodium chloride	Roth, Karlsruhe
Sodium dodecyl-phosphate	Roth, Karlsruhe

Materials and Methods

Sodium hydroxide (NaOH)	Merck, Darmstadt
Sodium sulphite	Roth, Karlsruhe
Sorbitol	Roth, Karlsruhe
Sucrose	Roth, Karlsruhe
Trichloroacetic acid	Roth, Karlsruhe
Tris	Applichem, Darmstadt
Yeast extract	Roth, Karlsruhe

2.1.3. Antibodies and working concentration

Mouse anti-GFP	Roche Diagnostics, Mannheim
Rabbit anti-mouse, Horse Radish Peroxidase (HRP)	DAKO, Glostrup, dilution 1:1000
Rabbit anti-mouse, Alkaline Phosphatase (AP)	DAKO Glostrup, dilution 1:2000
Goat anti-rabbit, AP	DAKO Glostrup, dilution 1:2000
Goat anti-rabbit, HRP	DAKO Glostrup, dilution 1:2000
Rabbit anti-SERP	(Ansorge <i>et al.</i> , 1996)
Rabbit anti-PV1	(Nyalwidhe and Lingelbach, 2006)
Goat anti-GST	GE Healthcare, 1:2000

2.1.4. Enzymes

Restriction Enzymes (RE)

All REs were from New England Biolabs (NEB): *AvrII*, *BamHI*, *BglII*, *EcoRI*, *KpnI*, *NheI*, *NotI*, *PvuII*, *SpeI*, *XbaI*, *XhoI*, *XmaI*.

Other enzymes

DNase I	Applichem, Darmstadt
RNase	Roth, Karlsruhe
Klenow fragment, DNA polymerase I	NEB
KOD polymerase	Novagen, Darmstadt
Phusion high-fidelity polymerase	Finnzymes, Espoo Finland
Taq polymerase	NEB
Superscript III reverse transcriptase	Invitrogen, Groningen
T4-DNA-Ligase	Invitrogen, Groningen

Materials and Methods

2.1.5. Molecular biological kits and reagents

Eppendorf gel extraction kit	Eppendorf, Hamburg
Seqlab miniprep kit	Seqlab, Göttingen
QIAEX II gel extraction kit	Qiagen, Hilden
QIAGEN plasmid maxi kit	Qiagen, Hilden
QIAprep spin miniprep kit	Qiagen, Hilden
TRIzol reagent	Invitrogen, Karlsruhe

2.1.6. Cell culture materials

Albumax	Invitrogen, Karlsruhe
Blasticidin S	InvivoGen, San Diego, USA
Ganciclovir	InvivoGen, San Diego, USA
Gelafundin	B. Braun AG, Melsungen
Gentamycin	PAA, Pasching, Austria
Giemsa	Merck, Darmstadt
Human erythrocyte concentrate (A/rh ⁺)	Uni-clinical centre Marburg
Human plasma (A/rh ⁺)	Uni-clinical centre Marburg
Hypoxanthine	PAA, Pasching, Austria
RPMI 1640	Gibco, Karlsruhe
RPMI 1640	PAA, Pasching, Austria
WR99210	Jacobus Pharmaceuticals

2.1.7. Cells and organisms

Strain	genotype	reference
<i>E. coli</i> DH5 α	<i>supE44</i> Δ <i>lacU169</i> (Φ 80 <i>lacZ</i> Δ M15) <i>hsdR17</i> <i>recA1</i> <i>gyrA96</i> <i>thi-1</i> <i>relA1</i>	Hanahan 1983; Bethesda Research Laboratories 1986
<i>E. coli</i> PMC103	<i>mcrA</i> Δ (<i>mcrBC-hsdRMS-</i> <i>mrr</i>)102 <i>recD</i> <i>sbcC</i>	Doherty, Lindeman <i>et. al.</i> , 1993
<i>E. coli</i> BL21-CodonPlus-RIL	<i>E. coli</i> B F ⁻ <i>ompT</i> <i>hsdS</i> (r _B - m _B -) <i>dcm</i> ⁺ Tet ^r <i>gal</i> <i>endA</i> Hte [<i>argU</i> <i>ileY</i> <i>leuW</i> Cam ^r]	Stratagene

Materials and Methods

<i>P. falciparum</i> 3D7	isolated in the Netherlands	The Walter and Eliza Institute of Medical Research, Melbourne, Australia
Transfected <i>P. falciparum</i>	various transfection	This study

2.1.8. Media and solutions

2.1.8.1. Solutions for protein-based experiments

Acrylamide solution

30% (w/v) Acrylamide

0.8% (w/v) Bisacrylamide

Ammonium peroxy-sulphate (APS)

10% APS in ddH₂O

Alkaline phosphatase (AP) buffer

100 mM Tris-HCl, pH 9.5

100 mM NaCl

5 mM MgCl₂

AP developing solution

66 µl NBT(nitro blue tetrazolium) stock solution

33 µl BCIP(5-bromo-4-chloro-3-indolyphosphate) stock solution

BCIP stock solution

5% BCIP in Dimethylformamide

Blocking solution

Stored at -20°C

5% milk powder in PBS, pH 7.4

Materials and Methods

Colloidal coomassie staining solution

0, 08% coomassie brilliant blue G250 (CBB G250)

1, 6% ortho-phosphoric acid

8% ammonium sulfate

20% methanol

Electrophoresis buffer

0.124 M Tris

0.96 M Glycin

0.05 % SDS

Enhanced chemiluminescence solution (ECL)

50 mM luminol in DMSO

0.8 mM p-coumaric acid in DMSO

200 mM Tris/HCl, pH 8.8

0.01% H₂O₂

Glycin buffer

100 mM glycine in PBS, pH 7.6

NBT stock solution

5% NBT in 70% dimethylformamide

Phosphate buffered saline, pH 7.4 (PBS)

140 mM NaCl

2.7 mM KCl

1.5 mM KH₂PO₄

8.1 mM Na₂HPO₄

Ponceau red staining solution

0.2% ponceau S

3% trichloroacetic acid

Materials and Methods

Protease inhibitor cocktail stock solution

200 µg/ml of each of the inhibitors antipain, chymostatin, aprotonine, pepstatin, trypsin, leupeptin, elastinal and Na-EDTA in PBS. Working solution 1:200 dilution

2 X SDS-PAGE: sample buffer (reducing), stored at 4°C

100 mM Tris/HCl, pH 6.8

5 mM EDTA

20% glycerol

4% SDS

0.2% bromophenol blue

100 mM DTT

4x Separating gel buffer

1.49 M Tris/HCl , pH 8.8

0.4% SDS

4x Stacking gel buffer

500 mM Tris/HCl, pH 6.8

0.4% SDS

Western blot transfer buffer

48 mM Tris/HCl, pH 9.5

39 mM glycine

0.0375% SDS

20% methanol

2.1.8.2. Solutions for DNA-based experiments

Agarose

0.8 to 1.5% agarose dissolved in 1x TAE

Buffer A for DNA extraction

50 mM NaOAC, pH 5.2

100 mM NaCl

Materials and Methods

1 mM EDTA

Cresol red loading buffer pH 8,8

36% sucrose

0.1 g cresol red

6x DNA loading buffer

1% bromophenol blue

30% glycerol

50 mM Tris/HCl, pH 8.0

5 mM EDTA

1 kb+ DNA ladder

1 volume 1kb⁺ DNA ladder

19 volumes 6x DNA loading buffer

DNA purification solutions

Merlin I

50 mM Tris/HCl, pH 7.5

10 mM EDTA

100 µg/ml RNase

Merlin II

0,2 M NaOH

1% SDS

Merlin III

1 M potassium acetate (KOAC)

35.7 ml glacial acetic acid

Merlin IV

66.84 g guanidine hydrochloride in 33.3 ml Merlin III

Stir, gently heat 5 to 10 min

pH adjusted to 5.5 with NaOH

Materials and Methods

Merlin V

200 mM NaCl

20 mM Tris/HCl pH 7.5

5 mM EDTA

50% EtOH

PFGE lysis buffer

0.5 M EDTA

10mM Tris/HCl, pH 8.0

1% sarkosyl

2 mg/ml proteinase K (proteinase K added fresh just prior to use)

3M sodium acetate (NaOAc) pH 5.2

Southern blotting hybridisation buffer

Depurination

0.2 N HCl: 17 ml concentrated HCl in 1 liter dH₂O

Denaturation

1.5 M NaCl

0.5 M NaOH

For 1 liter solution

87.6 g NaCl

100 ml 5M NaOH or 50 ml of 10M NaOH

Store at RT up to 3 months

Neutralisation

1 M Tris pH 7.4

1.5 M NaCl

For 1 liter solution

87.6 g NaCl

122.1 g Tris base

pH to 7.4

Materials and Methods

20X SSC

3M NaCl

0.3M sodium citrate

pH 7.0

10X SSC for transfer

6X SSC for fixation

Hybridisation/Pre-hybridisation buffer

6X SSC

5X Denhardt's solution

0.5 % SDS

50 % formamide

Filter through 0.45µm membrane

Add freshly 100 µg/ml salmon sperm DNA (SIGMA, DNA sodium salt from salmon testes, product number D1626, CAS # 9007-49-2)

Washing solutions

Wash 1 2X SSC, 0.1% SDS

Wash 2 0.1X SSC, 0.1 % SDS

50x TAE

2 M Tris

2 M acetic acid

50 mM EDTA

TE

10 mM Tris

1 mM EDTA

pH 7.4 to 8.0 depending on the purpose

2.1.8.3. Bacteriological media

LB (Luria-Bertani) agar

35 g/l LB-agar

Materials and Methods

Superbroth, pH 7.0

35 g/l pepton

20 g/l yeast extract

5 g/l NaCl

SOC-medium

20 g/l peptone

5 g/l yeast extract

10 mM NaCl

2.5 mM KCl

autoclaved

20 mM MgCl₂

20 mM glucose

Media were sterilised by autoclaving and allowed to cool to 50°C. Appropriate antibiotics were then added to a final concentration of 50 µg/ml.

Antibiotics

	<i>Stock</i>	<i>working concentration</i>
Ampicillin (sodium salt)	50 mg/ml	50 µg/ml
Carbenicillin	50 mg/ml	50 µg/ml
Chloramphenicol	34 mg/ml	34 µg/ml

2.1.8.4. Media and solutions for parasite culture and transfection

Antibiotics for selectable markers

WR99210

a) *20 mM WR99210 stock solution*

8.6 mg WR99210 in 1 ml DMSO, stored long term at -70°C

b) *WR99210 working solution*

Dilute 1/1000 in RPMI-Hepes (= 20 µM). Filter sterilise, store at -70°C or stable for 1 month at 4°C.

Recommended working concentration: 5 nM (3 µl of working solution in 12 ml culture medium).

Materials and Methods

Blasticidin S hydrochloride

Stock solution from supplier: 10 mg/ml, stored at -20°C.

Working concentration 4 µg/ml

Ganciclovir

From the manufacture's instruction (Invivogen), ganciclovir is only soluble at pH ≥ 12.

Stock solution at 20 mM

51 mg ganciclovir in about 8 ml water, adjust to pH 12 with 1 M NaOH, complete dissolve Ganciclovir.

Lower pH to 10.7 ~ 11 with HCl.

Fill up with water to 10 ml solution.

Filter sterilise, aliquot and store at -70°C or stable up to 1 month at 4°C.

Working concentration: 20 µM (dilute 1/1000 of stock solution into culture medium).

Cytomix stock buffers

Cytomix was adapted from Van den Hoff (van den Hoff *et al.*, 1992).

- a) 10 M KOH
- b) 250 mM Hepes/20 mM EGTA
5.96 g Hepes (free acid)
0.76 g EGTA
To 80 ml with ddH₂O
pH to 7.6 with 10 mM KOH (~ 1,4 ml)
to 100 ml with ddH₂O
- c) 10ml 1 M phosphate buffer pH 7.6
8.66 ml 1M K₂HPO₄
1.34 ml 1 M KH₂PO₄

Cytomix 100 ml, Stored at 4°C

- 6 ml 2 M KCl
- 7.5 µl 2M CaCl₂
- 1 ml 1 M K₂HPO₄/KH₂PO₄

Materials and Methods

10 ml of 250 mM Hepes/20 mM EGTA pH 7.6

500 µl 1M MgCl₂

To 90 ml with ddH₂O

sterilised filter

Freezing solution

28% glycerol

3% d-sorbitol

0.65% NaCl

RPS medium

500ml RPMI 1640 medium (PAA or Gibco)

Supplement with:

50ml of heat-inactivated human plasma or 50ml of 5% albumax

20 µg/ml gentamycin

200 µM hypoxanthine

5% Sorbitol

Dissolve 5 g sorbitol in 100 ml water, filter sterilise and store at 4°C.

Thawing solutions

Sterile 12% NaCl

Sterile 1.6% NaCl

Sterile 0.9% NaCl + 0.2% glucose

Malaria culture medium (RPS)

2.1.9. Plasmids

Table 1. List of plasmids used in this study

Plasmid	Resistance	Features	Reference
pARL2	WR99210 Ampicillin	Basic vector	(Przyborski <i>et al.</i> , 2005)
pARL2-GFP	WR99210 Ampicillin	GFP expression, <i>hDHFR</i> cassette	(Przyborski <i>et al.</i> , 2005)

Materials and Methods

pARL-BSD-GFP	Blasticidin S Ampicillin	<i>hDHFR</i> was removed, replaced by <i>bsd</i> cassette GFP expression	Przyborski, (personal communication)
pHTK	WR99210 Ampicillin	Basic vector Ganciclovir sensitive For double-crossover recombination	(Duraisingh MT, 2002)
pHTK-ΔPV1-3	WR99210 Ampicillin	Ganciclovir sensitive Containing 3'-flank region of PF11_0302	
pHTK-ΔPV1	WR99210 Ampicillin	Knock-out construct Ganciclovir sensitive Containing 2 flank regions of PF11_0302	This study
pARL-DHFR-PV1g	WR99210 Ampicillin	PV1-GFP fusion	This study
pARL-ΔPV1g	WR99210 Ampicillin	Knock-in construct Truncated PV1 fused with GFP is non-expressed in episomal form.	This study
pARL-mutPV1	WR99210 Ampicillin	Knock-in construct Mutated PV1 at very C-terminal end	This study
pARL-BSD-PV1g	BSD Ampicillin	For double transfection PV1-GFP fusion	This study
pGem-T-Easy		Subcloning vector	Promega, Madison USA
pGEX-5x-3	Ampicillin	Recombinant protein expression GST tag	GE Healthcare Life Sciences
pGEX-PV1	Ampicillin	GST-PV1 fusion protein	This study

2.1.10. Synthetic oligonucleotides

All oligonucleotides were synthesised from MWG-Biotech AG.

Table 2. List of PCR primers used in this study

Order	Primer name	Sequence 5' → 3'
Knock-out primers		
1	PV1-ko5F	CGGACTAGTGTGATTAAGAAAAAGAATTTAAAAT
2	PV1-ko5R	CGTAGATCTCTATTAGTTTTGATTCTTATTATGG
3	PV1-ko3F	GACGAATTCGGATCTCTGGAATCGGTAATGTTG

Materials and Methods

4	PV1-ko3R	GCGCCATGGGTTTATGTAAATATATACATATAG
Integration primers (for integration PCR)		
5	PV1-ig-5F	CAGCATTTGAATATTAATTAATC
6	PV1-ig-5F2	GCATCGTAAAATTATAGATATTTCTATG
7	PV1-ig-3R	TTTGAACATGGTCATATGTACTC
8	PV1-internalF	ACAAAGATCAACTTATGGACTTACC
9	PV1-internalR	AAGACATTACCTGATGAAGCATTAC
10	DHFR-ig5R	TTCTTGCCGATGCCCATGTTCTG
11	DHFR-pm-5R2	TTTATCATGCACATTGGAATAATAC
12	DHFR-ig3F	AAATATAAACTTCTGCCAGAATACCC
Primer specific for vectors and Southern blot probes		
13	DHFR probeF	AATTAGCAAATAAAGTAGAC
14	DHFR probeR	TTGTAATTTCTGTGTTTATG
15	pHTK-5F	GTATATATATATATATATATATAGGTATAG
16	pHTK-5R	GGTTAACAAAGAAGAAGCTCAGAGATTGCATG
17	pHTK-3F	AATTCATGTTTTGTAATTTATGGGATAGCG
18	pHTK-3R	GGCTTAACTATGCGGCATCAGAGCAGATTG
19	pHTK-backboneF	TAGACAGATCGCTGAGATAGG
20	pHTK-backboneR	TTGATCCGGCAAACAAACC
21	TK gene1	GGCCCGAAACAGGGTAAATAACG
22	TK gene2	CTTCCGAGACAATCGCGAACATC
23	pARL-F	CGTTAATAATAAATACACGCAG
24	pARL2-Not70-F	GCGGATAACAATTTACACAGG
25	pARL-R	CAGTTATAAATACAATCAATTGG
26	DHPS-F	GGTGGAGAATCCTCTGCTCC
27	DHPS-R	CCAATTGTGTGATTTGTCCAC
Knock-in primers/ GFP fusion		
28	PV1-XhoF	GGCTCGAGATGATTAATAAATAATTAGCTAGC
29	PV1-AvrR	GGCCTAGGGCTCGATATTGGTGTGTTTTGATC
30	dPV1-NotF	ATGCGGCCGCACAACCAGTAACGGATTTACATG
31	dPV1-XhoR	ATCTCGAGTTAACTCGATATTGGTGTGTTCTGGTC
Other primers		
32	PF11_0303F	TTTACAGCTACGGAAATTATATC
33	PF11_0303R	CTGTAATGTCTACCTAAATATCTATC
34	GFP-AvrF	TACCCTAGGATGAGTAAAGGAGAAGAAC
35	GFP-KpnR	GGCGGTACCTTTGTATAGTTCATCC
Recombinant protein expression primers		
36	PV1-GST-BamF	CAGGATCCACAATGTGGTGGCCCCCTAAGAG

Materials and Methods

37	PV1-GST-XhoR	CAGCTCGAGTTAGCTCGATATTGGTGTGTTTTG
----	--------------	-----------------------------------

2.2. Methods

2.2.1 Bioinformatics methods

For *in silico* analysis of proteins and nucleic acids the following programs were used:

Blast	http://ncbi.nlm.nih.gov/cgi-bin/BLAST
ClustalW	http://www.ebi.ac.uk/clustalw/ (Larkin <i>et al.</i> , 2007)
MyHITS	http://myhits.isb-sib.ch/cgi-bin/motif_scan (Hulo <i>et al.</i> , 2008)
MnM	http://mnm.engr.uconn.edu/MNM/SMSSearchServlet (Rajasekaran <i>et al.</i> , 2009)
OPI	http://chemlims.com/OPI/MServlet.ChemInfo (Zhou <i>et al.</i> , 2005)
PFP	http://dragon.bio.purdue.edu/pfp/ (Hawkins <i>et al.</i> , 2006)
ScanSite	http://scansite.mit.edu/motifscan_id.phtml (Obenauer <i>et al.</i> , 2003)
SignalP	http://www.cbs.dtu.dk/services/SignalP/ (Bendtsen <i>et al.</i> , 2004)
SMART	http://smart.embl-heidelberg.de/ (Schultz <i>et al.</i> , 1998)

Nucleic acid and protein sequences were downloaded from PlasmoDB (www.plasmodb.org) and ApiDB (www.apidb.org) (Aurrecochea *et al.*, 2009).

Primer designs and vector constructs were *in silico* confirmed in Clone Manager 7 (Sci Ed Central). Protein sequence alignment was followed ClustawW (Larkin *et al.*, 2007) with parameters of Gonnet series, the gap opening 10, gap extension 0.2.

2.2.2 Transfection of plasmid constructs

Plasmid constructs for transfection were cloned using the standard cloning strategy (Sambrook and Russell, 2001) into *E. coli* strain strain PMC103. For difficult constructs as pHTK-derived vectors, carbenicillin was used for selection of positive clones. A large number of colonies were screen by colony PCR. Plasmids from positive clones were confirmed by restricted digestion and automated sequencing.

2.2.2.1 pHTK- Δ PV1

Two DNA segments of approximately 1 kb from the *PfPVI* encoding gene (*PF11_0302*) were amplified from 3D7 genomic DNA and introduced into the flanking regions of the human *DHFR* (*hDHFR*) cassette to mediate the integration of the plasmid into the parasite genome (Fig. 2.1). Specifically, the 805 bp of 3-flank

Materials and Methods

segment of the *PF11_0302* was amplified by the primers PV1-ko3F 5'-GACGAATTCCGATCTCTGGAATCGGTAATGTTG and PV1-ko3R 5'-GCGCCATGGGTTTATGTAAATATATACATATAG. The amplified product encompasses 94 nucleotides of the encoding sequence as well as 711 nucleotides of un-translated region downstream of the natural stop codon. The DNA segment was inserted into *EcoRI/NcoI* digested pHTK vector to generate the pHTK Δ PV1-3 plasmid (restriction sites were typed in italic in the oligonucleotide sequences). The pair of primers PV1-ko5F 5'-CGGACTAGTGTGATTAAGAAAAAGAATTTAAAT-3' and PV1-ko5R 5'-CGTAGATCTCTATTAGTTTTGATTCTTATTATTGG-3' amplified the 5-flank segment of the *PF11_0302* gene. The underlined nucleotides in the PV1-ko5R primer are encoding two artificial stop codons. In case the single-crossover occurs it helps to prevent the expression of the full length *PfPV1*. The product of 844 bp includes 352 nucleotides of the 5' untranslated region, upstream of the PV1 start codon as well as the codons representing the first 164 amino acids of the translated proteins. The fragment was then inserted into *SpeI/BglII* – digested pHTK Δ PV1-3 vector to create the pHTK Δ PV1 construct. Note that the final pHTK Δ PV1 vector still retains the 5' to 3' direction of targeting sequence in respect of the drug resistance cassette.

2.2.2.2 pARL-DHFR-PV1g

This vector express PfPV1 protein fused with GFP, under the selection of hDHFR selectable marker. Full length encoding PfPV1 sequence without stop codon was amplified by RT-PCR, using the primer PV1-XhoF 5'-GGCTCGAGATGATTAATAATATTAGCTAGC and PV1-AvrR 5'-GGCCTAGGGCTCGATATTGGTGTGTTTTGATC. The amplified DNA fragment was ligated to *XhoI/AvrII*-restricted pARL2-GFP (Przyborski *et al.*, 2005) to create pARL-DHFR-PV1g plasmid.

2.2.2.3 pARL-BSD-PV1g

The sequence encoding the PV1-GFP fusion protein in vector pARL-DHFR-PV1g was placed between *XhoI* and *KpnI* restriction site. The DNA fragment was cleaved and inserted into *XhoI/KpnI*-restricted pARL-BSD plasmid (Przyborski, personal

Materials and Methods

communication), thus generating the pARL.BSD-PV1g plasmid which also expresses PV1-GFP fusion protein but resistant to BSD in stead of WR99210.

2.2.2.4 pARL- Δ PV1g

The basic vector for all pARL-derivative constructs was from pARL-1a (Crabb *et al.*, 2004). The vector contains the PfCRT promoter to drive the expression of the transgene. To create a knock-in parasite line, a truncated version of PfPV1 was generated so that the transgene could only be expressed upon integration into the PV1 locus. The pARL-DHFR-PV1g was digested by *NotI/NheI* to remove the region of the CRT promoter and the first 19 nucleotides of the *PfPV1* gene. Sticky ends of linear plasmids were filled in by Klenow activity of DNA polymerase I (NEB). Plasmid was circularised by T4 DNA ligase, creating the pARL- Δ PV1g construct. Successful removal of the promoter region was assured by automated sequencing.

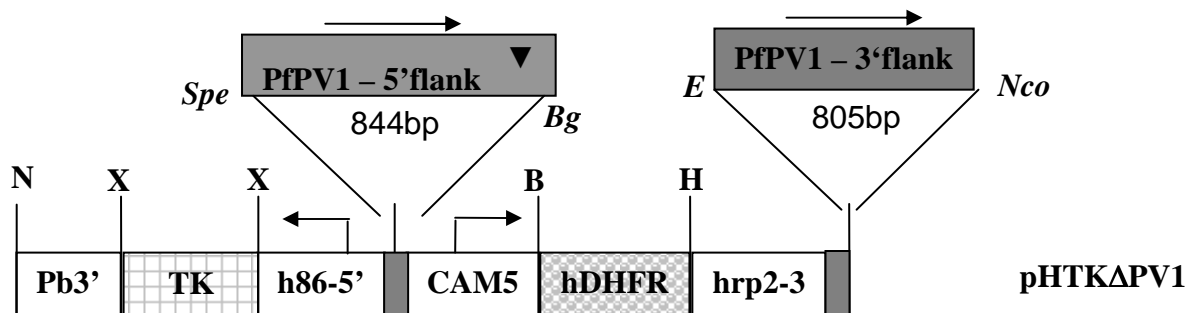
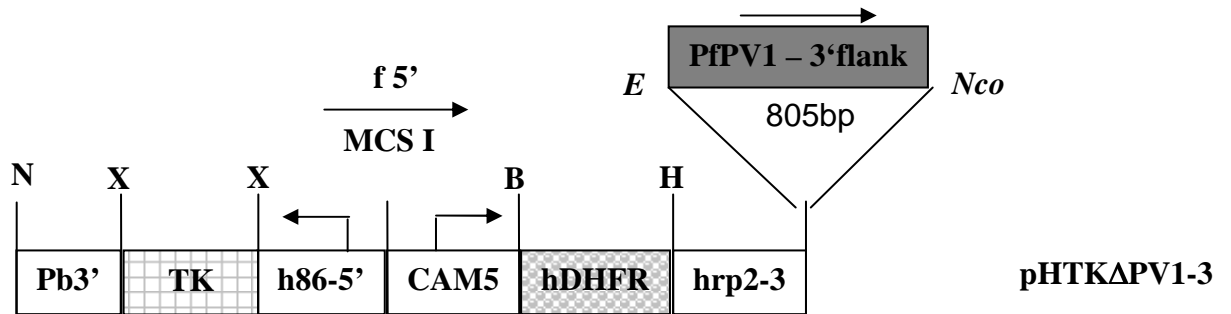
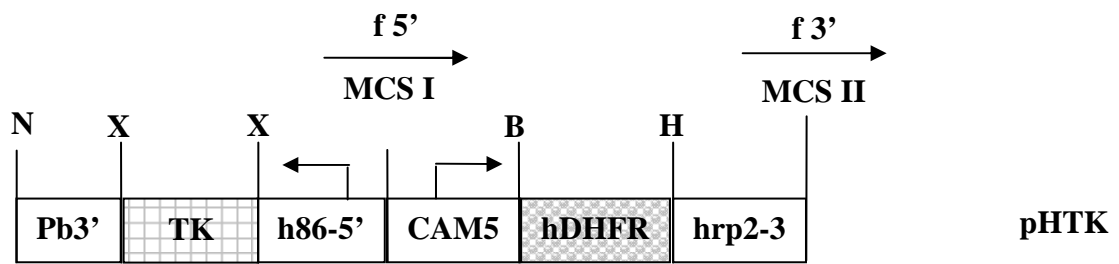
2.2.2.5 pARL-mutPV1

A truncated PV1 encoding fragment was created by primers dPV1-NotF 5'-ATGCGGCCGCACAACCAGTAACGGATTTACATG and dPV1-XhoR 5'-ATCTCGAGTTAaCTCGATATTGGTGTGTT**c**TG**g**TC. The italic nucleotides are restriction sites of *NotI* and *XhoI*, respectively. The underlined nucleotides represent the original stop codon. Bold, small letters are substituted nucleotides in silent mutations which result in codons for the same amino acids. Forward oligonucleotides were primed at nucleotide 205th of the PV1 encoding sequence, relevant to Thr69 residue of PV1 protein. The 1100 bp DNA product was digested and consequently ligated to *NotI/XhoI*-restricted pARL2 to create pARL-mutPV1 construct.

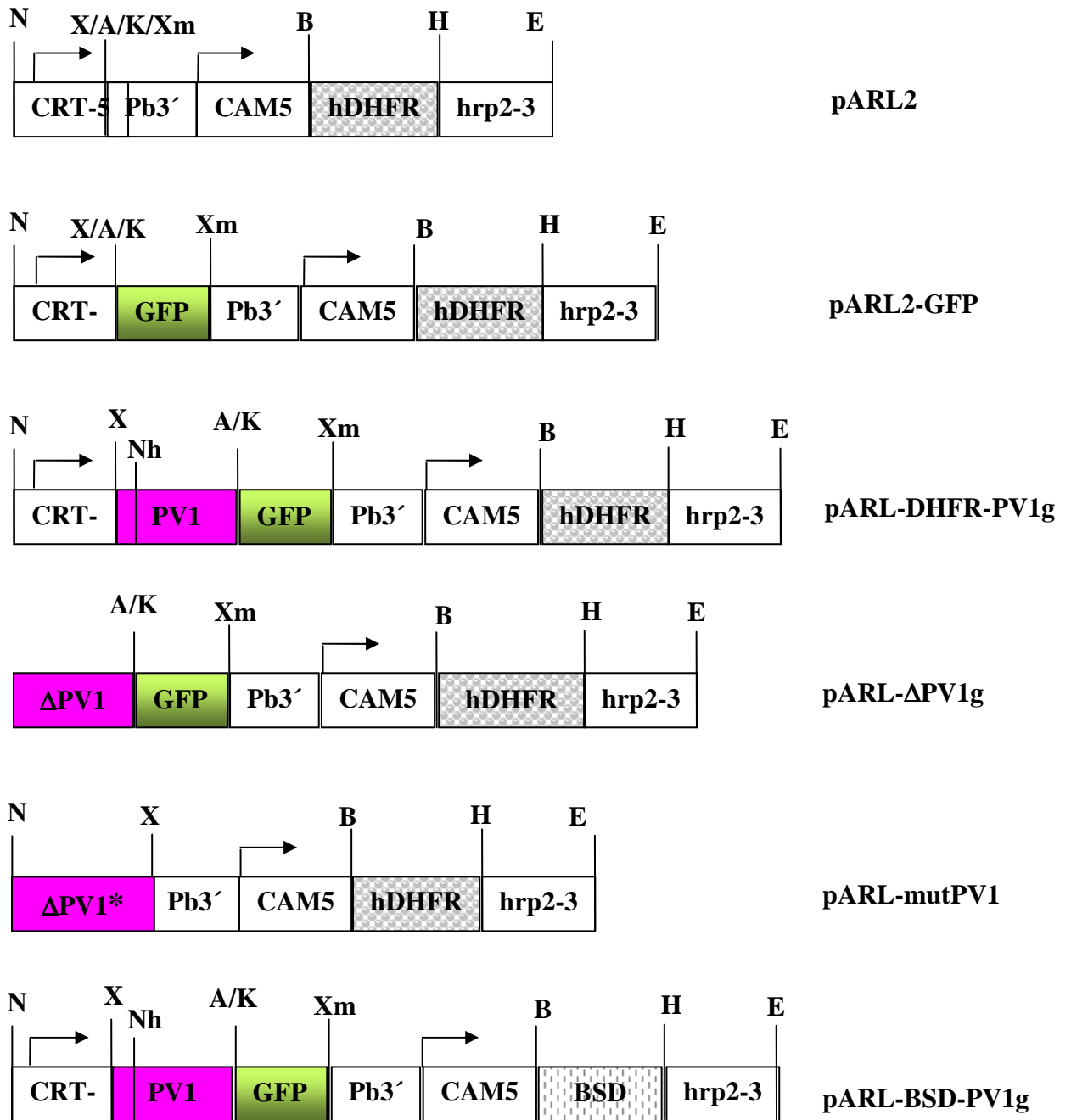
Figure 2.1: Vector maps for *P. falciparum* transfection plasmids

In all plasmids but pARL-BSD-PV1g, the hDHFR cassette is comprised of ~ 1kb of calmodulin (CAM) 5'- untranslated region (UTR), 0.56 kb *hDHFR* gene, and 0.6 kb *hrp2* 3'-UTR. In pARL-BSD-PV1g, the *hDHFR* gene was replaced by the *BSD* gene. **pHTK** is a double-crossover plasmid used for gene disruption (Duraisingh MT, 2002). The 5' and 3' target sequences need to be cloned into the multicloning sites (MSCI and MSCII), respectively, in the same direction of the *hDHFR* cassette, as shown by the arrows. From the 5' to 3' the MSCI are *MluI*, *SacII*, *SpeI*, *BglIII*, *HincII*, *HpaI*, and within the MSCII are *EcoRI*, *ClaI*, *NcoI*, *AvrII*, *BbeI*, *KasI*, *NarI*, and *SfoI*. The expression of *TK* gene is controlled by the *HSP 86* 5'-UTR and *P. berghei* 3' termination region of *DHFR-TS* gene. Note that the expression cassette is head-to-head orientation against the *hDHFR* cassette. Two flanking regions of PV1 encoding sequence was depicted in the two construct **pHTK Δ PV1-3** and **pHTK Δ PV1**, respectively. The black down-pointing triangle (\blacktriangledown) in the 5'-flanking fragment represents the premature stop codon. **pARL2** vector (Duraisingh MT, 2002; Przyborski *et al.*, 2005) is a basic vector used mainly for expression of GFP-tagged proteins. It uses a tail-to-head orientation of the expression cassettes to avoid the bidirectional influence of the CAM promoter on the expression of the gene of interest. The GFP fusion proteins are controlled by the *CRT* promoter and the *Pb* 3'-UTR as shown in **pARL2-GFP**, **pARL-DHFR-PV1g** and **pARL-BSD-PV1g** vectors. In **pARL- Δ PV1g** and **pARL-mutPV1**, the *CRT* promoter was removed so that the sequences of interest are only expressed under the endogenous promoter upon the integration into the targeting locus. The asterisk (*) in the truncated Δ PV1 region indicates the modified nucleotides at the 3'-end sequence. Restriction sites used in cloning include *NotI* (N), *XhoI* (X), *AvrII* (A), *KpnI* (K), *XmaI* (Xm), *NheI* (Nh), *BamHI* (B), *HindIII* (H), *EcoRI* (E), *NcoI* (Nco), *SpeI* (Spe) and *BglIII* (Bg).

Materials and Methods



Materials and Methods



2.2.3 Parasite

2.2.3.1 Parasite culture

P. falciparum parasites (strain 3D7 or transfected strains) were cultivated in RPS following the standard procedure (Trager and Jensen, 1976), with either human A+ or O+ erythrocytes, depending on the ensuing experiments. The parasitemia was observed regularly by Giemsa-stained smears under microscopy and the infected erythrocytes were replaced by fresh human erythrocytes when culture reached a maximum of 10% parasitemia at the latest. Media was changed regularly and parasite cultures were gassed with 5% CO₂, 5% O₂ and 90% N₂ and incubate at 37°C. Parasite were synchronised by 5 % sorbitol at ring stage (Lambros and Vanderberg, 1979). Trophozoites-infected erythrocytes were enriched to a parasitemia higher than 90% by gelafundin floatation (Pasvol *et al.*, 1978).

2.2.3.2 Parasite transfection

Synchronised ring stage parasites with a parasitemia of 5 to 10% were used for transfection. To synchronise the culture, parasites were either treated with gelafundin one day prior to transfection or with Sorbitol two days prior to transfection. Cell pellet from 5 ml of culture (app. 200 µl) in addition of 200 µl fresh blood (O⁺, donated by Jude M. Przyborski or Nina Gehde) were required for each transfection. A large amount of plasmid DNA was required for transfection of *P. falciparum*, at least 50 µg of the vector (usually 80 - 100 µg). DNA was precipitated in ethanol and the pellet was dried in a laminar flow hood to assure the sterilised condition. After DNA was fully dissolved in 30 µl of sterile TE (pH 8.0), 385 µl sterile Cytomix was added. The Cytomix/plasmid sample was mixed with the parasitized erythrocyte pellet and transferred to a 0.2 cm Gene Pulser cuvette (BioRad). Electroporation was carried out at 0.310 kV and 950 µF (high capacitance). The resulting time constant should have a magnitude between 7 and 12 msec. After electroporation the cells were immediately transferred to a culture flask containing 12 ml prewarmed RPS and 400 µl fresh blood (O⁺). Four to six hours post transfection drug selection with WR99210 (WR) was started. 3 µl of 20 µM WR were added daily the first 5 to 6 days until no more parasites were visible. Accordingly the culture was fed twice a week with the same concentration of WR (5 nM) and media changes were carried out. Every two days the culture was checked for living parasites *via* Giemsa-stained smears. Fresh RBS was added once a week (~100 µl). As soon as parasites were visible (average 21-30 days)

Materials and Methods

three 1 ml aliquots containing predominantly ring stage parasites with a parasitemia of at least 2% were resuspended in 1 ml freezing solution and immediately frozen in liquid nitrogen.

For double transfection, parasites already bearing the pHTK Δ PV1 episomally were co-transfected with pARL-BSD-PV1g following the standard protocol above. The double transfected parasites (db-transfected) were put under drug selection of both 5 nM WR and 4 μ g/ml blasticidin (Invivogen). Parasites resistant to both drugs were first visible on Giemsa-stained smears after 21 days.

2.2.3.3 Drug selection of integrated plasmid containing parasites

For negative selection of pHTK Δ PV1-transfected parasites with the purpose of double-crossover homologous recombination, 20 μ M of ganciclovir was added to the WR99210 resistant population. The WR selection continues during ganciclovir treatment. Three batches of cell culture were carried out independently in parallel in attempt of obtaining the integrant. Parasites mostly died after adding ganciclovir and were visible again in Giemsa-stained smears at various times in different cultures (12 days or 40 days or unable to recover, respectively). The recovered parasites were cultured until parasite growth was firmly established.

In another approach to select parasites with the plasmid vector integrated by homologous recombination, the pHTK Δ PV1-transfected parasites were grown for 3 weeks without positive drug selection (WR) then reapplied drug pressure and continued to culture until parasites reappeared in the Giemsa-stained blood smears. The on and off drug cycling could be extended to 3 or more cycles until no parasite death was observed after the addition of WR.

For the double transfected parasites, on the background of WR and blasticidin-S resistance, 3 cycles of WR selection were applied as describe above. Genomic DNA was extracted at each cycle. After the 3rd cycle, two independent populations were separated. The db-transfected A population was merely put under WR and blasticidin-S selection and the db-transfected B population was negatively selected by adding ganciclovir as above. The B parasites re-appeared after 10 days in the presence of 3 different drugs: 5 nM WR, 4 μ g/ ml blasticidin-S and 20 μ M ganciclovir.

Materials and Methods

All parasites from the attempted homologous recombination studies were in mixed population and these cultures were cloned by limiting dilution (Rosario, 1981) before further analysed by Southern Blotting to determine if integration into the relevant gene had been obtained.

2.2.3.4 Parasite cloning by limiting dilution

The transfected parasite culture was a mixed population of episomal plasmid and the integrated plasmid-containing parasites. Single clones were picked up via limiting dilution in a 96-well microtitre plate at a dilution of 0.3 parasites per well (Rosario, 1981). Briefly, the parasitemia of ring stage cultures were calculated, the number of RBC per μl culture was counted using a Neubauer hemocytometer and the number of parasites per μl of cell culture suspension was then determined. The dilution of cell culture suspension was added to the fresh RPS so that approximately 30 parasites were seeded into the 96-well microplate. Fresh medium and 8 μl of RBC per well were fed every week. Parasite growth was monitored after 2 to 3 weeks by Giemsa-stained smear. The positive clones were eventually transferred to 5ml and later to usual culture volume. Considering the time from the start, 4 to 5 weeks were required to establish a firmly culture for a single parasite clone.

2.2.4 Monitoring transfectants: genetic analysis

2.2.4.1 PCR analysis

For the detection of the expected homologous integration event, a quick screening method was first performed using the combination of various primers (see the primer map (Figure 3.5 in Result section). The same basic PCR master mix comprised of *Taq* polymerase, 20 pmol of each primer in diverse combination, 200 μM of each dNTP in suitable PCR buffer was used for different templates. Typically, 1 μl of genomic DNA was used for a 50 μl -volume PCR reaction. The basic PCR program run through 35 cycles of 95°C/30 sec, 50°C/30 sec and 68°C/2 min 30 sec. Optimised conditions were also tested, using different polymerases, increasing concentration of PCR components such as Mg^{2+} , primers, DNA template or changing time requiring for each step.

2.2.4.2 Southern blot analysis

Various DNAs were double digested with *Xba*I and *Eco*RI or *Nhe*I and *Pvu*II then proceeded for Southern blotting (SB) hybridisation with different probes, using the standard SB protocol (Sambrook and Russell, 2001; Southern, 1975). Generally, 10 µg of genomic DNA and 10 units of each RE (New England Biolab) were used in the double digestion in 100 µl total volume, incubated overnight or 16 hours at 37°C. Frequently two probes were required for an identical blot, hence samples were arranged in favor of duplicate lanes in the same gel. The 10 µg digested genomic DNAs were split into 2 distant lanes on a 0.8% agarose gel at 5 µg per slot. If the number of samples exceeded the available wells, a second gel was prepared.

Gel electrophoresis was run overnight or 16 hours at 17 Voltages. After staining with Ethidium Bromide (EtBr), the stained gel was aligned with a transparent ruler and photographed under UV illumination. The gel was then depurinated in 0.125 M HCl for 20 min, denatured in denaturation buffer (0.5M NaOH, 1.5 M NaCl) for 30 min, neutralised in neutralisation buffer (0.5 M Tris pH 8.0, 1.5 M NaCl) for 30 min, changed into the new neutralisation buffer and continued soaking in 15 minutes. DNAs on the gel were then blotted onto a pre-wet Hybond-N+ membrane (GE Healthcare) in 10X SSC overnight. DNA fixation on the membrane was carried out by baking at 80°C for 2 hours. The membrane was wrapped by SaranWrap and stored at 4°C until needed.

Pre-hybridisation was carried out in a roller bottle at 0.1 ml hybridisation buffer per 1 cm² of membrane at 42°C for at least 2 hours. During the pre-hybridisation, the probes were labelled with [α -³²P]-dATP by HexaLabel Plus kit (Fermentas) following the manufacturer's protocol. The probes were added to the fresh hybridisation buffer at 10-20 ng/ml or 0.5 – 2 × 10⁶ incorporated counts per ml solution. The membrane was hybridised overnight at 42°C with gentle agitation. After the hybridisation, the blot was washed 3 times of 20 min/ RT in Washing solution 1 (2X SSC, 0.1% SDS), followed by 2 times of 20 min/50°C in Washing solution 2 (0.1X SSC, 0.1% SDS). From the last stringency wash, the blot was wrapped in Saran Wrap and exposed to X-Ray film.

Materials and Methods

If re-probing was required, the blot was re-used by hot SDS stripping protocol (GE Healthcare's instruction). The boiling solution of 0.1% SDS was poured onto the blot and allowed to cool. This step was repeated at least 3 times. The removal of the probe was checked by exposing the stripped blot to X-Ray film for 1 week. If the signal was persistent, the same procedure was repeated.

2.2.4.3 Pulsed field gel analysis (PFGE)

The PFGE was performed using the CHEF-DR III Variable Angle System (Bio-Rad). 0.8 % agarose (Certified Megabase Agarose – BioRad) gel was prepared in 0.5X TBE. The chromosome blocks (see 2.2.5.4 below) were equilibrated for at least 30 min in the running buffer at room temperature before they were loaded on the gel. After loading, the wells were sealed with 1% (w/v) low melting point agarose and the gel was run at the appropriate running conditions (Hinterberg and Scherf, 1994): 0.5 X TBE/18° C in 2 phases ramping switch 90 – 300 s pulse in 24 hours at 3 V/cm (or 95 volts) and 300 – 720 sec in 24 hours at 2.5 V/cm (or 85 volts). After the run was complete, the gel was stained with ethidium bromide and photographed on a UV transilluminator. For efficient transfer, the large DNA fragments separated by PFGE were nicked by UV irradiation in 5 minutes prior to transfer to hybridization membranes. The DNA can then be hybridised using standard Southern blot protocol.

2.2.5 Preparation of nucleic acid materials

2.2.5.1 Preparation of transfection plasmids

Because the transfection of foreign DNA into *P. falciparum* requires a large amount of DNA material, the transfection plasmids were prepared in a large volume, using the QIAGEN MaxiPrep kit. The volume of the bacterial overnight culture was raised to 400 ml Superbroth and the plasmids were extracted following the manufacturer's instruction, with a slightly modification of using double volume of resuspension-, lysis- and neutralisation buffer. The isolated plasmids were precipitated in 100% Ethanol. The DNA pellet was stored in 70% ethanol at -20° until used.

2.2.5.2 Preparation of *P. falciparum* genomic DNA

For the best yield of genomic DNA, a culture with 6-10% trophozoites was used (Crabb *et al.*, 2004). Cell pellet was resuspended in 10 ml cold PBS. After addition of

Materials and Methods

100 µl of 10% Saponin, the tubes were inverted 5 to 6 times and incubated for 10 min on ice. Afterwards the cell lysate was centrifuged at 3000 rpm/ 5 min. Saponin lyses the erythrocyte membrane and the PVM, hence the pellet contains the intact parasites and membraneous particles from RBCM and PVM. The supernatant was discarded and the parasite pellet was washed with PBS until no more haemoglobin was visible. The washed pellet was either directly further treated or stored at -20°C. 250 µl PBS, 250 µl 2X buffer A and 100 µl 20% SDS were added, the tubes were inverted and incubated for 2 min at room temperature. A double volume of phenol/chloroform was added and mixed thoroughly. The mixture was centrifuged at 5000 rpm for 10 min. The aqueous phase containing DNA was transferred to a clean tube and extracted twice with 1 volume of phenol/chloroform, once with chloroform. The final aqueous phase was then precipitated by adding 1/10 volume of 3 M sodium acetate (pH 5.2) and 2.5 volumes of 100% ethanol. The precipitated DNA was kept at -20°C for at least 1 hour or overnight storage. DNA pellet was washed with 70% ethanol. The pellet was resuspended in 100 µl TE (pH 8.0) and stored at 4°C.

2.2.5.3 Preparation of *P. falciparum* RNA

For isolation of RNA from *P. falciparum* a saponin-lysis with several washing steps was performed as described above. The pellet was resuspended in 37°C Trizol (Invitrogen). After a double cycle of freezing/thawing, 200 µl chloroform were added, mixed and centrifuged for 15 min at 13000 rpm. The upper phase was transferred to a new Eppendorf tube and 1 volume isopropanol was added. The sample was incubated for at least 1 h at -80°C, centrifuged 13000 rpm/ 30 min/ 4°C, the supernatant was discarded, the pellet was air-dried and resuspended in a selected volume of TE (pH 7.4 to 7.6) with 1 µl RNase out (Invitrogen).

2.2.5.4 Preparation of *P. falciparum* chromosome blocks

To resolve chromosomal DNA of *P. falciparum* by PFGE, chromosomal DNA was embedded into agarose plugs. A parasite culture containing 5-7% trophozoites was saponin-lysed and the parasites were pelleted by centrifugation. To prepare the blocks, the parasite pellet was resuspended in three times the pellet volume of warm (50°C) PBS. The same volume of warm (50°C) 2% (w/v) low melting point agarose in PBS was added and the mixture was transferred into the plug molds (Bio-Rad) and allowed

Materials and Methods

to set on ice. Once set, the blocks were transferred into PFGE-lysis buffer and incubated at 50°C for 48 hours. Chromosome blocks were stored in PFGE-storage buffer at 4°C until used.

2.2.6 Methods on parasite proteins

2.2.6.1 Fractionation of infected erythrocytes by SLO

Cell fractionation using SLO (kindly provided by Professor S. Bhakdi) was carried out as described previously (Ansorge *et al.*, 1996). The trophozoite-iRBCs were enriched by gelafundin floatation. Subsequently 10^8 iRBCs were incubated in 4 hemolytic units of SLO. The samples were incubated 6 min at RT, centrifuged at 4000g/ 5 min to extract the erythrocyte cytosol from the permeabilized host cells. This resulted in the release of all haemoglobin and RBC cytosol contents. Following SLO lysis, the pellet (named SLO- pellet to distinguish from other pellets below) was washed three times in PBS or until visibly clear from haemoglobin. The SLO pellet contains intact parasites, the vacuolar content and membranous particles. To separate the soluble proteins (SLO-soluble fraction/ SLO-SF) from membranous fractions (SLO-MF), the SLO pellet was lysed in 10 mM Tris, 1 mM EDTA and protein inhibitor cocktail (PIC, Calbiochem) and subjected to three cycles of freezing/thawing. The soluble fraction was collected by centrifugation at 18.000 rpm/ 30min/ 4°C. Equal equivalents of each fraction were analysed by SDS-PAGE and immunoblot analysis.

2.2.6.2 Labelling the newly synthesised parasite proteins with [³⁵S]L-methionine

The ring stage iRBCs equivalent to 10^9 parasites (3D7) were washed twice in methionine-free RPMI 1640 medium and cultivated to the next stage in methionine-free RPS culture medium, with the addition of 100 µCi [³⁵S]L-methionine (Helmby *et al.*, 1993). The culture flask was incubated at 37°C as usual for approximately 24 hours or until late trophozoites (36 - 40 hours) developed. The iRBCs were fractionated by SLO as described above (2.2.6.1).

2.2.6.3 Fluorescence microscopy

For live-cell imaging gelafundin-enriched parasites stained with Hoechst 33258 (Invitrogen) were directly applied on a glass slide and imaged immediately at room

Materials and Methods

temperature. Images were acquired using the appropriate filter sets on a Zeiss Axio (Carl Zeiss, Jena) observer inverse epifluorescence microscope system.

2.2.7 Immunoblotting analysis

The immunoblotting analysis was performed following the standard protocol (Sambrook and Russell, 2001). Briefly, proteins were first separated on 10 % SDS-PAGE. After SDS-PAGE, the gel and a piece of slightly bigger size of nitrocellulose membrane were soaked with transfer buffer (39 mM Glycin, 48 mM Tris, 0.0375% SDS, 20% methanol) for 5 min. The transfer sandwich was assembled from anode to cathode with 3 pieces of Whatmann 3MM paper soaked with transfer buffer, nitrocellulose membrane, separation gel and 3 pieces of Whatmann paper soaked with transfer buffer at 1mA/cm² in one hour. Proteins were stained with Ponceau-S, marker bands were marked and the membrane was washed with 1 x PBS until the colouring was removed. The membrane was incubated in blocking solution (5% skim milk in PBS) for one hour to block unspecific protein binding sites. Subsequently the membrane was incubated in the first antibody [rabbit anti-SERP (1:500) (Ansorge *et al.*, 1996), mouse anti-GFP (1:1000, Roche), mouse anti-PfHSP70 (1:1000, a gift of T. Blisnick), rabbit anti-PV1 (1:500) (Nyalwidhe and Lingelbach, 2006) or goat anti-GST (1:2000, GE Healthcare)] at 4°C overnight. The next day the membrane was washed three times with 1x PBS for 15 min followed by one hour incubation with the appropriate secondary antibody, either horseradish peroxidase-conjugated (HRP) or alkaline phosphatase-conjugated (AP) anti-mouse, anti-goat or anti-rabbit antibody, respectively (DAKO, Santa Cruz, 1:2000). Specific proteins were detected by ECL (GE Healthcare) or by AP detection.

2.2.8 Expression and purification of recombinant proteins

2.2.8.1 Constructing the expression vector

For pGEX-PV1, the DNA sequence corresponding to the PV1 protein without the N-terminal signal peptide was amplified using the primers PV1-GST-BamF 5'-CAGGATCCACAATGTGGTGGCCCCTAAGAG and PV1-GST-XhoR 5'-CAGCTCGAGTTAGCTCGATATTGGTGTGTTTTG. Restriction sites are italic typeface, stop codon is underlined. The PCR product was digested with the enzymes *Bam*HI and *Xho*I and ligated to the pGEX-5x-3 vector (GE Healthcare) downstream

Materials and Methods

of the GST encoding sequence to create the pGEX-PV1 vector. The sequence was confirmed by automated sequencing.

2.2.8.2 Over-expression and solubility test of recombinant proteins in *E. coli*

For the expression of GST-PV1 fusion protein, the construct was transformed into *E. coli* BL21-CodonPlus-RIL (Stratagene). *P. falciparum* has a high codon bias of AGA arginine, CUA leucine and AUA isoleucine (Nakamura *et al.*, 2000). The *E. coli* strain used here contains extra copies of the corresponding tRNA genes, allowing a high level expression of proteins of interest. This RIL-plasmid confers a chloramphenicol resistance. 5 ml overnight culture were seeded into 50 ml LB medium with ampicillin and chloramphenicol. Bacteria were grown to OD₆₀₀ of 0.8 – 1.0 and the protein expression was induced at 1 mM IPTG in 4 hours at 30°C. Every hour the cell pellet from 1 ml culture was harvested and stored at -20°C until needed. The cell pellet was resuspended in 50 µl lysis buffer (100 mM NaCl; 25 mM Tris/HCl, 1 mM PMSF pH 8.0). Lysozyme was added to 1 mg/ml and the resuspension was sonicated 3 x 15 sec. The cell lysate was centrifuged at 13,000 rpm/5 min/ 4°C and the supernatant was saved as soluble fraction. The insoluble fraction was resuspended in 25 µl lysis buffer and 25 µl 2X sample buffer. In each step, a sample volume equivalent to 200 µl of culture was analysed by SDS-PAGE.

2.2.8.3 Purification of GST fusion protein from *E. coli*

The purification of the PV1GST fusion protein was modified from standard protocol (Smith and Johnson, 1988) and from the manufacturer's instruction (GE Healthcare). 400 ml of bacterial culture were grown to suitable OD. After induction, the volume culture was split to 2 x 200 ml and spun down at 6000 rpm/ 15min/ 4°C (GSA Sorvall rotor). Cells from 200 ml of culture were subjected to purification. The rest was stored at -80°C until needed. Cells were resuspended in 10 ml binding buffer (1 X PBS, 5mM DTT, 1mM PMSF) and lysed by sonication in 3 minute, 10 sec ON/ 10sec OFF. After sonication, Triton X-100 was added to the final concentration of 1% and the cell lysate was clarified by centrifugation at 16000 rpm/ 30 min/ 4°C (SS34 Sorvall rotor). The supernatant after centrifugation was loaded onto the equilibrated bulk-pack column of 200 µl bed volume of Glutathione S-Sepharose 4B (GE Healthcare). The unbound proteins were washed from the column 3 times with binding buffer. The PV1GST fusion protein was eluted by elution buffer (20 mM Glutathione, 50 mM

Materials and Methods

Tris-HCl pH 8.0, 120 mM NaCl). All samples were analysed by SDS-PAGE. The GST protein alone was also expressed from the vector pGEX-5x-3 and purified for further use as control. For GST pull-down assay, both PV1GST and GST protein were dialysed against 1X PBS for 16 hours at 4°C before added to the pull-down experiment.

2.2.9 GST pull-down assay

SLO-SF of late trophozoites (36 – 40 hr post invasion) was pre-cleared before the assay. Briefly, the lysate of 2×10^8 parasites was incubated with 50 μ l of 50% slurry of Gluthione Sepharose 4B and 25 μ g of GST [followed (Sambrook and Russell, 2001)] for at least 2 hours at 4°C. The mixture was spun down at 13000 rpm/ 2min/ 4°C and the pre-cleared cell lysate in the supernatant was transferred to a fresh tube. The *in vitro* protein interaction assay for *P. falciparum* was adapted from the standard protocol (Sambrook and Russell, 2001) and from the previous publications (Bracchi-Ricard *et al.*, 2005; Murphy *et al.*, 2004). In short, an equimolar amount of PV1GST and GST alone was used in the assay. The molecular mass of PV1GST protein was calculated by Compute pI/Mw at Expsy (Gasteiger, 2005) and the mass – molar quantity was converted by calculation software at http://molbiol.edu.ru/eng/scripts/01_04.html. Approximately 200 pmol of protein, equal to 15 μ g of PV1GST or 5 μ g of GST alone were bound to 50 μ l Glutathione Sepharose beads first, at least 2 hours at 4°C. A control of the Glutathione Sepharose 4B beads alone was also performed in parallel. Pre-cleared lysate from SLO-SF of 2×10^8 parasites (200 μ l) was then mixed to the complex and incubated overnight at 4°C with gentle agitation. After 5 washing steps with TBST (Tris buffer saline and Tween 20: 10 mM Tris HCl- pH 8.0, 150 mM NaCl, 0.1% Tween-20), the complex was boiled in SDS-PAGE buffer, and centrifuged to remove the beads. An amount of 2×10^8 cells equivalent was loaded in each lane. For a sensitive approach, the protocol was applied to the SLO-SF lysate from [³⁵S]-L-methionine labelled parasites and the gel was exposed to an X-ray film for 1 week at –80°C or longer. In addition, a normal cell lysate was also subjected to the assay, the observed bands on the gel were obtained and investigated by mass spectrometry (kindly helped from Dr Omid Azim-Zadeh and Bsc. Caroline Odenwald).

3. Results

3.1. PV1 identification, orthologs and bioinformatics analysis

Data from PlasmoDB (Aurrecochea *et al.*, 2009) and OrthoMCL database (Chen *et al.*, 2006) have shown that PfPV1 orthologs are highly conserved in *Plasmodium* species. However, BLASTP searches against the genomes of other Apicomplexa (www.apidb.org) (Aurrecochea *et al.*, 2009) and the NCBI- BLASTP cannot find any similarity in other Apicomplexa nor other genera. The protein shares 26.7% identity, 44.4% similarity with PKH_092690 from *P. knowlesi*, and 24.8% identity, 41.3% similarity with Pv092070 from *P. vivax* [by ClustalW2, (Larkin *et al.*, 2007)], (Figure 3.1). However, the predictions for PfPV1 lack any information about domain structure and function. Domain searches using SMART (Letunic *et al.*, 2009; Schultz *et al.*, 1998) only reveal a coiled-coil region from residue 294 to 333 besides a low compositional complexity region in the sequence from 157 to 170 (¹⁵⁷DPNNKNQNEDNVDN¹⁷⁰). Interestingly, PfPV1 possesses an exclusively glutamine-rich region at amino acid residues 302-346 which does not exist in other *Plasmodium* species (Figure 3.1). This glutamine-rich region is also part of the coil-coil region above, which is defined by Scansite (Obenauer *et al.*, 2003) as a DUF2040 domain (DUF: domain of unknown function), assigned in residues 315 – 337. Globplot (Linding *et al.*, 2003) predicts an additional globular domain at the N-terminus, between residues 1-156 (Figure 3.1A) and other intrinsically disorder regions [157,167], [212, 228], [263, 270], [371, 392] and [404, 452].

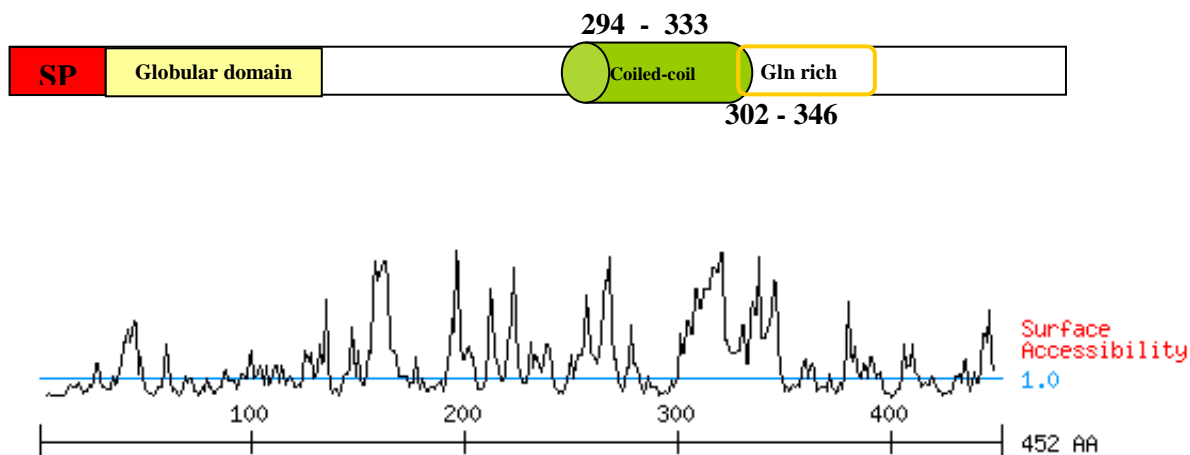
Various motif scanning sites, MyHits (Hulo *et al.*, 2008), Minimotif Miner - MnM (Rajasekaran *et al.*, 2009), Scansite (Obenauer *et al.*, 2003) and PFP (Hawkins *et al.*, 2006) gave no significant hints to the function of PfPV1. MotifScan MyHits (Hulo *et al.*, 2008) barely predicted weak matches for motifs of N-glycosylation, casein kinase II (CK2) phosphorylation site, N-myristoylation, protein kinase C (PKC) phosphorylation site and the glutamine rich region from 302 – 346 as depicted above. The prediction for orthologs from *P. vivax* and *P.knowlesi* also resulted in those motifs. Giving that the parasite lacks any evidence of N-glycosylation (Gowda and Davidson, 1999; von Itzstein *et al.*, 2008), all the prediction of N-glycosylation sites on PfPV1 and the orthologs were likely negative results. From the latest update of MnM (Rajasekaran *et al.*, 2009) and based on the conserved region of cross species,

Results

some motifs were predicted (Table 3). However whether or not they are true functional motifs requires experimental studies. Previous attempts to identify post-translational modifications by mass spectrometry did not discover any modification pattern, even though particular attention was paid to myristoylation and phosphorylation (Nyalwidhe, unpublished observation). Nevertheless, it remains possible that PfPV1 may be post-translationally modified.

In combination with Ontology Based Pattern Identification - OPI (Zhou *et al.*, 2005), PlasmoDB classifies PfPV1 into GO groups: GO:0007154 (cell communication, based on biological process); GO:GNF0206 (cytoadherence, Literature Combined database) (Aurrecoechea *et al.*, 2009) as well as the groups from literature resources of PV localisation, GO:PM16470785 (Nyalwidhe and Lingelbach, 2006) and the interaction network by Y2H, GO:PM16267557 (LaCount *et al.*, 2005).

A



Results

B

P. vivax	<u>MKKAALSILLLLLPVYSLNLDNENQ</u> --EPEEINTITGKLVQVNSEHEKILSIINEIFTKK	58
P. knowlesi	-KKVALSIVLILLPVYSLSIDNANQ--EPEEIKNITAKLVQVNSEHEKFLSVINEIFTKK	57
P. falciparum	<u>-IKIILASFLFFFFYFSSSIYGNVVPKSAEAVHTLTAKLDTENKAHQKYIDIINGVFSEN</u>	59
	* . . * : : : * . * : : * . * : : : *	
P. vivax	EESCKF S FSN-NGFRCAFSRFDVNFNNSKAVNALFTSENEQVIKDAE EYK VRLM L ELH	117
P. knowlesi	DDSC K F S FSN-NGFKCAF S KFDVNFNNGSKEMNALFNNANEQ I IKDAE EYK VRLM L ELH	116
P. falciparum	MENF V F S ITTSNG F TC S INKL D V I FDNKV T GMQ K V F SDENV Q Y I KEAS L E F K N N L E Y M K	119
	: . * : : * . * : : : * * : : * . * : : * : : *	
P. vivax	NLRPPNTNLKNFK K F Q G I CM F F S ELRR K F F HL Y R N DESGD G EGSSR G EITSGD Q L T E	177
P. knowlesi	NLRPP T N L KN F K D F Q G I CM F F S ELRR K F F HL Y R N ES N EDGD V NQ N DD I T N V D Q L T E	176
P. falciparum	G V MP S EN D FS N VR K E F Q K V C V K Y F S E LRR K F F Q I Y R DP N N K NQ N ED N V D N H M N I E E S Q E	179
	: . * . : : * . : : * * : : * : : * : : * : : * : : * : : *	
P. vivax	RMES S YDSASTEDGS N AG K D S Q D L S ELMEED-----DE H NP D AP N M Q SS S Y S FS S H	229
P. knowlesi	RLE S TYDSASTEDGS I SG K D K Q D L S EVMEED-----E E N N L D V P H V Q-SS S Y S FS S H	227
P. falciparum	F F SG F NP F GT M K I R K EQ N PD L S Q K D S L IL N EN N ND S LT S AD Q K N N M V P M E NR S FS S Y S Q Q	239
	: . . : : * . : : * . * : : : * : : * : : * : : * : : *	
P. vivax	T S KK I M F D G -NN V I E EN S S V NDGG D D Q SE D L Q Q G P M T K E K A V S I M L K N T S F T I E G K C T E	288
P. knowlesi	T S KK I V F D G -NN V I E EN S S I NDG S DD Q N E N L E Q G P M T K E K A L S I F L K N S S F S I E G N I T E	286
P. falciparum	S S H V V S F D G H D E H V E Q Q E Q H S G D N T Q E D K D Q L M D L P F N K D K V F S T F L K N V T L L I E G N C T E	299
	: * : * * : : * : : * . * : : : * : * : : * . * : : * * : : * * : : *	
P. vivax	EDE-----K K E K P F S V F F N S Q L S	306
P. knowlesi	EDQ-----N K E K P F S V F F N S Q L S	304
P. falciparum	A Q Q Q A Q E Q T Q E Q T E E Q E E E Q N E K E I E S D K Q V Q K D G E Q K E N D V Q K K Q K A N A F T I Q F S S L S	359
	: : * : : * : : * * : : * * : : * * : : * * : : *	
P. vivax	R N H F S T V C N S N G K N F L R K A D G G S P F V E P L N P D D L N R M M A D M L K F F S Q S D G N R M L L P F L	366
P. knowlesi	R N H I S T V C N A N G K N M L R G S G S N N P F M E P L N P D D L N K M M N D M V K F F S Q N D G N G M L L P F L	364
P. falciparum	R K H I S T C N A S S G N V F L R K G N K---P F E H F N S P N F E N M M K G V F G I I Q N P F E N G Q P T F P F	416
	* : * * * . * * : . * : . . * . * : . : * * : . : . : . . * * : :	
P. vivax	G K M N F M D A L G S L G L P P G L D L E S M F N D F L Q G N G -T P C C R G A R P T I G G P S N K Q D P S A D D S D	425
P. knowlesi	N R M N F N E A L G N L G L P S G L D I E S M F N D F L Q K S G S N P C R G A R P Q I D Q P K K E D P P T D D S D	424
P. falciparum	K N I N S I S G I G N V D I P-----K N F M N D F L N N G N -----D Q N T P I S S ---	451
	: * . . : * : : * : : * : : * : : * : : * : : * : : *	
P. vivax	EQH 428	
P. knowlesi	NQQ 427	
P. falciparum	---	

Figure 3.1 Structure, feature and conservation of PfPV1. (A) Schematic representation of full-length PfPV1 showing the signal peptide (SP) at the N-terminus (residues 1-21, red box), a predicted globular domain (residues 1 – 156, light yellow box), a coiled-coil region (residues 294 – 333, green can) and a glutamine-rich region (residues 302-346, open rectangle). Features were predicted by SMART (Letunic *et al.*, 2009; Schultz *et al.*, 1998) and Globplot (Linding *et al.*, 2003). The surface accessibility map was plotted from Scansite (Obenauer *et al.*, 2003). (B) Sequence similarity by ClustalW2 (Larkin *et al.*, 2007) between proteins encoded by *P. vivax* Pv092070, *P. knowlesi* PKH_092690 and *P. falciparum* PF11_0302, respectively. Sequences were retrieved from PlasmoDB. Genome sequencing from other *Plasmodia* are not completed therefore the alignment of the whole group is not available. Identical (*), highly similar (:), similar (.) residues and gaps (---) are indicated. The conserved residues are shown in bold type. The predicted N-terminal signal peptides are underlined.

Results

Table 3. Mini motifs predicted in PfPV1

Known motif	Position(s) in PfPV1	Conserved in other <i>Plasmodium</i> Homologous sequences	Function
[S/T]Q	202	<i>P.v</i> ---KDG S QDLSELMEE--- <i>P.k</i> ---KDK K QDLSEVMED--- <i>P.f</i> ---PDL S QKDSLILNE---	This consensus motif is phosphorylated by ATM; phosphorylation Thr; no modification required
PxxxD	276	<i>P.v</i> ---LQQG PMTKE KAVSI--- <i>P.k</i> ---LEQG PMTKE KALSI--- <i>P.f</i> ---LMDL PFNKD KVFST---	This consensus motif in peptide binds platelet fibrinogen receptor; no modification required
SxxxS	202,234	<i>P.v</i> GS QDLSELMEE-----DEHNPDAPNMQQ SSYSF SSH <i>P.k</i> KK QDLSEVMEDD-----EENNLDPVPHVQ- SSYSF SSH <i>P.f</i> LS QKDSLILNENNNDSLTSADQKNNMVP MENR SF YSQ	This consensus motif in beta-catenin is phosphorylated by an unknown target; phosphorylation ; no modification required
[S/T]xxx[S/T]	202, 234	<i>P.v</i> GS QDLSELMEE-----DEHNPDAPNMQQ SSYSF SSH <i>P.k</i> KK QDLSEVMEDD-----EENNLDPVPHVQ- SSYSF SSH <i>P.f</i> LS QKDSLILNENNNDSLTSADQKNNMVP MENR SF YSQ	This consensus motif in glycogen synthase is phosphorylated by GSK3 beta; phosphorylates N-terminal Ser/Thr; C-terminal Ser/Thr must first be phosphorylated
Sxx[S/T]	238, 357	<i>P.v</i> SSYSF SSHT SKKIMFDG <i>P.k</i> SSYSF SSHT SKKIVFDG 238 <i>P.f</i> RSFSY SQQ SSHVVSFDG <i>P.v</i> KKEKPFVFF NSQL SRNHFST <i>P.k</i> NKEKPFVFF NSQL SRNHIST 357 <i>P.f</i> QKANAF TIQF SS SSL SRKHIST	This consensus motif is phosphorylated by casein Kinase I; phosphorylation Ser/Thr; first Ser must be phosphorylated
[FILVW]xxx[FILV]xxx[FILVW]	74, 283, 355	<i>P.v</i> NG FR CA FS RFDVNFN <i>P.k</i> NG FK CA FS KFDVNFN 74 <i>P.f</i> NG FT CS IN KL DV IFD <i>P.v</i> EK AV SIM LK NT SF TIE <i>P.k</i> EK AL SIF LK NS SF SIE 283 <i>P.f</i> DK V ES T FL KN V TL L IE <i>P.v</i> FSV FF NS QL SRNH F STV <i>P.k</i> FSV FF NS QL SRNH I STV 355 <i>P.f</i> F TI Q F SS SL SRKH I STT	This consensus motif binds the #1 calmodulin domain of calmodulin; no modification required Type 1-5-10
[FILVW]xxx[FAILVW]xx[FAILVW]xxxxx[FILVW]	416	<i>P.v</i> LLL PF L G K M N F M D AL G S L GL PP G L D LES <i>P.k</i> M LP F L N R M N F N EAL G N L GL PS G L D IES 416 <i>P.f</i> T FP F FK N I NS I S G I GN V D IP-----KN	CaM binding motif 1-5-8-14, the relevant sequence in P.v or P.k is either 1-5-8-14 or 1-5-10, the residue positions are not conserved in this case.
[FILVW]xxxxx[FILV]xxxxx[FILVW]	109	<i>P.v</i> EEY K V R L M L E L H N L R P <i>P.k</i> EEY K V R L M L E L H N L R P 109 <i>P.f</i> EAS L E F K N N L L E Y M K G V M P	CaM binding motif 1-8-14, the corresponding

Results

Rxx[S/T]	233	<i>P.v</i> DEHNPDAPNMQQ[SSYS]FSSH 229 <i>P.k</i> EENNLDVPHVQ-[SSYS]FSSH 227 <i>P.f</i> DQKNNNMVPMEN[RSFS]YSQQ 239	sequence in P.v and P.k is type 1-5-10. This consensus motif is phosphorylated by CamKII; phosphorylation Ser/Thr; no modification required
[S/T]x[K/R]	36	<i>P.v</i> EPEEINTITGK[LQV]QNSEHEKIL 48 <i>P.k</i> EPEEIKNITAK[LQV]QNSEHEKFL 47 <i>P.f</i> SAEAVHTLTAK[LDT]ENKAHQKYI 49	This consensus motif in peptide is phosphorylated by PKCalpha; phosphorylation Ser/Thr; no modification required
[K/R]R	148	<i>P.v</i> FFSEL[RR]KFFHLYRNDESGQDGE[SSR] <i>P.k</i> FFSEL[RR]KFFHLYRNNESNEDGDVNQN <i>P.f</i> YFSEL[RR]KFFQIYRDPNNKNQNE[DNVD]	This consensus motif in mating factor is proteolyzed by Kexin2; cleaves after C-terminal Arg; no modification required

Table 3. Mini motifs were predicted in PFPV1 by MnM (Rajasekaran *et al.*, 2009). There were 69 motifs found, only some highlighted motifs were listed here, based on the conserved region with other *Plasmodium* species, the surface prediction score (0.8 – 1.0) and the cell localisation (consider PV localisation as the extracellular or secreted). In a consensus motif, redundant amino acids in a position are put inside square brackets; x is any amino acid. *P.v*: *P. vivax*; *P.k*: *P. knowlesi*; *P.f*: *P. falciparum*. The annotations of motif functions were extracted from the MnM homepage.

3.2. Strategy one: Gene targeting by double cross-over homologous recombination using a negative selection system

3.2.1. Double cross-over integration of pHTK Δ PV1 under the selection of ganciclovir still required WR99210 cycling

In order to study the importance of PfPV1 in asexual *P. falciparum* life cycle we decided to knockout the encoding gene. To avoid the time consuming process of cycling of on and off WR99210 drug (WR), we decided to target the PF11_0302 gene by double crossover recombination with the negative selection strategy (Duraisingh *et al.*, 2002). The 5'-flank and 3'-flank regions of PF11_0302 were respectively inserted into *SpeI/BglIII* and *EcoRI/NcoI* site, in the same direction of expression of the *hDHFR* cassette of vector pHTK to create the vector pHTK Δ PV1 (Figure 2.1). Transfectants were obtained after 21 days under the selection of WR99210. Three transfected parasite flask cultures containing the episomal plasmid were then put under the negative selection of ganciclovir by activity of TK encoded in the vector. Parasites were dead after adding ganciclovir and re-appeared in Giemsa stained smears at various times in subsequent culture: line 1 re-appeared after 12 days, line 2 after 40 days and line 3 was unable to recover. To detect the integrating event, we carried out PCR reactions by combining a chromosome specific primer (Figure 3.2 A, primer a] or d]) with a vector specific primer (Figure 3.2 A, primer b] or c]). However, we failed to detect any integration (Figure 3.2 B, reaction [a + b] and [c + d]). In fact, the full length PfPV1 was still intact, evidenced by the product at 1.38 kb fragment (Figure 3.2 B, reaction [e + f]). Technically it might be the results from a mixed population of integrated and non-integrated parasites so both line 1 and line 2 were cloned by limiting dilution. We were unable to obtain any single parasite clone from line 2, and only one clone, the 1D8 was picked from line 1. The genomic DNA was digested with *XbaI* and *EcoRI* and subsequently probed in Southern blot hybridisation with a 5'-end probe (Figure 3.2 C). However we were unable to detect any integration event, evidenced by the plasmid band (8.4 kb) and an endogenous band (4.1 kb) in the blot (Figure 3.2 C).

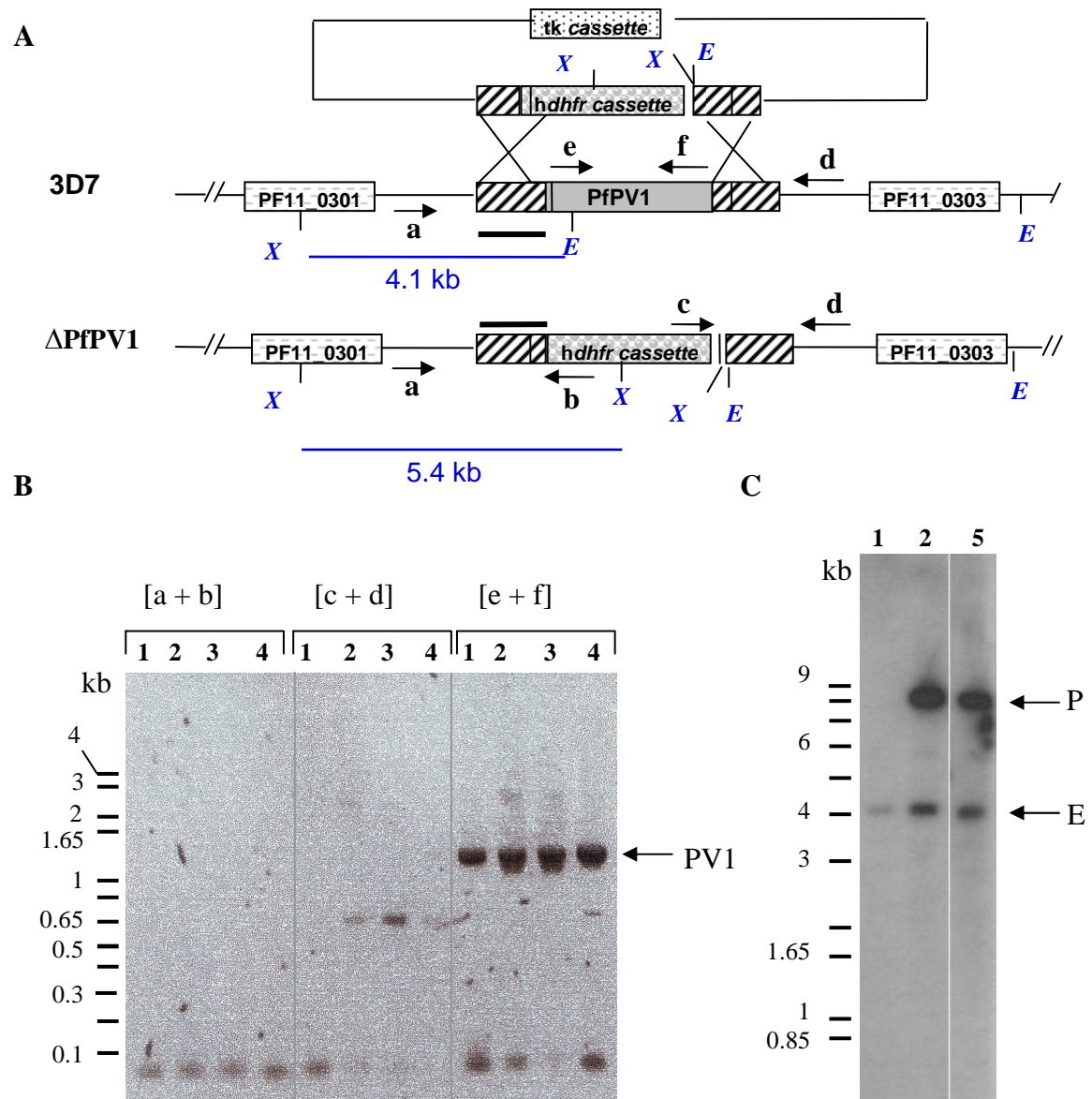


Figure 3.2. The *PfPV1* locus cannot be targeted by simple negative selection. (A), Schematic representation of integration of the knockout plasmid pHTKΔPV1 into the chromosomal PV1 locus (Chr 11). The *PfPV1* locus is flanked by two genes, PF11_0301 and PF11_0303. PV1- 5 flank probe is depicted as solid line (—); Enzymes used in southern blot were *Xba*I (X) and *Eco*RI (E). Primers used in PCR: chromosome specific, primer a] and d]; vector specific, primer b] and c]; primer for the amplification of *PfPV1* encoding gene: primer e] and f]. **(B)**, PCR for the detection of integration, the expected product of reaction [a + b]: 2.4 kb; reaction [c + d]: 1.6 kb. Reaction [e + f] amplifies the whole *PfPV1* encoding sequence at 1.38 kb as labelled in the picture. DNA templates were from 3D7 parental parasites (lane 1); episomal pHTKΔPV1 containing parasites shortly after visibly reappeared (lane 2); transfected parasite after adding ganciclovir, recovered after 12 days (lane 3), after 40 days (lane 4). **(C)**, Southern blot of restricted genomic DNA from 3D7 parental parasites (lane 1), episomal pHTKΔPV1 containing parasites (lane 2), and the 1D8 clone (lane 5), the uneven black stain under the plasmid band at lane 1D8 was merely from the noise background of the blot, as it was from the same stain in the empty neighbour lane. The blot was probed with 5' flank fragment of the *PfPV1*, labelled by [α -³²P]dATP. DNA markers are shown in kb. Endogenous band (E): 4.1 kb, episomal plasmid (P): 8.4 kb.

Results

As the time requirement was not shortened by promptly adding ganciclovir, we returned to a traditional gene disruption protocol by drug cycling of positive selection. Parasites were subjected to three rounds of with or without WR over several months. Ganciclovir was also added after each cycle and simultaneously kept in the culture with other lines. Adding ganciclovir after 2 cycles of WR killed the parasites and the parasites visibly reappeared after 8 days, we named the population as 2 cyc-WG (ie, adding ganciclovir after 2 cycles of WR). The normal 3 cycles WR was still kept in culture and ganciclovir was also added afterward. At this point ganciclovir did not completely kill the population, there was a mix of dead and ill-looking parasites under the microscope. However, the parasitemia was recovered after 5 days and the culture was labelled as 3 cyc-WG population.

To analyse the integration, we examined the genomic DNAs by Southern blots. Similar to the first attempt with the 1D8 parasite, after 3 cycles of WR without ganciclovir we were unable to detect any integration event (Figure 3.3 B, left panel, lane 2, 3 and 4). Alternatively, adding ganciclovir after 2 WR cycles caused the loss of the episomal plasmid band, as shown in Figure 3.3 B, lane 5, the disappearance of the 8.4 kb band. Interestingly, there was one smear at the expected size of integration (5.4 kb) although the endogenous band (4.1 kb) was still there. We supposed that this might refer to the mixed population between the integrated and non-integrated parasites. Assuming that the 3 cyc-WG parasites would also obtain the same result we did not repeat the blot for the mixed population but went directly to isolate single clones by limiting dilution. 4 clones were obtained: C2, C3, E10, and F8. Analysis revealed the presence of the 4.1 kb endogenous band, in addition to a size shift between 5 and 6 kb (Figure 3.3 B, middle and right panel), closely to the expected integration band. C2 clone gave a “supposed integration” signal slightly shorter than other clones. We concluded that by combination of WR cycling and the selection of ganciclovir, the pHTK Δ PV1 did integrate into the chromosome, as shown in the integration band of 5.4 kb by the PV1 5-end probe.

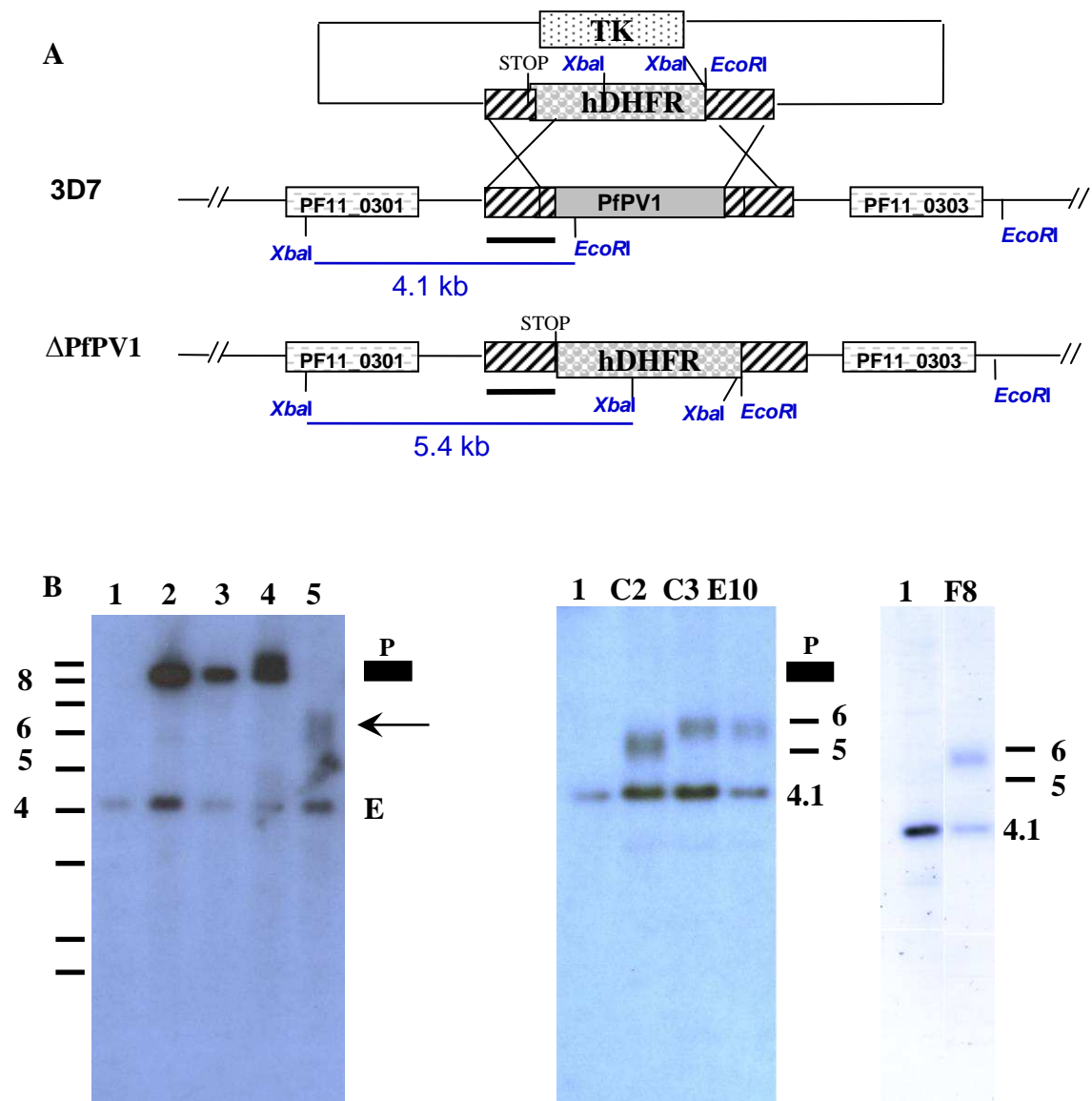


Figure 3.3. The episomal pHTK Δ PV1 only disappeared after adding ganciclovir to rounds of WR99210 cycling. (A), Schematic representation of integration of the knockout plasmid pHTK Δ PV1 into the chromosomal PV1 locus (Chr 11). The *PfPV1* locus is flanked by two genes, PF11_0301 and PF11_0303. PV1-5'probe is depicted as solid line (—). The REs used for diagnostic digest were *Xba*I and *Eco*RI. The stop codon at the end of 5-flank region was introduced. The expected sizes of hybridised bands with 5-end probe are indicated as 4.1 kb for 3D7 (wild type) and 5.4 kb for integrated parasite. (B), Southern blot of restricted genomic DNAs hybridised with 5' probe. Lane 1, 3D7 parental parasite; lane2, episomal pHTK Δ PV1 containing parasite, cycle 0 of WR; lane 3, pHTK Δ PV1 parasite, WR-cycle 2; lane 4, pHTK Δ PV1 parasite, WR-cycle 3; lane 5, 2 cyc-WG parasite, ganciclovir was added after cycle 2 of WR; lane P, signal from 0.5 μ g digested pHTK Δ PV1 plasmid. Because of the strong signal at 8.4 kb from the plasmid (P), the control lane was removed from the membrane after the first exposure, drawn as the solid rectangle■. Lane C2, C3, E10 and F8: single clone from 3 cyc-WG population. Blots from the middle panel and right panel were independently performed. DNA markers were shown in kb. The arrow bar (←) highlights the integrated smear, letter E marks the endogenous band (4.1 kb).

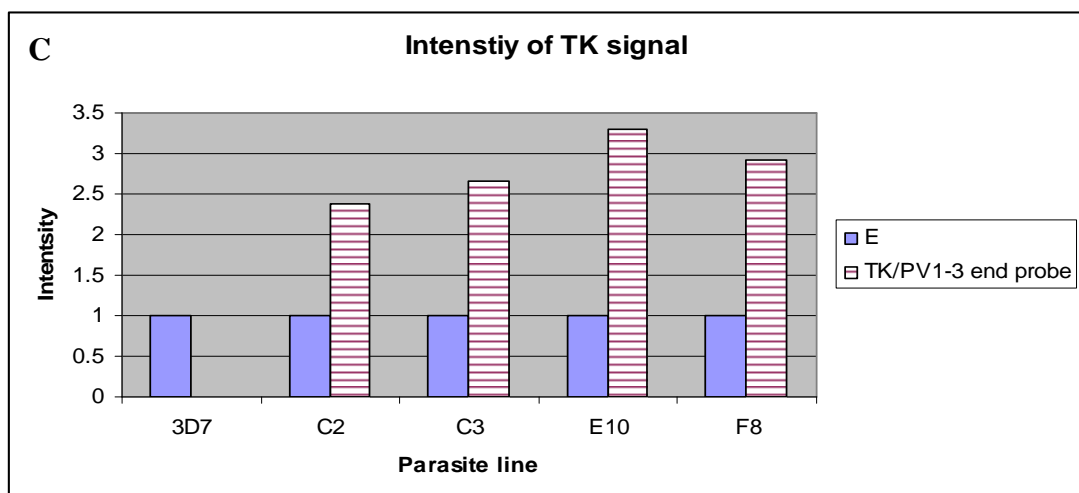
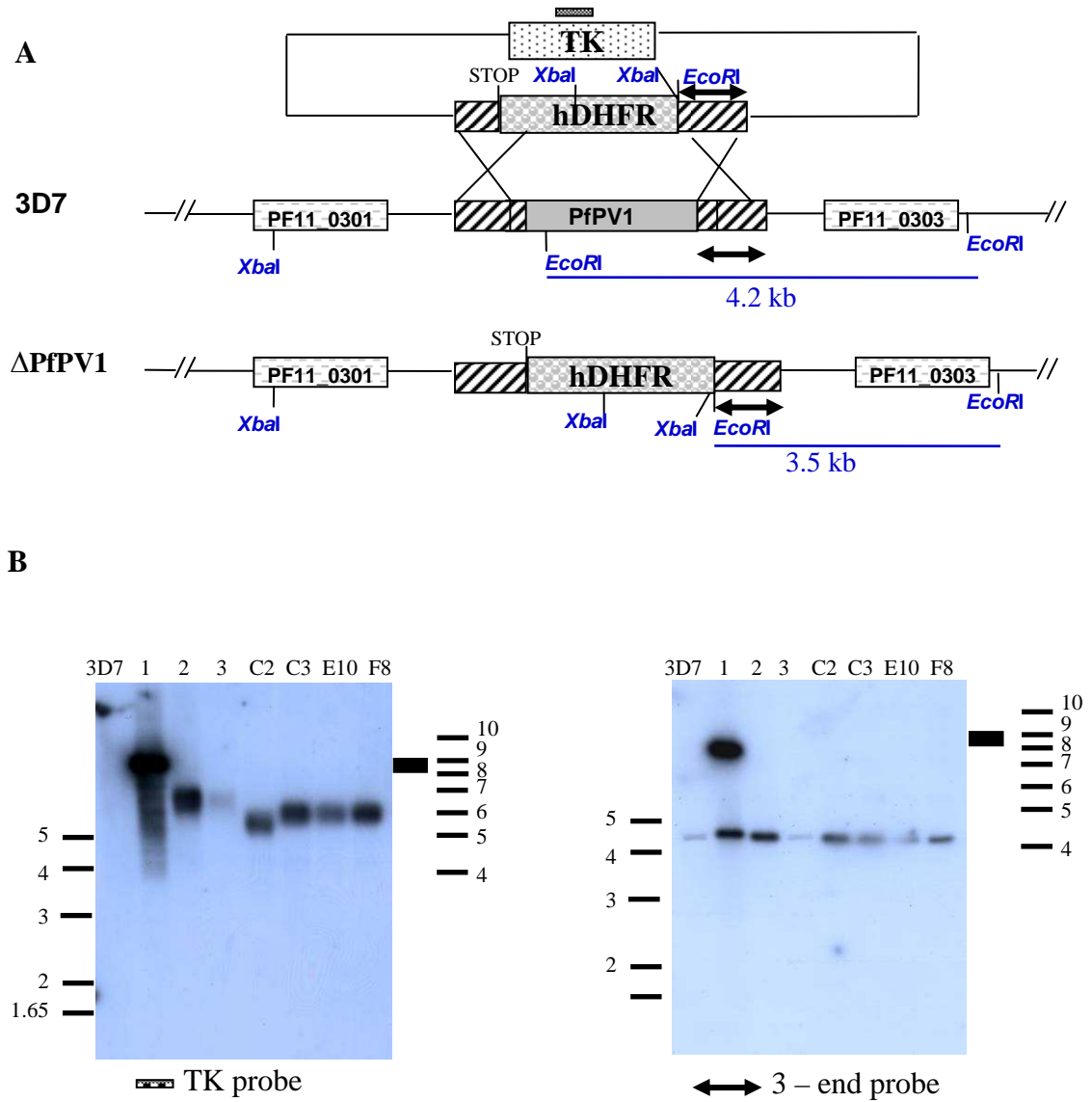
3.2.2. pHTK Δ PV1 integrated into chromosome but not in a simple double cross-over or a 5' or 3' single cross-over.

Giving that the endogenous band of the *PV1* locus still appeared in 4 clones above, and the band corresponding to the integrated size also appeared, we predicted that the integration indeed occurred, but to identify the nature of the recombination, we carried out more hybridisation analysis with the PV1-3' probe and the *TK* gene specific probe. The obtained signals were unexpected, and different from predicted results (Figure 3.4 B). Consistent with the result from 5' probe, hybridising the *Xba*I+*Eco*RI-digested genomic DNA with the PV1-3' probe also confirmed the disappearance of the episomal plasmid (8.4 kb) once ganciclovir was added after 2 or 3 cycles of WR, as shown in Figure 3.4 B, right panel, lane 2, 3, respectively. The 3' probe gave a band at approximately 4.2 kb in all parasite lines, referring to the endogenous gene locus. However, the expected 3.5 kb band of integrated DNA was not observed. It could be because of the single homologous recombination at the 5' end that the size corresponding to the endogenous band of 3' probe still exists. However, in that case there must be another band at around 7 kb from the plasmid backbone (schematic integration at Figure 3.5) but there was no such other band besides the endogenous size.

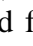

If the single cross-over in either 5' or 3' end happened, the *TK* gene in the plasmid backbone would also integrate into the chromosome, therefore we carried out the hybridisation with the *TK* probe. In fact, we performed the experiment with the *TK* probe first, stripped the membrane and re-probed with the 3' probe and collected the data for the 3' probe as above. For the *TK* probe although the episomal plasmids were gone, the blots of those clones were all positive (Figure 3.4 B, left panel). However, the obtained sizes were decreased gradually along the time of drug cycling. The first cycle of WR gave the same signal as the plasmid control (8.4 kb), but the fragments were shorter after adding ganciclovir in the second and third cycle (Figure 3.4 B, left panel, lane 1, 2, 3). In all single clones, a strong but cloudy signal at the range of 5 to 6 kb can be observed. A band shift was also observed in C2 compared to other clones, the same phenomena as with PV1-5' probe. Noticing that the intensity of the *TK* signal was much stronger than the PV1-3' end signal, we measured the density by

Results

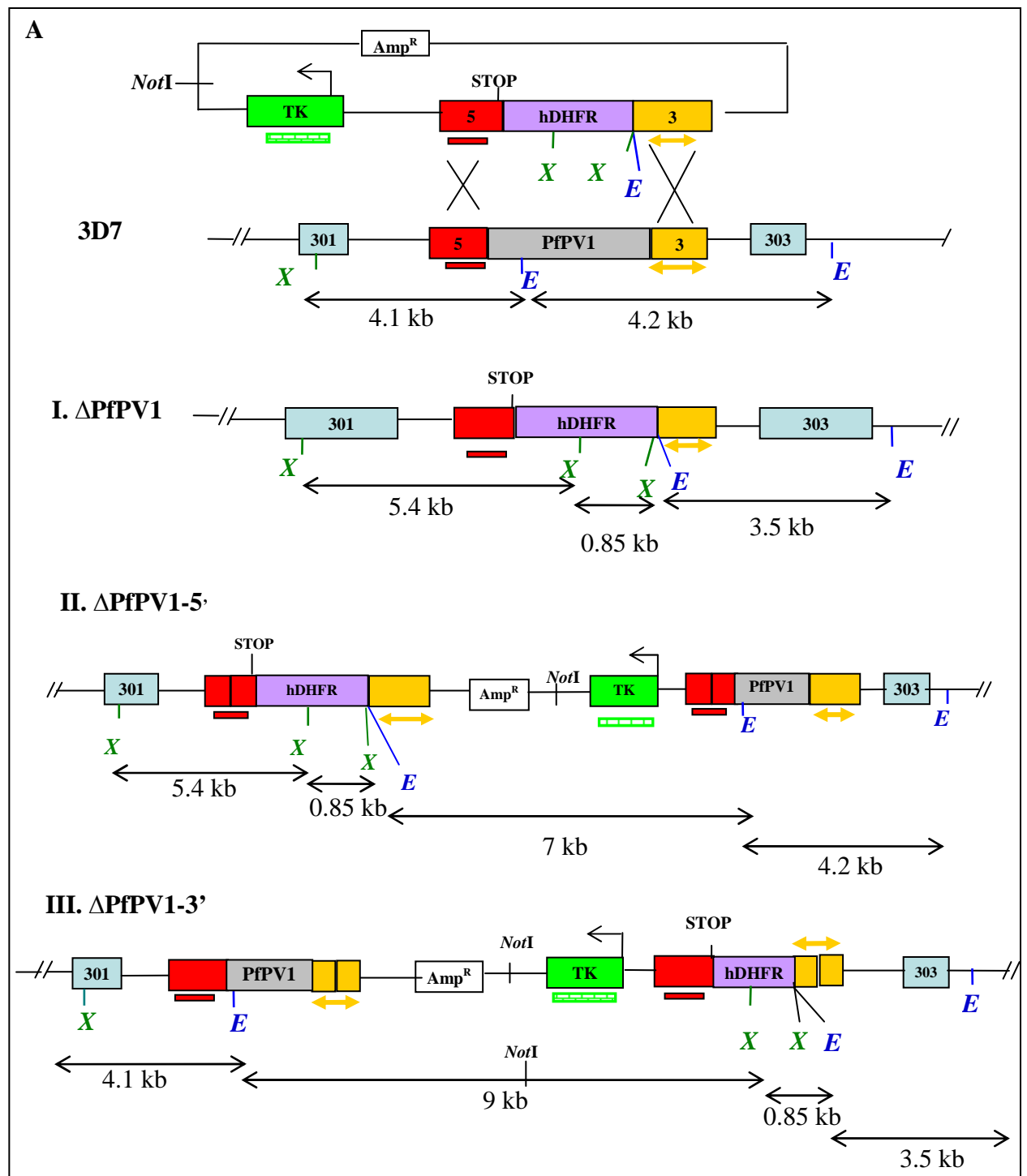
Multigauge software (Fujifilm), the TK intensity was approximately from 2 to 3.5 fold higher than that of the endogenous band (Figure 3.4 C).



Results

Figure 3.4. pHTK Δ PV1 integrated into chromosome but not in a simple double cross-over or a 5' or 3' single cross-over. (A), Schematic representation of integration of the knockout plasmid pHTK Δ PV1 into the chromosomal PV1 locus (Chr 11). The *PfPV1* locus is flanked by two genes, PF11_0301 and PF11_0303. The RE used for diagnostic digest is shown (*Xba*I and *Eco*RI). Probes for southern blot were depicted as: 3 end probe: straight line with arrowhead (\leftrightarrow), TK probe: small grid box (). The stop codon at the end of 5-flank region was introduced. The expected sizes of hybridized bands with 3-end probe were indicated as 4.2 kb for 3D7 (wild type) and 3.5 kb for integrated parasites. (B), Southern blot of restricted genomic DNAs. The blot was first probed with the TK fragment (left panel), stripped and re-probed with 3-end probe (right panel). Lane as labeled in the figure: 3D7: wild-type parasite; 1, episomal pHTK Δ PV1 containing parasite, cycle 1 of WR; 2, cycle 2-WG; 3, cycle 3-WG, DNA from this population was not high enough so the signal was weaker than the others' ; Lane C2, C3, E10 and F8: single clone from 3 cyc-WG population respectively. The strong signal at 8.4 kb from the plasmid control was cut off after the first exposure, drawn as the solid rectangle . Theoretically, the blot with TK probe would not give any signal once a double cross-over occurred, but the reaction happened in all clones here. (C), Density measurement of TK band vs PV1-3' band. Signal intensity was measured by Multigauge Software (Fujifilm). E: *PV1* endogenous band; TK/ PV1-3end probe: ratio of the TK signal vs PV1-3' endogenous band.

The existence of the *TK* gene can be explained by a single cross-over event. But the obtained results were not consistent with the expected result. If the homologous recombination happened at 5' or 3' end of the target gene, the hybridized product with TK probe would give a size of 7 kb or 9 kb, respectively (Figure 3.5). Moreover, besides the endogenous or/and the integrated band, the 5' probe and the 3' probe would also give another signal at the same size as the TK probe for the plasmid backbone but there were no such signals.



Results

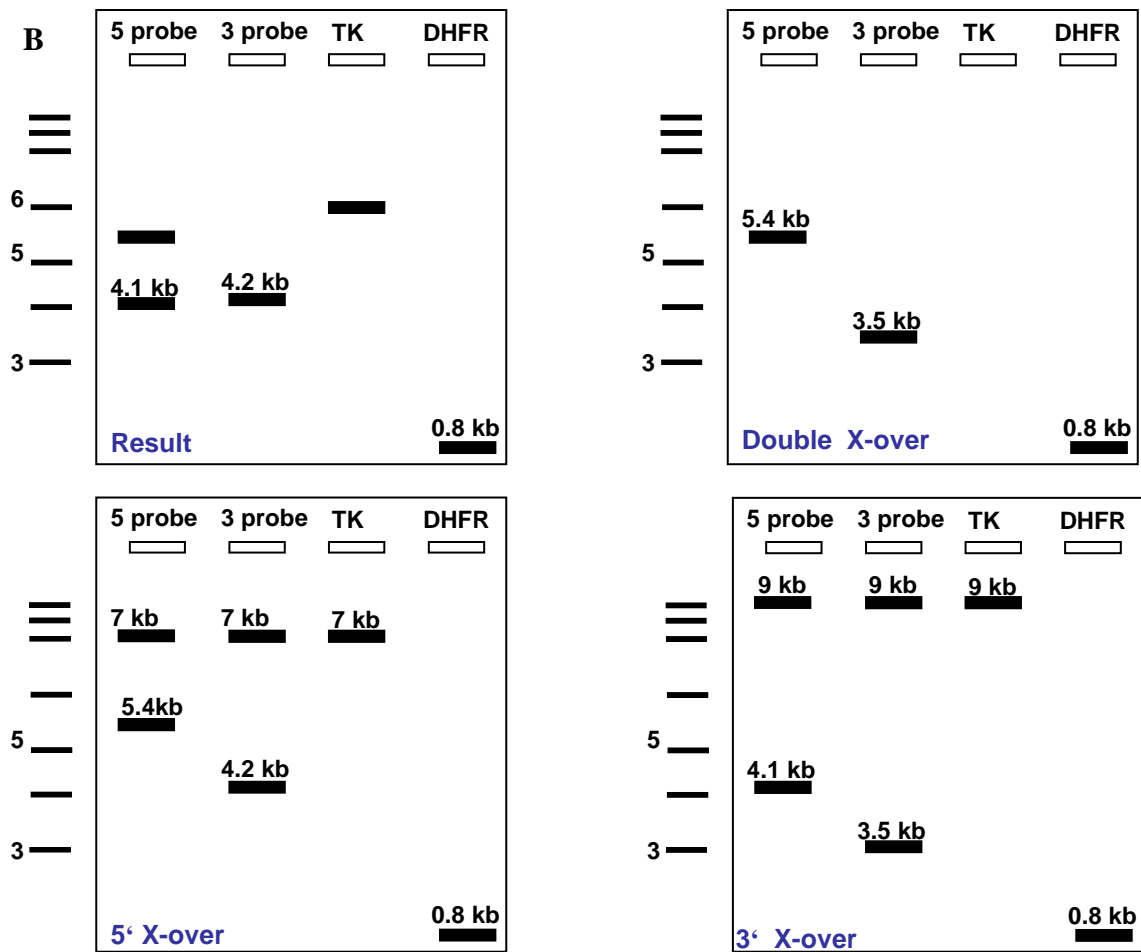


Figure 3.5. Schematic representation of possible integration event of pHTK Δ PV1 into PV1 locus. (A), genotypic analysis of *P. falciparum* transfected with pHTK Δ PV1. (I. Δ PfPV1), disruption of PfPV1 by double cross-over integration; (II. Δ PfPV1-5') and (III. Δ PfPV1-3'), the single cross-over recombination event for one copy of the full length plasmid integrated into 5' end or 3' end, respectively. The *PfPV1* locus is flanked by two genes, PF11_0301 (pale blue box, 301) and PF11_0303 (pale blue box, 303). The pHTK Δ PV1 plasmid contain the *Amp* resistance cassette (*AmpR*, white), *TK* cassette (green), *hDHFR* (lavender) and 5' (red) and 3' (gold) homologous region of PfPV1. The *NotI* site marks a full circle of plasmid. The premature stop codon (STOP) was introduced into the 5' region of PfPV1. Left arrow, transcription start site and the direction of *TK* cassette. The REs used for diagnostic digest were *XbaI* (X) and *EcoRI* (E). Probes for southern blot: 5' probe, red box (—); 3' probe: gold line with arrowhead (↔), *TK* probe: green, small grid box (□). The expected sizes of diagnostic bands are indicated in kb. In the case of the *EcoRI* site in the cloning join between the *hDHFR* cassette and the 3' region, the site is at the beginning of the homologous region and this site will not include in the cross-over recombination, hence it always sticks together with the *hDHFR* cassette. (B), Result and possible outcomes of the integration by southern blot with 4 different probes: PV1- 5', PV1-3', *TK* specific and *DHFR* probe. gDNAs were digested with *XbaI* and *EcoRI*. Upper, left panel, the obtained results; upper, right panel, expected sizes if a double cross-over occurred; Bottom, left panel, expected sizes if a single cross-over happened at the 5-end; Bottom, right panel, expected sizes if a single cross-over happened at the 3-end. At the result panel, the size of the integrated band with 5-probe was between 5 and 6 kb and the exact size was not indicated, same went to the result from the *TK* probe.

3.2.3. The TK encoding sequence might still exist in the integrant but appears not to be active

Despite adding ganciclovir, the parasites quickly recovered after a few days whereas the TK probe also yielded a positive signal in hybridisation (Figure 3.4). It is probable that either the TK activity was not efficient or there was no TK function at all. We carried out the PCR with TK specific primers and genomic DNAs from these clones. The primers TK gene F/R amplified a product of 605 bp from the 1131 bp coding sequence of *TK* gene. The TK probe was also from the same primers but with the DNA template from initial pHTK Δ PV1 vector. For control, we used a pair of primers to amplify the full length *PfPV1* coding sequence. The PV1 sequence was positive in all clones (Figure 3.6 B), confirming that the *PV1* gene locus was not disrupted. Meanwhile, the PCR of TK specific primers yielded a questionable result, inconsistent with the Southern blot. The expected 605 bp fragment was positive in gDNAs from episomal pHTK Δ PV1 containing parasite and mixed population of 3cyc-WG parasites. However, none of the clones yielded a product at 605 bp, but a faint band around 1 kb (Figure 3.6 A). We could not exclude the possibility that these are unspecific, but they only occur in gDNAs from single clones, not in gDNA from mixed population. Giving the fact that the integrated pHTK Δ PV1 parasites survived in ganciclovir, the TK probe (amplified from the same specific primers) yielded positive results for the clones in Southern blot but not the correct size in the PCR, we assumed that somehow upon the integration into the chromosome DNA, the *TK* gene rearranged and caused no toxic effect to parasite on ganciclovir treatment. The inefficiency of the TK selection system has previously been reported [see Introduction 1.5.2.2, (Duraisingh *et al.*, 2003a; Maier *et al.*, 2006)] with the explanation of insufficient TK activity from one copy upon single cross-over recombination. To our knowledge, this is the first report of a possible inactivation of the *TK* in the negative selection system in *P. falciparum*. In an attempt to analyse the sequence of the 1 kb fragment from the PCR above, we failed to clone them into subcloning pJET1 vector (Fermentas) and the event for TK was not further analysed.

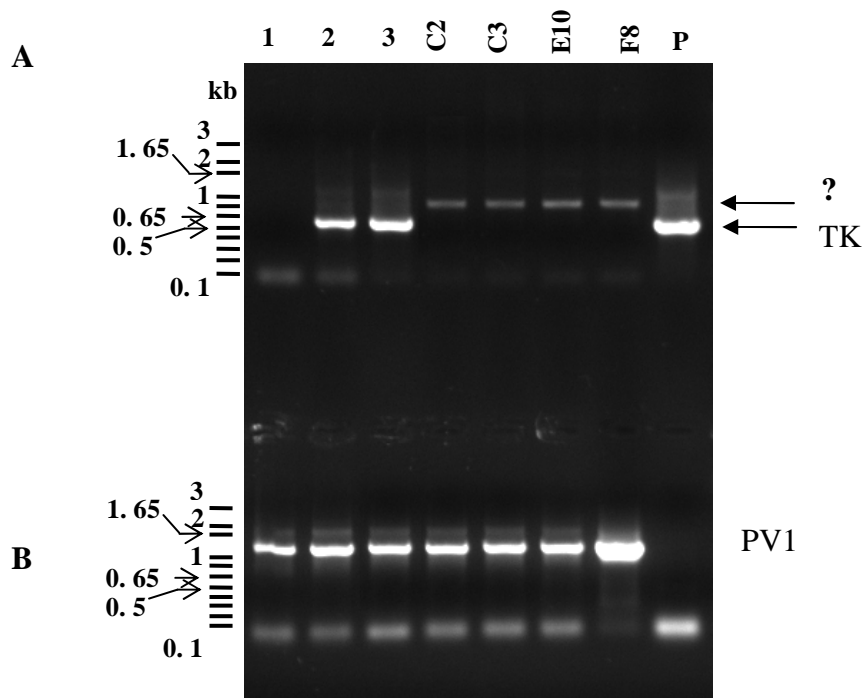


Figure 3.6. Inability to amplify the specific TK fragment from pHTKΔPV1-integrated parasite clones. (A), PCR by TK gene F/R primer, product: 605 bps. (B), PCR by PV1-XhoF/PV1-AvrR primers, amplify full length *PV1*, product at 1372 bps. Lane 1, 3D7 wild type parasite. Lane 2, episomal pHTKΔPV1 containing parasite. Lane 3, mixed population parasite after 3 cyc WR + Ganciclovir. Lane C2, C3, E10, F8: single clone, respectively. Lane (P), pHTKΔPV1 vector control. PCR components were followed standard conditions. PCR program: 35 cycles of 95°C/30 sec, 50°C/30 sec, 68°C/ 1min 30 sec. The question mark depicts the unknown 1 kb product from single clones.

3.2.4. Analysis of transfectants with the DHFR probe

Probing the blot with the hDHFR probe revealed an ambiguous result. The hDHFR probe was amplified by DHFR probe F/R primers, encompassing the last 250 bps of *hDHFR* gene and 62 bps of *hrp2* - 3' region. Theoretically, the hDHFR probe would detect a 0.85 kb fragment from *XbaI* and *EcoRI* double digested DNA containing the hDHFR cassette (CAM 5' - *hDHFR* gene - *hrp2*-3') used in this study (see Figure 3.5 for the schematic RE map). Indeed, there was no band at 3D7 parasite (Figure 3.7 B, lane 1), confirming the absence of *hDHFR* in wild type genome. The 0.85 kb fragment was observed in pHTKΔPV1 control, the episomal plasmid and the DNA from 2 and 3 WR cycles. Upon the negative selection by ganciclovir, the 0.85 kb band was invisible, as shown in 2 cyc-WG parasites and the single clones C2, C3, E10 and F8. The PCR with hDHFR probe primers were positive in all clones (Figure 3.7 A).

Results

Thus the invisibility of the 0.85 kb fragment in Southern blot analysis is very likely because of the low copy number of hDHFR cassette once the plasmid integrated into the chromosome. As shown in Figure 3.7 B, the hDHFR signal was visible only in episomal plasmid containing parasites. There were other faint bands around 6 and 9 kb in all pHTK Δ PV1 containing parasites, presumably unspecific signals from the plasmid. Probing the blot from single clones with the hDHFR probe also revealed the band at 9kb. The size of pHTK Δ PV1 is 9257 bp and hybridisation of the hDHFR probe with the digested pHTK Δ PV1 control detected a specific band at 0.85 kb and a faint undigested plasmid signal slightly higher than the 9 kb band from genomic DNA of the clones (Figure 3.7 B, lane P). We do not speculate that the 9 kb band is the result from the integration into other gene locus than *PfPV1*. There are several reasons supporting this interpretation. First, the parasites resist against WR implicating that the hDHFR is fully active. Since the first *Xba*I site is inside the hDHFR gene it is unlikely that this site was altered. The second *Xba*I is next to *Eco*RI in the multiple cloning site of the original vector (see Figure 3.5 for the schematic RE map), meaning both two sites are at the edge of the 3' homologous region and naturally these sites will not be included in the cross-over recombination. Hence these regions always stick together with the hDHFR cassette. While *Eco*RI activity is affected by site preferences and star activity, *Xba*I is not. The digestion was completed as shown in the blot, hence in any possibility, episomal or integrated hDHFR cassette (even the unspecific integration) would always react with the specific probe to give a signal at 0.85 kb. Moreover, if the integration happened at an unrelated gene locus, the PV1- 5' and 3' probe would detect other cross-reacted bands than the endogenous 4.1 kb/ PV1- 5' probe (Figure 3.3), 4.2 kb/PV1 3' probe (Figure 3.4) and the integrated band 5.4 kb from the PV1- 5' probe (Figure 3.3).

To further confirm the targeting of pHTK Δ PV1 into the right locus on chromosome 11, we attempted to undertake the pulse field gel electrophoresis (PFGE) and hybridise the membrane with both PV1 probe and hDHFR probe. Unfortunately, at the point of this experiment, despite several trials, we failed to establish the PFGE condition and could not provide more evidence for the targeting of pHTK Δ PV1 into the *PfPV1* locus. Nevertheless, with all the analysed data above, we firmly suggest that the pHTK Δ PV1 integrated into the *PfPV1* locus on chromosome 11 in a manner

Results

that maintained both the endogenous locus, introduced the WR resistance marker - the *hDHFR* gene as well as inactivated the *TK* gene.

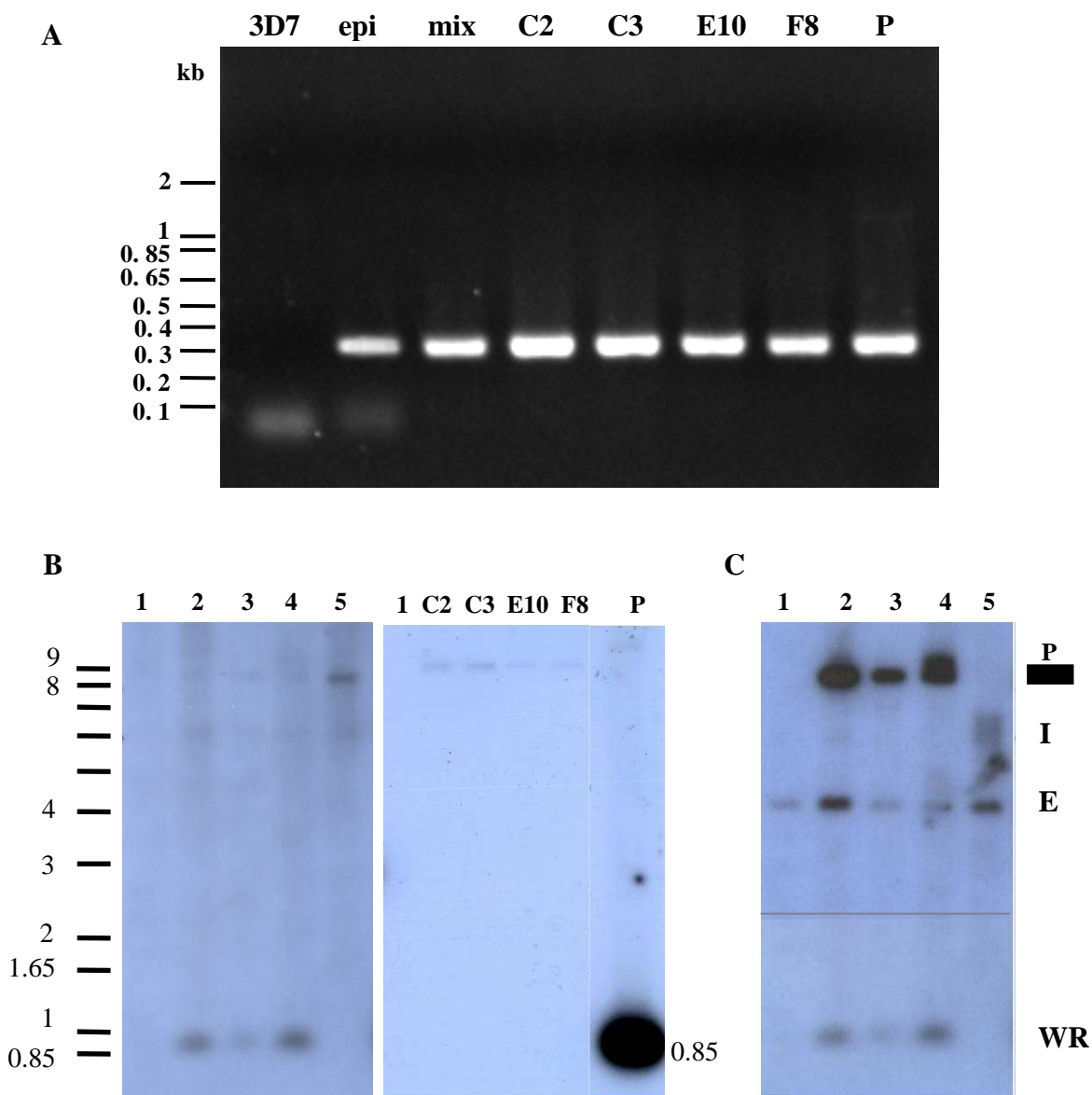


Figure 3.7 Analysis of the integrated pTKΔPV1 into *P. falciparum* by the hDHFR probe. (A). A specific fragment of *hDHFR* (312 bps) was amplified in all clones, the primer pair hDHFR probe F/R was used for both PCR and for the probe in southern blot. 3D7: parental parasite; epi: episomal pHTKΔPV1 containing parasite (cycle 0 of WR); mix: parasites in mixed population after adding ganciclovir into cycle 3 of WR; C2, C3, E10, F8: single clone, respectively; P: pHTKΔPV1 plasmid control. The amount of DNA input might not be the same in all reactions therefore the product signal intensity also varies. **(B).** Southern blot with hDHFR probe. Lane 1, 3D7 parental parasite; lane 2, episomal pHTKΔPV1 containing parasite (cycle 0 of WR); lane 3, pHTKΔPV1 parasite, cycle 2; lane 4, pHTKΔPV1 parasite, cycle 3; lane 5, 2 cyc-WG parasite, ganciclovir was added after cycle 2 of WR; lane P, signal from 0.5 μg digested pHTKΔPV1 plasmid. Because of the strong signal at 0.85 kb from plasmid, the lane was cut from the membrane after the first exposure. Lane C2, C3, E10 and F8: single clone, respectively. **(C),** overlap of the result from Figure 3.2 B (PV1 5' probe) and Figure 3.6 B, left panel (hDHFR probe). The membranes for both probes were identical, P, plasmid band; I, integrated band; E, endogenous PV1 band; WR, hDHFR band.

Results

3.2.5. The PfPV1 appears to be essential for asexual stage development of *P. falciparum*

As shown in Figure 3.6 B, the full length PfPV1 protein encoding sequence is still intact, we checked the expression of PfPV1 protein by Western blot (Figure 3.8). All clones express a positive band at around 55kDa, similar to the wild type 3D7 parasite, indicating that the *PfPV1* gene is fully expressed despite the integration of the transfected vector into the chromosome.

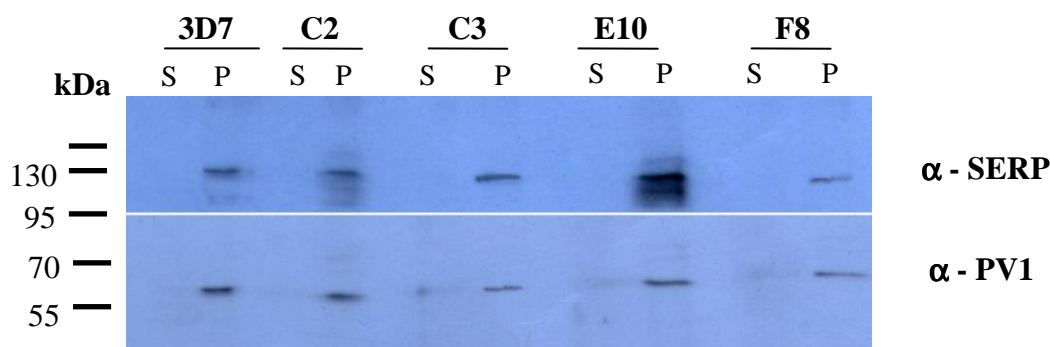
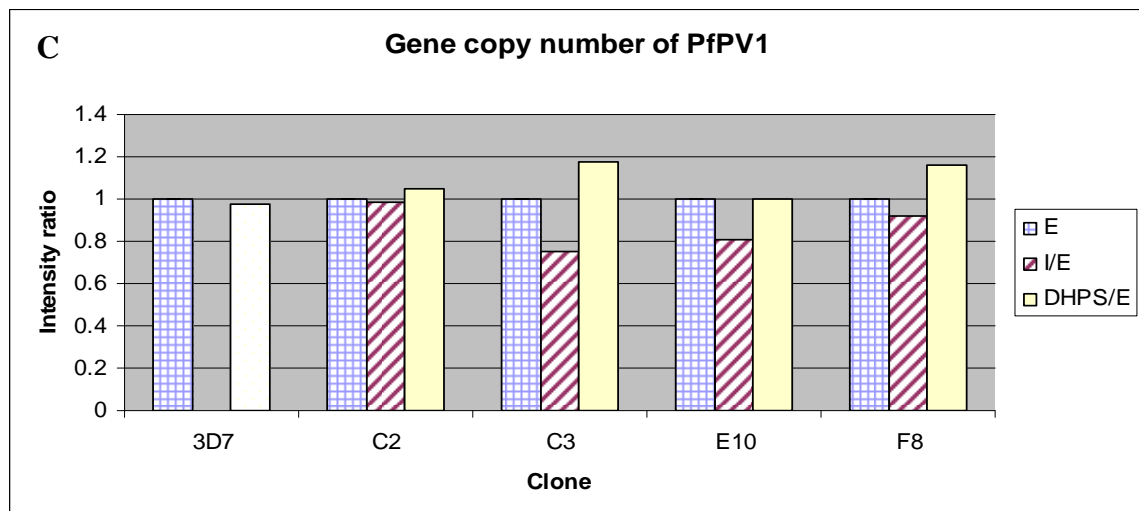
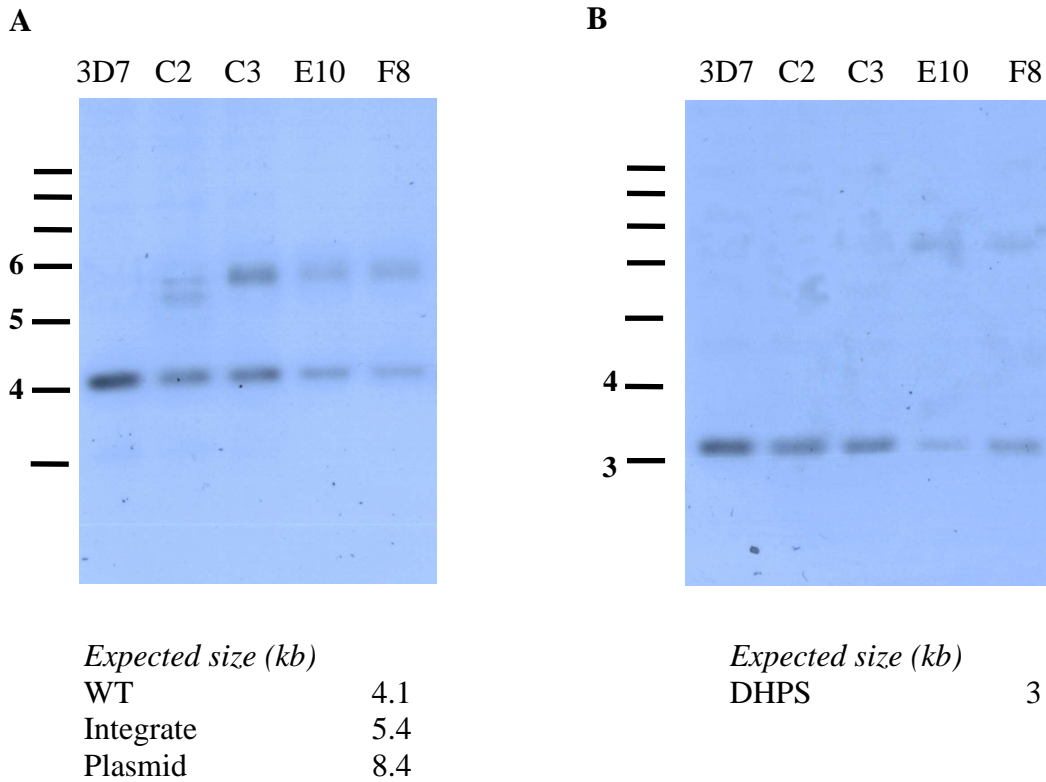


Figure 3.8. Protein PfPV1 still expresses in pHTKΔPV1-integrated clones. A total of 1×10^7 cell equivalents were loaded and probed with anti-SERP as the PV marker and anti-PV1 antibodies. Size marker is shown in kDa. Cell fractionation by SLO was carried out as described in Material and Methods. S: supernatant from SLO lysis. P: pellet after SLO lysis, this fraction contains the PV and the parasite proteins.

From the Southern blot in Figure 3.3, we noticed that the signal intensity of the endogenous PV1 band is visibly equal to that of integrated band. We then carried out the quantitative Southern blot (Figure 3.9), comparing the signal of the endogenous band from the blot hybridised with the PV1-5' probe and the signal from a probe against the single copy gene dihydropteroate synthase (*DHPS*). The intensities of the bands were determined by Multigauge Software Fujifilm (Figure 3.9 C). In PV1-5' probed blot, the endogenous 4.1 kb fragment (E) and the integrated 5.4 kb band (I) were observed at close ratio 1:1 in all clones (Figure 3.9C). The same blot was stripped and hybridised with DHPS probe. We observed the 3 kb DHPS fragment in all parasites (Figure 3.9 B). Comparing the signal intensity of the DHPS fragment and the endogenous PV1 band we verified the single copy of the PV1 gene as well as the integrated band (Figure 3.9 C). We assumed that the parasite has duplicated the PV1 locus before integration to accommodate both the selection cassette and the

Results

maintenance of the endogenous gene. This suggests that PfPV1 has an important, if not essential function for *P. falciparum* during their erythrocyte development. Because of the importance of the gene, it is not easily possible to disrupt the endogenous locus.



Results

Figure 3.9. Quantitative southern blot confirms the single copy of endogenous *PfPV1* locus after the integration. To ensure an equal loading, the blot was first probed with the PV1-5' fragment (A), stripped and re-probed with the DHPS probe (B). The 648 bps DHPS probe was amplified by the pair of primer DHPS-F/DHPS-R.(C), density measurement of *PfPV1*-related band. Signal from the endogenous band of PV1-5 end probe in each lane was compared with the respective lane at the DHPS probed hybridization by density measurement (Multigauge Software, Fujifilm). All the signal intensities were at closely 1:1 ratio, ensuring the single copy of *PfPV1* gene. Lane 3D7; parental 3D7 cell line; lane C2, C3, E10, F8: single clones, respectively. E: *PV1* endogenous band; I: integrated band; I/E: ratio of integration band vs *PV1* endogenous band; DHPS/E: ratio of the single copy *DHPS* gene vs *PV1* endogenous band.

3.3. Strategy two: episomal expression of PV1-GFP followed by integration into the endogenous PV1 coding region

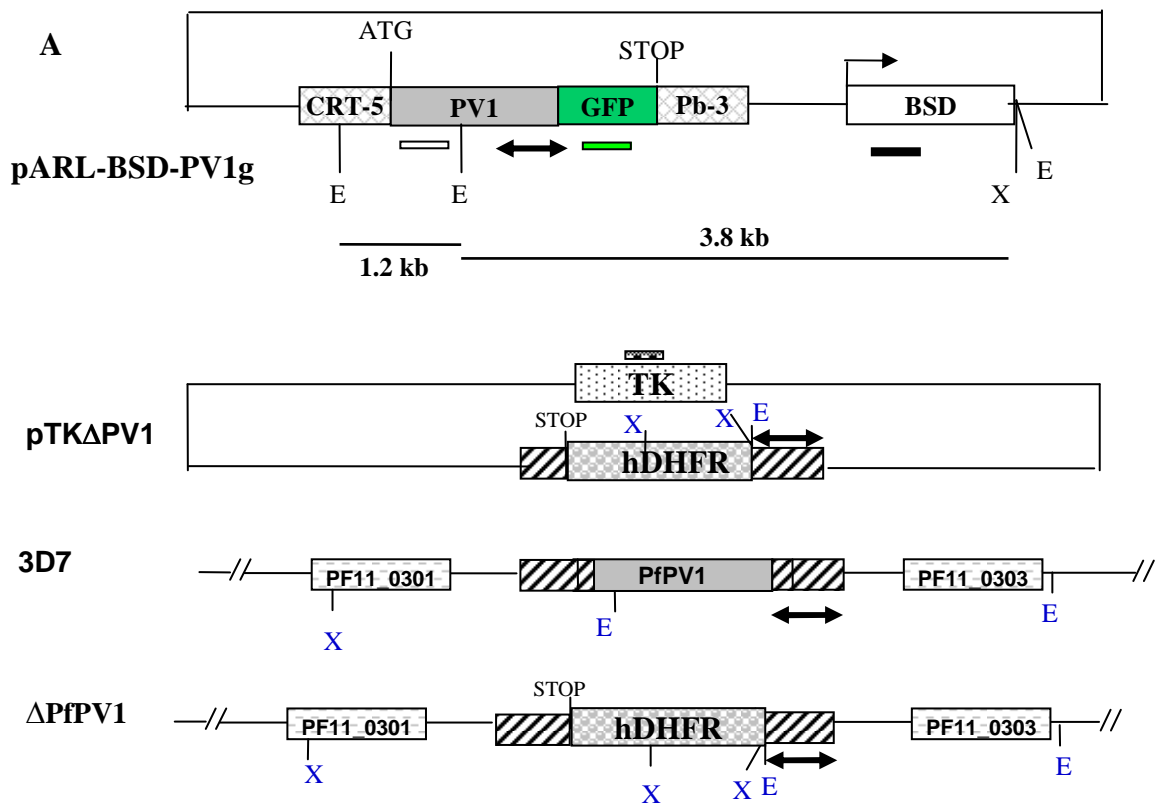
3.3.1. The episomal pHTK Δ PV1 in the double transfected parasites only disappears after negative selection with ganciclovir

As it appeared that the deletion of PV1 might be lethal, we designed a complementation experiment. We expected to be able to disrupt the endogenous gene locus through the pHTK Δ PV1 vector and concomitantly express a copy of *PfPV1* from an episomal plasmid, which should not recombine with the endogenous gene locus. For this purpose, parasites already bearing the episomal pHTK Δ PV1 were co-transfected with the pARL-BSD-PV1g vector containing a Blasticidin S deaminase (BSD) cassette as selectable marker. The *PfPV1* was fused to the N-terminus of GFP and the fusion PV1-GFP encoding sequence was controlled by the *CRT-5* promoter (Figure 3.10A). Double transfected parasites were grown under blasticidin S pressure and cycles of WR99210. Using the fluorescent microscopy, we observed the glowing of the fusion PV1GFP protein and its localization in the PV (Figure 3.11 A). Thus the episomal *PV1GFP* transgene could be expressed in blood stage parasites. After 3 cycles of WR, ganciclovir was added. Parasites were dead and re-appeared after 10 days. We then isolated single clones by limiting dilution and carried out the Southern blot hybridisation.

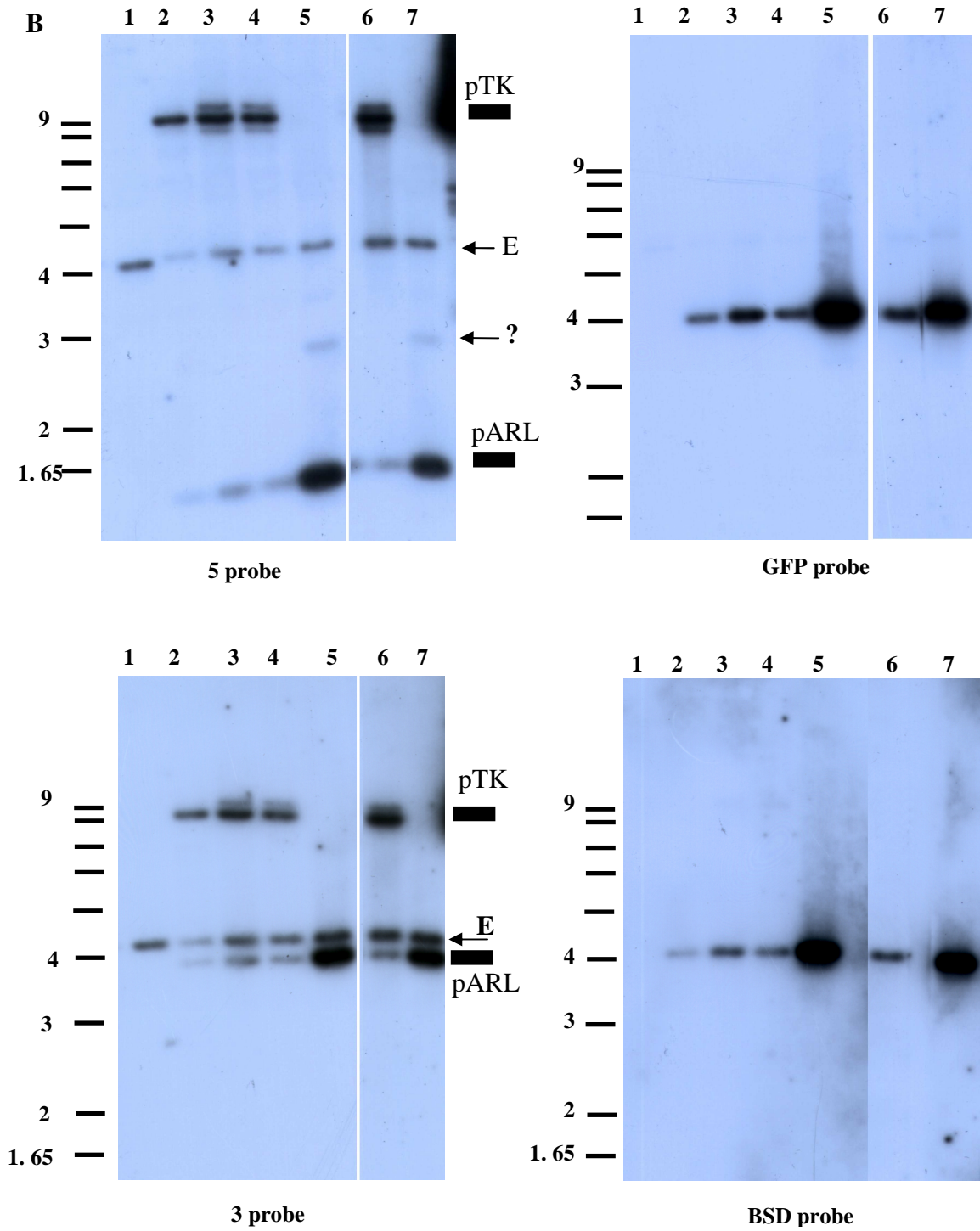
We first analysed the mixed population of double transfected parasites, using gDNAs from each cycle of WR (Figure 3. 10 B). The pARL-BSD-PV1g existing episomally can be detected at a 3.8 kb band with PV1-3' probe as well as the BSD specific and the GFP probe. In all lanes except the wild type 3D7, we also observed the expected

Results

1.2 kb fragment from pARL-BSD-PV1g plasmid when incubating the blot with PV1-5' probe. The PV1-5' probe also gave a positive fragment of pHTK Δ PV1 episome (8.4 kb band) even after prolonged more than 3 cycles of WR (Figure 3.10 B, lane 6). Similar to the pHTK Δ PV1 single transfected (Figure 3.3 B, lane 5), in the double transfected parasites, the episomal pHTK Δ PV1 band only disappeared once ganciclovir was added to the culture, as shown in Figure 3.10 B, lane 5, from the 3rd WR cycling population. However, the expected 5.4 kb integration band was not present; instead we detected a minor band of approximately > 2.5kb (Figure 3.10 B, 5' probe, lane 5 and 7). The possibility that this fragment is due to cross-reactivity between the PV1-5' probe and the pARL-BSD-PV1g plasmid was ruled out because this band was absent from the WR cycling, non-ganciclovir population and from the control pHTK Δ PV1 and pARL-BSD-PV1g plasmid.



Results



Size (kb) \ Probe	PV1-5'	PV1-3'	GFP	BSD
Endogenous	4.1	4.2	-	-
Integration from pHTKΔPV1	5.4	4.2	-	-
pHTKΔPV1	8.4	8.4	-	-
pARL-BSD-PV1g	1.2	3.8	3.8	3.8

Results

Figure 3.10 Genotypic analysis of double transfected parasites with pHTK Δ PV1 and pARL-BSD-PV1g vector. (A), Schematic representation of pARL-BSD-PV1g vector, pHTK Δ PV1 vector, the wild type locus (3D7) of PfPV1 and the expected integration event. Details on pHTK Δ PV1 vector and chromosome DNA are referred in Figure 3.5A. For pARL-BSD-PV1g vector, the start codon ATG and the stop codon are displayed. The fusion PV1-GFP protein was controlled by *P. falciparum* CRT promoter and *P. berghei dhfr-ts* 3' UTR. Left to right arrow: the direction of BSD cassette. The RE used for diagnostic digest were *Xba*I (X) and *Eco*RI (E). Probes for southern blot are depicted based on pARL-BSD-PV1g vector: 5' probe, open box (□); 3' probe: solid line with arrowhead (—▶), BSD probe: solid box (■). For the rest of plausible event, see Figure 3.5A. The expected sizes of diagnostic bands are indicated in kb. (B), Southern blot of double transfected parasites with 4 different probes: PV1-5', PV1-3', BSD and GFP probe. The respective probe for the blot is labeled. gDNAs were digested with *Xba*I + *Eco*RI. Membranes were hybridised with PV1-5' and GFP probe first, stripped and re-probed with PV1-3' and BSD probe, respectively. Lane 1, 3D7 wild type parasite; lane 2, lane 3 and lane 4, double transfected parasites after first, second and third cycle of WR, respectively. During the period of WR cycling, parasites were always put under pressure of BSD. Lane 5, after three cycles of WR, ganciclovir was added, parasites found dead and reappeared after 10 days. Lane 6, double transfected parasites after 4 cycles of WR, no ganciclovir; lane 7, parasites derived from lane 5, continued growing without BSD but WR and ganciclovir in 2 months. The strong signal from the plasmid controls might cause the noise background after prolonged exposure. We removed these lane after the first exposure and marked it as the solid signal, pTK for pHTK Δ PV1 and pARL for pARL-BSD-PV1g vector; none other band out of the expected fragments was detected. E, endogenous band.

3.3.2. The *PfPV1* gene might act as selectable marker itself to maintain the pARL-BSD-PV1g vector when blasticidin S was removed

In addition to isolate single parasites, another batch of post-ganciclovir population (DNA after 3 cycles of WR, added ganciclovir) was removed from blasticidin S pressure for more than 2 months. Surprisingly, the signal corresponding to the plasmid pARL-BSD-PV1g was still detected by all probes: PV1-5', PV1-3', GFP and BSD specific probe (Figure 3.10 B, lane 7). This phenomenon led to the question why parasites kept maintaining the *BSD* gene without the selection with blasticidin S. One possibility is, if PV1 is essential, and the endogenous locus is altered, the episomal copy may act as selectable marker itself and keep maintaining the pARL-BSD-Pv1g vector even though the drug pressure was already removed. Another interesting point is at the disappearance of the pHTK Δ PV1 fragment, the intensity of the pARL-BSD-PV1 signal was much stronger in comparison to the endogenous band (Figure 3.10 B, lane 5 and 7).

3.3.3. Single clones from double transfected parasites possess different genotypes

We were able to isolate 19 clones (out of 96 wells) from the mixed population after adding ganciclovir into 3 cycles of WR parasites (continuously under the pressure of blasticidin S). This number of clones was acceptable considering that 30 parasites were seeded into the 96 well-microplate. Among these single lines, clones D3 and F9 were the two slowest growing clones, especially D3 clone. This parasite line took 2 weeks longer than other clones to have enough material for the first DNA extraction. The D3 clone did not react with anti-GFP antibody in the immunoblot and did not glow under the fluorescent microscope; hence it provided the evidence of loss of the pARL-BSD-PV1g vector in this line (Figure 3.11). For later experiments, we cultured the D3 clone without adding blasticidin S. On the other hand, the F9 clone only slowly grew at the beginning of recovering from the 96-microwell plate. Once the parasites fully recovered under the normal culture condition, the F9 parasite grew as normal as the others. The GFP expression of F9 clone was also confirmed by fluorescent microscopy and immunoblotting (Figure 3.11). We picked up B10 clone as representative for normal growth lines.

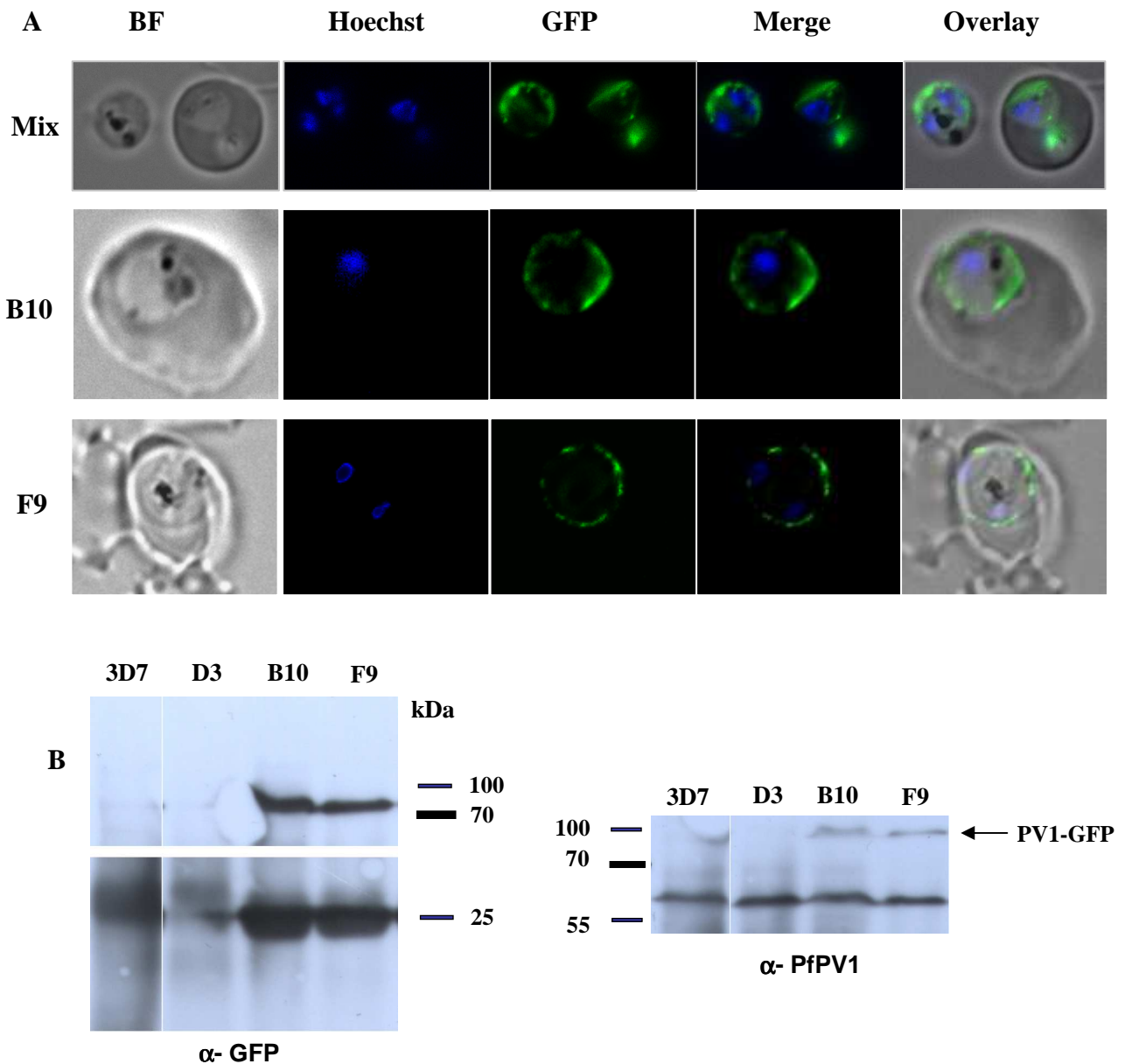


Figure 3.11. Not all clones from the double transfected parasites can co-express both PV1 and PV1GFP fusion protein. (A), Fluorescence microscopy of the mixed population of double transfected parasites and the B10 and F9 clone. The D3 clone did not glow and is not shown here. The nuclei were stained with Hoechst 33258 (blue). The PV1-GFP fusion protein was observed in a region surrounding the parasite (green). The merging of two colour channels was shown, as well the overlay with bright field (BF). (B), Immunoblot of double transfected parasite clones. A total of 1×10^7 cell equivalents after SLO fractionation were loaded and probed with anti-GFP or anti-PV1 antibody. Size marker is shown in kDa. PfPV1 protein is expected at 55 kDa but always appears slightly higher than its calculated MW. PV1GFP fusion protein is expected at ~80 kDa, GFP alone is around 26 kDa. In the blot with anti-GFP antibody, the parasite 3D7 did not react as expected. The dark signal on the 3D7 lane was from the haemoglobin contamination. D3 clone also did not react with anti-GFP antibody, provided the evidence of loss of the pARL-BSD-PV1g vector in this line. The B10 and F9 clone both had the signal of PV1GFP fusion protein at ~80 kDa and the degraded GFP signal at ~26 kDa. In the blot with anti-PV1 antibody, the endogenous PfPV1 protein was observed in all lanes and the fusion PV1GFP protein was only detected at B10 and F9 clone.

Results

From the fact that the mixed population kept *BSD* without drug pressure even after 2 months, we removed blasticidin S on clonal parasites for 3 weeks and analysed by Southern blot. Genomic DNAs were collected right after 3 weeks of non-blasticidin. We continuously applied the WR pressure during the removal of blasticidin S. Because of time limitations, we only carried out the Southern blot using PV1-5' and TK probes. In agreement with mixed population, single clones F9 and B10 in PV1-5' probed blot gave a strong 1.2 kb signal from pARL-BSD-PV1g backbone vector even after 3 weeks of blasticidin S removal (Figure 3.12 A). The unknown >2.5 kb band which appeared at mixed population (Figure 3.10, PV1-5' probe, lane 5, lane 7 and Figure 3.12 A) also occurred in both clone F9 and B10. There is one band at ~5kb from the F9 culture before blasticidin removal. This uncharacterised band also occurred in the pARL-BSD-PV1g control lane in this particular blot. Because the control was directly loaded from the digested plasmid and the identical initial plasmid sample had been used for the blot in Figure 3.10 had previously shown to result in only the 1.2 kb fragment (Figure 3.10, PV1-5' probe), we considered this ~5 kb signal merely a cross-reaction which occurred only in this current experiment. Southern blot of clone F9 showed an ambiguous result, especially the high molecular weight and fuzzy bands at unknown sizes detected before the removal of blasticidin S (Figure 3.12A, F9 clone). These bands were absent from both populations of B10 clone (with or without blasticidin S). However, after removing blasticidin S, the F9 clone gave the same result as B10 clone. Due to the time limitation, we did not further investigate if the blasticidin S reversion could cause any effect on the double transfected parasites.

The D3 clone has obviously lost the pARL-BSD-PV1g vector since the 1.2 kb band disappeared. Interestingly, while losing the episomal *PfPVI* copy, the D3 clone displayed a similar pattern to parasites with single transfected pHTK Δ PV1: a band at the same size of the endogenous *PfPVI* gene (4.1 kb) and another band at integrated size (5.4 kb) (Figure 3.12 A, PV1-5' probe). Moreover, while the *TK* gene disappeared at F9 and B10 clones, faintly presented at mixed population, it appeared at D3 clone in the same pattern of pHTK Δ PV1 single transfected parasite (Figure 3.12 B). The disappearance of *TK* in the F9 and B10 clone led to the assumption that the negative selection indeed created a pressure to force the integration of pHTK Δ PV1 removing the *TK* encoding gene. However, the integration might not happen at the right locus because the expected fragment (5.4 kb) was not observed.

Results

Integration PCRs were also performed but no product was obtained despite the combination of alternative integration specific primers. To further analyse the genotype of the double transfected parasites, we performed PFGE and the blot was first probed with *PfPV1* probe and *Exp-1* probe as control of a gene locus on chromosome 11 (Figure 3.12 C). We have planned to strip the blot and re-hybridise the blot with the hDHFR probe and the BSD probe. However, because of the time consuming required for completely removing the old probe, these analyses could not be carried out. The DNA blocks used for the PFGE were from blasticidin-treated F9 clone and non-blasticidin D3 clone. The PV1 internal probe using in the PFGE confirmed that the Pfpv1 gene was undisrupted on chromosome 11 in both double transfected F9 clone and D3 clone which share the same genotype as pHTK Δ PV1 transfected parasite. The Pfpv1 internal probe can also detect the Pfpv1 sequence in the entire pARL-BSD-PV1g plasmid. We suggest that the smeary pattern on F9 clone was from the pARL-BSD-PV1g plasmid. Whether that pattern was from the episome or integrated pARL-BSD-PV1g into another chromosome was difficult to differentiate and require more controlled probes. Unfortunately, due to time constraints, we did not continue with these analyses.

With these data above, once again, it is confirmed that the *PfPV1* gene locus is not easily disruptable. Although there is the episomal copy of the gene in double transfected parasites, it is not controlled by the endogenous regulators. Moreover, the Pfpv1 was fused to GFP and this might affect function of the protein. Hence, the over-expressed fusion protein might cause negative effect or unable to fully complement the endogenous gene. We therefore conclude that the Pfpv1 plays an essential function in erythrocytic development of *P. falciparum*.

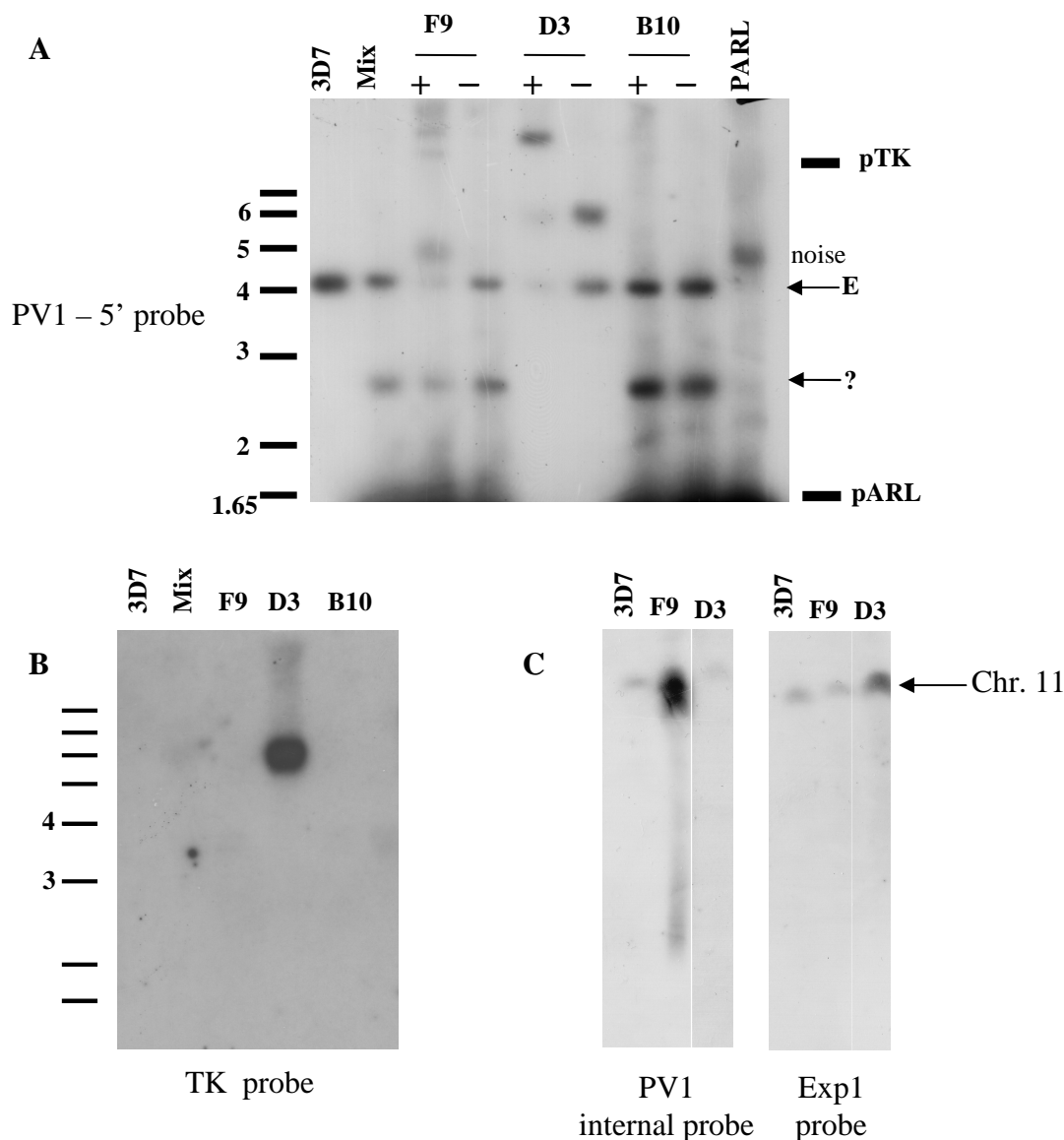


Figure 3.12 Single clones from double transfected parasites display different genotypes. (A), Southern blot with the PV1-5' probe. Lane 3D7, wild type parasite; Mix, parasites after three cycles of WR99210, + ganciclovir, + blasticidin S; F9, D3, B10, single clone isolated from the mixed population, respectively. (+), blasticidin S was continuously applied on the culture; (–), blasticidin S was removed from the culture in 3 weeks. The signal from 1.2 kb fragment of episomal pARL-BSD-PV1g plasmid was too strong thus the respective part on the membrane was removed after the first exposure. Even though, the intensified band can still be observed here. (B), Southern blot with TK probe confirmed for the first time the loss of *TK* gene. DNA samples as in blot A, except this time all the DNAs from clones were from (+) blasticidin S – treated parasites. pTK signal from pHTKΔPV1 backbone and pARL for pARL-BSD-PV1g vector; E, endogenous band; noise: the cross-reacted signal from the hybridization. The band at >2.5 kb was presented with a question mark. (C). PFGE analysis of F9 and D3 clone. *Exp1* probe is used as a control of chromosome 11. The PV1 internal probe was specific for intact PfPV1 encoding sequence hence it occurs on endogenous locus and the episomal copy from pARL-BSD-PV1g. PFGE condition as shown in Material and Methods.

Results

3.4. Identification of interaction partners of PfPV1 by GST pull-down assay

In order to identify proteins that interact with PfPV1, in previous experiments we had studied the immunoprecipitation and blue native PAGE (Nyalwidhe, unpublished data) but none of these identified any interaction. Here we carried out the pull-down assay of the recombinant PfPV1-GST fusion protein and the parasite extract.

3.4.1. Purification of the recombinant PfPV1-GST protein

The recombinant PfPV1-GST fusion protein was over-expressed in *E. coli* (Material and Methods). The fusion protein was partially insoluble (data not shown) but the soluble portion was much higher. We purified the soluble fraction following the instruction from the manufacturer (Material and Methods). The purified PfPV1-GST was obtained at apparent 80 kDa (Figure 3.13 A). Antibody to GST recognized both the PfPV1-GST fusion protein and the degraded GST (Figure 3.13 B). We used this purified protein for further experiments.

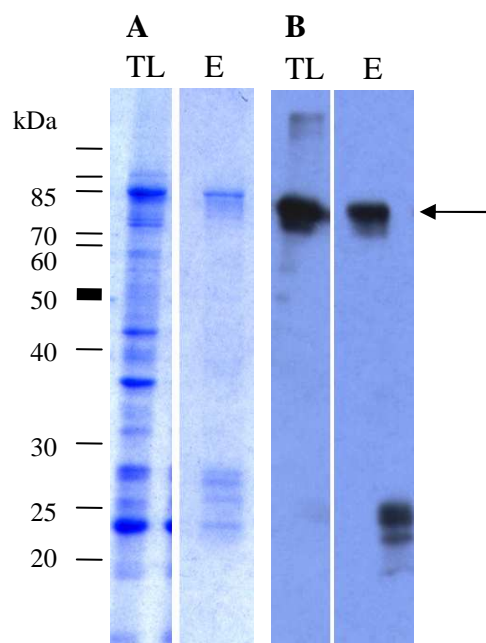
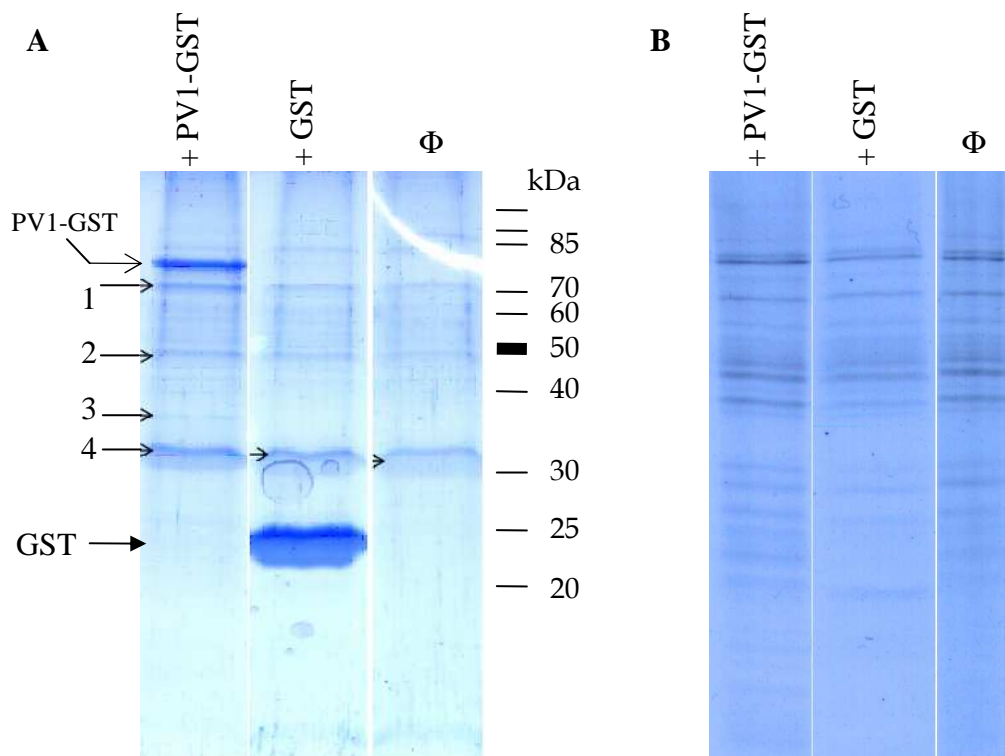


Figure 3.13 Purification of PfPV1-GST fusion protein. (A) SDS-PAGE of purified PfPV1-GST fusion protein. (B) Western blot, with anti-GST antibody. Lane TL, total lysate from *E. coli* cell pellet. The pellet was resuspended, lysed, separated by centrifugation and the supernatant was further purified (Material and Methods). Lane E, final elution after purification. Sample amount was loaded equivalent to a volume of 200 μ l of initial bacterial culture. Protein ladder is displayed in kDa. PfPV1-GST fusion protein was expressed at approximately 80kDa, pointed at arrow bar. The 26 kDa signal on panel B was from the degradation of GST alone. Anti-PfPV1 antibody also recognised the PfPV1GST fusion protein, but because of the high background blot, the data is not shown here.

Results

3.4.2. GST pull-down assay was not able to detect any interaction

To identify PfPV1 interacting proteins we used the chimeric PfPV1-GST protein as bait in the GST pull-down assay. Late trophozoites of 3D7 parasites were fractionated by SLO and the soluble proteins after SLO (SLO-SF) were incubated with the PfPV1-GST protein, along with the control of GST protein and the Glutathione Sepharose 4B beads. We did not detect any distinguished band in three samples, except for some fragments containing PfPV1 peptides exclusively appeared at the PfPV1-GST containing test tube (Figure 3.14A, band number 1 and 3), probably the degraded product from PfPV1-GST. The parasite extract was also cross-reacting with the Glutathione sepharose beads since bands were observed at the test tube of parasite extraction bound to beads without bait protein (Figure 3.14, lane Φ). We analysed some most abundantly identical bands, they were PfEF (band number 2) and PfGADPH (band 4). To increase the sensitivity of the assay, we labelled the parasite proteins with ^{35}S -Methionine. However, we still did not detect any difference, and the cross-reacting bands were identical in all samples. Therefore, at this point, under the conditions of this experiment, we cannot detect any interacting partners of PfPV1.



Results

Figure 3.14 GST pull-down assay of PfPV1-GST fusion protein and parasite extract from SLO pellet did not detect any interacting proteins. Three test tubes were prepared for the assay, each tube contained Glutathione Sepharose 4B beads, SLO supernatant extracted from 2×10^8 parasites and the chimeric PfPV1-GST protein (lane +PV1-GST), GST protein (lane +GST) or beads without bait protein (lane Φ). **(A)** Coomassive gel prepared for mass spectrometry, parasite proteins were not labeled. Bands were identified by Mass spectrometry: 1. PfPV1; 2, Pfef; 3, PfPV1; 4, PfGADPH. The PV1-GST fusion protein and GST protein in the test tube were marked with arrow. Protein ladder was shown in kDa. **(B)** X-ray film exposure from pull-down assay with ^{35}S - labeled parasite proteins also gave identical bands in all test tubes.

4. Discussion

Malaria is one of the most lethal infectious diseases worldwide. Understanding the biology of the causative agent *Plasmodium* will lead to better control of the disease. The biogenesis and maintenance of the parasitophorous vacuole within the infected erythrocyte is an essential factor for parasite survival. The PV has been postulated to be involved in various pivotal functions, however little is known about the PV contents and their respective functions. Our group had previously provided the first PV's proteome research (Nyalwidhe and Lingelbach, 2006) and has continuously exposed more members of this important compartment. Among several hypothetical proteins found in the first round of analysis, there were two proteins predictably containing a signal peptide, hence in agreement with being exported from the parasite, adding further support to the validity of our data (Nyalwidhe and Lingelbach, 2006). The protein PfPV1 encoded by PF11_0302 gene was further analysed and its location inside the PV was confirmed biochemically and morphologically [(Nyalwidhe and Lingelbach, 2006) and unpublished data]. In order to address the function of this protein we used a gene knock-out strategy by double-crossover and a negative selection (Duraisingh *et al.*, 2002). We also searched for the interacting proteins of PfPV1 using the GST pull-down assay.

4.1. PfPV1 knock-out studies

For the knock-out strategy, we used the negative selection strategy to select the double-crossover recombination. Initially we did not obtain any integration event after the first trial with ganciclovir selection without WR cycling. Therefore we put the knock-out construct transfected parasites on three WR cycles and added ganciclovir afterward. This time we were still unable to delete the encoding gene of PfPV1 protein but interestingly we obtained both endogenous and knock-out band from the specific Southern blot hybridisation and the episomal plasmid was also eliminated (Figure 3.3). Our data also showed that the TK encoding sequence was maintained in the parasite despite the ganciclovir pressure. Concerning the target gene, the same phenomenon was also observed in previous report (Maier *et al.*, 2008). The authors did a large scale gene knock-out work for 83 genes, using the same double-crossover strategy with both pHTK (Duraisingh *et al.*, 2002) and ScCDUP system (Maier *et al.*,

Discussion

2006). There were 3 genes that gave the exact pattern as our result, showed both wild-type and knock-out bands. Maier *et al* did not describe more details about the problem but went to the same conclusion with ours, that the targeting into the endogenous loci was accompanied by a duplication event for maintaining expression of the gene. We concluded that the *PfPVI* gene is essential for in vitro growth.

Our suggestion was further validated by complementing experiment, although the results were confused at the first look. We were not able to obtain the knock-out parasites. Instead we collected various parasite lines with different genotypes in respect of foreign constituents from transfected vectors. There was one clone, the D3 clone which lost the complementary copy of *PfPVI* displayed the same genotype as the single transfected *pHTKΔPV1* parasite clones (Figure 3.12). The D3 clone also kept the TK encoding sequence and displayed both the endogenous and integrated fragment. Meanwhile, the F9 and B10 clone, which expressed the episomal *PfPVI*GFP fusion protein, lost the *TK* and did not generate the correct integration band but integrated into somewhere instead (Figure 3.12).

At a brief look, it was somewhat a surprising result. However, it could be interpreted in several ways. It could be that the intracellular concentration of *PfPVI* is important for the parasites. The episomally chimeric *PfPVI*-GFP protein was controlled by *CRT* promoter but not *PfPVI*'s endogenous promoter. Although the localisation of *PfPVI*GFP protein in the PV was confirmed by microscopy and biochemical experiments, the expression profile could also affect protein activity. Data extracted from PlasmoDB show that, whereas both *CRT* and *PfPVI* are expressed throughout the erythrocytic development stages, the expression intensity percentile of *PfPVI* is always kept at a constant level in respect to the spectrum of all expression intensities at one time point (Figure 4.1). Moreover, the *PfPVI* was fused to GFP and this might affect function of the protein, thus not strong enough to completely compensate the function of the endogenous one. One interesting result is when the episomal *pHTKΔPV1* fragment disappeared, the intensity of *pARL-BSD-PV1* signal was much stronger than the endogenous *PV1* and persistently maintained even after the removal of blasticidin S (Figure 3.9 B, lane 5 and 7). It might be because the parasite needs time to gain enough copies of the episomal *PVI* to keep a proper function.

Discussion

From the results of F9 and B10 clone, we suggested that the episomal expression was limitedly complementing the activity of PfPV1, at least in low level. In these two clones, the loss of the *TK* cassette is an evidence of losing the full length pHTKΔPV1 backbone. We assumed that, under the pressure of negative selection of ganciclovir and to keep the parasite resistant to WR, the *hDHFR* cassette and a possibly unknown part of pHTKΔPV1 must recombine into the parasite chromosomes to eliminate the *TK* cassette. Therefore the unexpected 2.5 kb band (Figure 3.12A) was probably from an unspecific integration which at this point was not identified. We supposed that at the critical point, some parasites did not duplicate the endogenous *PfPV1* locus because of the limitedly complementary expression from episomal copy, as happen in F9 and B10 clone. Conversely, some other parasites, such as D3 clone, for unknown reasons lost the episomal copy of *PfPV1*, and had to duplicate the endogenous locus to maintain the expression and obtained the same genotype as single pHTKΔPV1 transfected parasites (Figure 3.12).

Overall, we were unable to disrupt the *PfPV1* gene, however the integration did happen when the gene was duplicated (Figure 3.9). These data support our suggestion that the PfPV1 is essential for the survival of erythrocytic parasites. One might argue that further data need to be performed to ensure that the locus is open to recombination. We have independently transfected into 3D7 parasite two replacement plasmids. The pARLΔPV1g plasmid contains a fragment of PV1 gene fused to GFP yet the *CRT* promoter region is removed from the vector. Only upon the integration into the *PV1* locus would the GFP express under the endogenous PfPV1 promoter. The second knock-in construct is the pARL-mutPV1 plasmid bearing two silent mutations at the very end of the *PV1* gene. Through the WR cycling we suppose that the single homologous recombination would happen at the *PV1* locus and the integration would be detected by sequencing, the transfected parasites are on culture now. Currently we are also collecting the DNA blocks for PFGE followed by Southern blot to monitor the chromosomes of both experiments: the single and double transfected parasites.

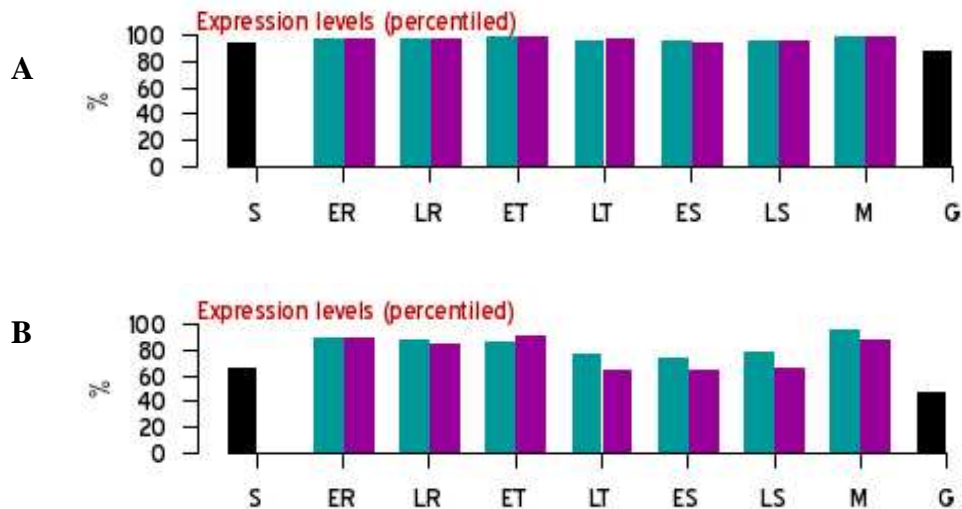


Figure 4.1 Expression profile of PfPV1 (panel A) and CRT protein (panel B). Profiles were taken from PlasmoDB (www.plasmodb.org). Shown is the percentiled expression level of the respective gene relative to all other genes at a time point. Data in green are of parasites synchronised by sorbitol, in purple of parasites synchronised by temperature and in grey is data below the confidence threshold. Data for gametocytes were obtained by sorbitol synchronisation and sporozoite data represent an average of two replicates. Abbreviations: S, sporozoite; ER, early ring; LR, late ring; ET, early trophozoite; LT, late trophozoite; ES, early schizont; LS, late schizont; M, merozoite; G, gametocyte

4.2. A possible genetic re-arrangement by integrated parasites to inactivate TK activity

Several major problems of gene targeting by single cross-over recombination strategy were time consuming by cycles of on/off positive drug selection and in some instances, the persistence of episomal concatamer. It is well established that the episomal plasmids are lost rapidly in the absence of drug selection as they are separated unevenly amongst the daughter parasites whereas the plasmids integrated into the genome are segregated normally with each chromosome (O'Donnell *et al.*, 2001; van Dijk *et al.*, 1995). The unstable nature of the episomally replicating plasmids can be exploited to isolate rare parasites in a transfected population that possess integrated forms. Drug cycling ensures that after subsequent on/off drug cycles, all transfected *P. falciparum* parasites obtained had integrated the plasmid by single cross-over homologous recombination. However, in instances where gene targeting is not favoured, transfected plasmids can change to stably replicating forms (SRFs) that are maintained episomally in the absence of drug selection (O'Donnell *et al.*, 2001). These SRFs are large concatamers of the parental plasmids, comprising

Discussion

from 9 to 15 plasmids in a head-to-tail array. The SRF DNA, although absent of single origin of replication, is effectively segregated between the daughter merozoites even in the absence of pressure selection. And it was proved that the replication happens through both rolling-circle and recombination dependent mechanisms (O'Donnell *et al.*, 2002). Thus even after several cycles of positive selection, the episomal concatemer might still exist and prevent the homologous recombination. To overcome these limitations, we used the negative selection system by the activity of *TK* gene (Duraisingh *et al.*, 2002). The *TK* enzyme converts prodrug such as ganciclovir to toxic metabolites. In principle, the only survival parasites were those with integration by double cross-over recombination, thus deleting the *TK* cassette and incorporating the positive drug marker into the target locus.

The ideal advantage of negative selection by *TK* activity was initially thought to avoid drug cycling and to eliminate the plasmid backbone (Duraisingh *et al.*, 2002), but there have been reports that the drug cycling of positive selection were also required (Kadekoppala *et al.*, 2008) and that some gene disruptions using the *TK* system have resulted in the absence of double crossover while maintaining the episomal plasmid or single crossover with insertion of the full plasmid including the *TK* gene (Duraisingh *et al.*, 2003a; Maier *et al.*, 2006). Our experiments also evidenced that we could not get the integration when adding ganciclovir right after the transfected population was recovered. The integration only happened when negative selection was applied on parasite population after several cycles of WR (Figure 3.3), yet the *TK* sequence was still detected by Southern blot, but not at the specific size by PCR (Figure 3.6).

The fact that pHTK Δ PV1 clones survived after adding ganciclovir while losing the episomal plasmid but still harbouring the *TK* encoding gene was explained by Maier as the insufficient expression of *TK* enzyme from one copy of the gene for potent negative selection (Maier *et al.*, 2006). From our data, we came to a disagreement with the speculation of integrating one copy of the *TK* gene into chromosome. Given that the integrated PV1 and the endogenous PV1 locus is at 1:1 ration (Figure 3.9), the density measurement of the signal in Figure 3.4 showed that the *TK* signal was stronger 2 to 3.5 fold compared to the endogenous signal and, therefore, the integrated PfPV1 band. Moreover, according to the first *TK* negative selection report in *Plasmodium*, the transfected parasites exhibit a marked “bystander effect” on addition

of ganciclovir (Duraisingh *et al.*, 2002). The “bystander effect” is the phenomenon when the neighbouring cells not expressing the negative selectable markers are killed alongside those expressing them. Therefore it is unlikely that the TK activity was not sufficient. We supposed that the concatameric plasmid was integrated into the parasite genome in multiple plasmid backbones. We were unable to amplify a 605 bp specific TK fragment in single clone parasites, but a ~1 kb band (Figure 3.6 A, clone C2, C3, E10 and F8). In the existence of SRF concatamer, no evidence of sequence rearrangement or additional sequence was detected (O'Donnell *et al.*, 2001) and our Southern blot also proved that the original TK was still intact in the episomal plasmid containing parasites (Figure 3.6, lane 2 and 3, mixed population). We assumed that upon integrating, the parasites re-arrange the TK-related sequence to inactivate its activity, therefore prevent the lethal effect from converting ganciclovir to toxic metabolite.

The genetic rearrangements to inactivate *TK* gene had been reported at high frequency in the murine leukemia virus-based vector (Parthasarathi *et al.*, 1995; Varela-Echavarría *et al.*, 1993) used in mammalian cell culture research, not surprisingly because of the nature of retrovirus-based system. In a closer parasitic system, Valdés *et al.* while testing *TK* gene as a negative selection system for *Trypanosoma brucei* reported the loss of TK activity due to the occurrence of point mutations and frameshifts (Valdes *et al.*, 1996). So far there has been no detailed explanation on problems of applying *TK* negative selection in *Plasmodium*. We report here for the first time a possibility of genetic rearrangement of this negative selection marker on transfected DNA upon the integration. It would be clearer if we successfully cloned and sequenced the unspecific ~1kb band appeared in our transfected clones (Figure 3.6). In the content of this thesis, we did not further analyse this event.

4.3. Blasticidin S resistance

Blasticidin S has been successfully used in many *P. falciparum* genetic transfection experiments (Mamoun *et al.*, 1999; Sidhu *et al.*, 2002; Wang *et al.*, 2002). In these studies, transfected parasites were selected through expression of the *Aspergillus* blasticidin S deaminase (*BSD*), which converts blasticidin S to a nontoxic deaminohydroxy derivative. We were surprised when the D3 clone derived from the

Discussion

double transfected parasites lost the BSD-containing vector but still survived under the blasticidin pressure. Although very weak and slowly grown, the D3 clone was able to maintain a parasitemia enough for visibly detected under the microscope. After we detected the positive clone in limiting dilution, to collect enough parasite material for DNA extraction, the D3 clone was 2 weeks delay to other clones. Fluorescent microscopy, immunoblot and Southern blot confirmed the loss of pARL-BSD-PV1g vector in this clone (Figure 3.11 and 3.12, lane D3). Recently, the problem of blasticidin resistance in *P. falciparum* studies has also been reported (Hill *et al.*, 2007). The authors, when attempting to generate a genetic disruption in the FCB parasite, ended up in blasticidin S-resistant parasites that lacked the *BSD* sequence from the transfection plasmid. After some experiments these authors concluded that a mutation in the plasmodial surface anion channel (PSAC) was responsible for blasticidin resistance. They envisioned that the selected changes in PSAC serve to alter its selectivity profile and prohibit blasticidin S access to its intracellular target. However, that resistance could be generated only from the FCB parasite, not from other parasite isolates used in their experiments (HB3, W2, and 7G8). The authors proposed that the FCB isolate presumably carries a permissive genetic background for the selection of required changes in PSAC.

In our case, it is possible that the D3 isolate also generated some alteration in its background thus resistant to blasticidin S. We could not answer whether its resistance was from the altered PSAC or else. So far there has been no report of blasticidin S resistance in the 3D7 parasite isolate. However, in our group we also observed some blasticidin S tolerance occurred only in 3D7 parasites already bearing an *hDHFR*-containing vector (Spork and Baser, personal communication). We therefore agree with Hill's statement, that the acquisition of blasticidin S resistance may require multiple changes at the level of the parasite genome. Therefore, even though the blasticidin S has shown the limitation to its use in transfection, so far the problem has only been observed in the unique background parasites. Given the usefulness of BSD application in many *P. falciparum* single transfections, we suggest that the use of blasticidin S is still reliable in meticulously analysed data.

4.4. Identifying interaction partners

In an attempt to identify interacting proteins with PfPV1 by GST pull-down assay, we performed experiments with proteins from trophozoite-stage parasites. Unfortunately, we did not detect any protein partner (Figure 3.14). Not shown in the content of this dissertation, but in immunoprecipitated studies, blue native PAGE or pull-down assay with His-tag recombinant, PV1 protein also yielded no interaction (Andrea Ruecker/2007 and Caroline Odenwald/2008, bachelor thesis).

Aside from the proteomic data in our group (Nyalwidhe and Lingelbach, 2006), PfPV1 has been spotted in LaCount's network (LaCount *et al.*, 2005) where the authors identified *P. falciparum* protein-protein interactions using a high-throughput version of the yeast two-hybrid assay (Y2H). They performed more than 32,000 yeast two-hybrid screens, of which 11% yielded positives in which the identities of both interacting protein fragments were determined. Six interactions were identified for PfPV1. There are three conserved, unknown function proteins encoded by PF14_0649, PFI0175w, PF11_0160 and other three proteins encoded by PF14_0197 (zinc finger protein, putative), PFB0300c (Merozoite surface protein 2 – MSP2) and PFE1590w (early transcribed membrane protein 5 – ETRAMP5) (Figure 4.2), whether or not these interactions are true positive require further investigation. Recombinant expression of the proteins mentioned above and *in vitro* binding between the individual proteins with PfPV1 might help to confirm the interaction. In our pull-down assays and in the previous experiments, we only examined the parasite extraction at trophozoite stage, particularly at the late trophozoite. Given the fact that in the whole asexual parasite cycle, the *PfPV1* gene is expressed at high level in the spectrum of all expression intensities (Figure 4.1A), we could not rule out the possibility that the proteins above are only interacting with PfPV1 in a certain time point. Because our data do not cover all of the stages, we temporarily could not state a conclusion about the interacting proteins.

Discussion

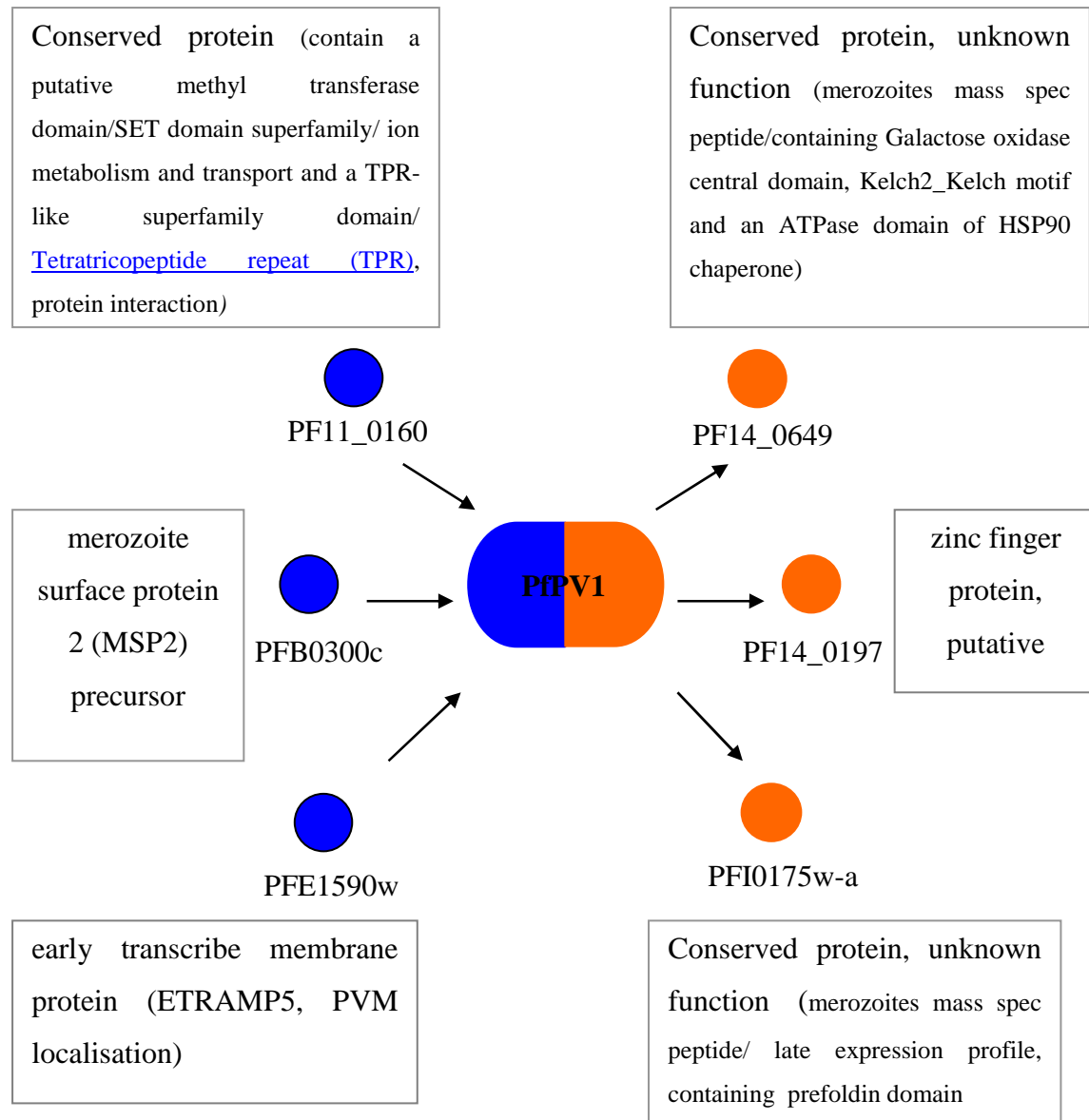


Figure 4.2 Y2H interactions of PfPV1 (LaCount *et al.*, 2005). Data was based on the protein interaction network for *P. falciparum* derived from yeast two-hybrid studies. Information of the interacting partners was provided in the box, collected from PlasmoDB (www.plasmodb.org) (Aurrecochea *et al.*, 2009). Blue: PfPV1 was prey; Red: PfPV1 was bait in the Y2H study.

4.5. Conclusion: PfPV1 – a conserved, unique protein with unknown but essential function

The *P. falciparum* genome predictably contains at least 5,409 open reading frames (ORFs) but over 60% lack sequence similarity to genes from any other sequenced organism (Gardner *et al.*, 2002). Also, detection of over 2,400 proteins by mass spectrometry showed that a large number of those hypothetical ORFs are transcribed and validated (Sam-Yellowe *et al.*, 2004). Thus, almost two third of the plasmodial proteins appear to be unique to this organism. Defining putative roles for these unannotated ORFs in the absence of homologs in other organisms remains challenging, discovery of their roles and identification of *Plasmodium* specific key regulatory elements will be fundamental to control this important pathogen.

PfPV1 is one of the unannotated proteins specific in *Plasmodium*. Location in the PV, unable to knock out, this protein also does not include any known functional domain, thus making the elucidation of its function is more difficult. At this point we can only present some predicted functions of PfPV1 through bioinformatics research, although the obtained scores are rather low (Table 3). We also present here the data extracted from PlasmoDB in searching for genes that have a similar expression profile to PfPV1 (Table 4). Of 100 defined matches, there are 13 genes predictably contain a signal peptide, half of their products are unknown function proteins, the others encode various products, from phosphatase to protease or multi-transmembrane proteins. The top 3 genes that score the highest profile similarity to *PfPV1* but do not contain a signal peptide all encode for metabolism transporters: PFE1150w - the multidrug resistance protein, PFA0375c – the lipid/sterol:H⁺ symporter and PFF1430c - a putative amino acid transporter (Table 4). The hypothesis that genes with similar functions have similar expression profiles has been widely considered as one of the methods in finding gene's cellular role in *Plasmodium* (Le Roch *et al.*, 2003). Although those clues are not the clarified hints but deserved to further exploration to understand the biological function of PfPV1. Extending the PfPV1 interaction assays to the whole erythrocytic stages could help to define the function of PfPV1.

Table 4. Expression profiles similarity to PfpV1

No.	[Gene]	[Profile Distance]	[Annotated GO Function]	[Product Description]	[SignalP Peptide]
	PF11_0302	0	N/A	conserved, unknown function	Y
1	PF14_0201	1.1811	molecular_function	surface protein, Pf113	Y
2	PF14_0614	1.2541	hydrolase activity	phosphatase, putative	Y
3	PF11_0246	1.3042	molecular_function	conserved, unknown function	Y
4	PFC0450w	1.3604	N/A	conserved , unknown function	Y
5	PFE1340w	1.438	N/A	conserved, unknown function	Y
6	PFL0065w	1.4732	molecular_function	conserved, unknown function	Y
7	PFL0790w	1.5361	molecular_function	conserved, ABC transporter transmembrane domain, unknown function	Y
8	PF11_0174	1.5644	cysteine-type peptidase activity	cathepsin C, homolog	Y
9	PF14_0761	1.5912	long-chain-fatty-acid-CoA ligase activity	acyl-CoA synthetase	Y
10	PF11_0212	1.6314	nucleotidyltransferase activity, RNA binding, molecular_function	tRNA nucleotidyltransferase, putative	Y
11	PF13_0265	1.6363	N/A	conserved, unknown function	Y
12	PF10_0208	1.6593	molecular_function	endomembrane protein 70, putative	Y
13	PFI0700c	1.6621	N/A	met-10+ like protein, putative	Y
14	<i>PFE1150w</i>	<i>0.7</i>	<i>ATP binding, multidrug efflux pump activity, ATPase activity, coupled to transmembrane movement of substances</i>	<i>multidrug resistance protein</i>	-
15	<i>PFA0375c</i>	<i>0.7945</i>	<i>hedgehog receptor activity</i>	<i>lipid/sterol:H+ symporter</i>	-
16	<i>PFF1430c</i>	<i>1.1409</i>	<i>amino acid transmembrane transporter activity</i>	<i>amino acid transporter, putative</i>	-
17	<i>PF11_0384</i>	<i>1.1989</i>	<i>molecular_function</i>	<i>cleft lip and palate associated transmembrane protein-related</i>	-
18	<i>PFD0415c</i>	<i>1.2852</i>	<i>N/A</i>	<i>conserved, unknown function</i>	-
19	<i>PF14_0477</i>	<i>1.2992</i>	<i>signal sequence binding, GTP binding, nucleoside-triphosphatase activity, 7S RNA binding</i>	<i>signal recognition particle SRP54, putative</i>	-
20	<i>PFI1085w</i>	<i>1.3033</i>	<i>N/A</i>	<i>ubiquitin-like protein, putative</i>	-
21	<i>PF14_0528</i>	<i>1.3126</i>	<i>molecular_function</i>	<i>hemolysin, putative</i>	-

Table 4. Expression profile similarity to PfpV1. Search on PlasmoDB for 100 genes that have a (glass slide) expression profile similar to that of PfpV1, distance method by Euclidean distance in 3D7 parasite, no time shift allowed. A secondary search found 13 genes that contain a predicted signal peptide. The list on this table was extracted for top 21 genes, first selected on signal peptide presence (genes from no. 1 to no. 13); followed by profile distance (genes from no. 14 to no. 21, in italic). N/A: not annotated yet; Y in SignalP peptide column: contains signal peptide. Data were extracted from PlasmoDB (Aurrecochea *et al.*, 2009).

References

References

- Adisa, A., Rug, M., Klonis, N., Foley, M., Cowman, A.F., and Tilley, L. (2003) The signal sequence of Exported protein-1 directs the green fluorescent protein to the parasitophorous vacuole of transfected malaria parasites. *J. Biol. Chem.* **278**: 6532-6542.
- Agop-Nersesian, C., Pfahler, J., Lanzer, M., and Meissner, M. (2008) Functional expression of ribozymes in Apicomplexa: Towards exogenous control of gene expression by inducible RNA-cleavage. *Int J Parasitol* **38**: 673-681.
- Aikawa, M., Miller, L.H., Johnson, J., and Rabbege, J. (1978) Erythrocyte entry by malarial parasites. A moving junction between erythrocyte and parasite. *J. Cell Biol.* **77**: 72-82.
- Aikawa, M., Miller, L.H., Rabbege, J.R., and Epstein, N. (1981) Freeze-fracture study on the erythrocyte membrane during malarial parasite invasion. *J. Cell Biol.* **91**: 55-62.
- Aikawa, M., Torii, M., Sjölander, A., Berzins, K., Perlmann, P., and Miller, L.H. (1990) Pf155/RESA antigen is localized in dense granules of *Plasmodium falciparum* merozoites. *Exp Parasitol* **71**: 326-329.
- Alexander, D.L., Arastu-Kapur, S., Dubremetz, J.-F., and Boothroyd, J.C. (2006) *Plasmodium falciparum* AMA1 binds a rhoptry neck protein homologous to TgRON4, a component of the moving junction in *Toxoplasma gondii*. *Eukaryotic Cell* **5**: 1169-1173.
- Alleva, L.M., and Kirk, K. (2001) Calcium regulation in the intraerythrocytic malaria parasite *Plasmodium falciparum*. *Mol Biochem Parasitol* **117**: 121-128.
- Ansorge, I., Benting, J., Bhakdi, S., and Lingelbach, K. (1996) Protein sorting in *Plasmodium falciparum*-infected red blood cells permeabilized with the pore-forming protein streptolysin O. *Biochem J* **315** (Pt 1): 307-314.
- Armstrong, C.M., and Goldberg, D.E. (2007) An FKBP destabilization domain modulates protein levels in *Plasmodium falciparum*. *Nat Methods* **4**: 1007 - 1009.
- Atkinson, C., and Aikawa, M. (1990) Ultrastructure of malaria-infected erythrocytes. *Blood Cells* **16**: 351 - 368.
- Aurrecoechea, C., Brestelli, J., Brunk, B.P., Dommer, J., Fischer, S., Gajria, B., Gao, X., Gingle, A., Grant, G., Harb, O.S., Heiges, M., Innamorato, F., Iodice, J., Kissinger, J.C., Kraemer, E., Li, W., Miller, J.A., Nayak, V., Pennington, C., Pinney, D.F., Roos, D.S., Ross, C., Stoeckert, C.J., Jr., Treatman, C., and Wang, H. (2009) PlasmoDB: a functional genomic database for malaria parasites. *Nucl. Acids Res.* **37**: D539-543.
- Balu, B., Shoue, D.A., Fraser, M.J., and Adams, J.H. (2005) High-efficiency transformation of *Plasmodium falciparum* by the lepidopteran transposable element piggyBac. *Proc Natl Acad Sci USA* **102**: 16391-16396.
- Bannister, L.H., and Mitchell, G.H. (1989) The fine structure of secretion by *Plasmodium knowlesi* merozoites during red cell invasion. *J Eukaryot Microbiol* **36**: 362-367.
- Bannister, L.H., and Dluzewski, A.R. (1990) The ultrastructure of red cell invasion in malaria infections: a review. *Blood Cells* **16**: 257-292; discussion 293-257.
- Bannister, L.H., Hopkins, J.M., Fowler, R.E., Krishna, S., and Mitchell, G.H. (2000) Ultrastructure of rhoptry development in *Plasmodium falciparum* erythrocytic schizonts. *Parasitology* **121**: 273-287.

References

- Bannister, L.H., Margos, G., and Hopkins, J.M. (2005) Making a home for *Plasmodium* post-genomics: ultrastructural organization of the blood stages. In *Molecular Approaches to Malaria*. Sherman, I.W. (ed). Washington, D.C: ASM Press, pp. 24 - 49.
- Baruch, D.I., Pasloske, B.L., Singh, H.B., Bi, X., Ma, X.C., Feldman, M., Taraschi, T.F., and Howard, R.J. (1995) Cloning the *P. falciparum* gene encoding PfEMP1, a malarial variant antigen and adherence receptor on the surface of parasitized human erythrocytes. *Cell* **82**: 77-87.
- Baumeister, S., Paprotka, K., Bhakdi, S., and Lingelbach, K. (2001) Selective permeabilization of infected host cells with pore-forming proteins provides a novel tool to study protein synthesis and viability of the intracellular apicomplexan parasites *Plasmodium falciparum* and *Toxoplasma gondii*. *Mol Biochem Parasitol* **112**: 133-137.
- Baumeister, S., Winterberg, M., Duranton, C., Huber, S., Lang, F., Kirk, K., and Lingelbach, K. (2006) Evidence for the involvement of *Plasmodium falciparum* proteins in the formation of new permeability pathways in the erythrocyte membrane. *Mol Microbiol* **60**: 493-504.
- Behari, R., and Haldar, K. (1994) *Plasmodium falciparum*: protein localization along a novel, lipid-rich Tubovesicular Membrane Network in infected erythrocytes. *Exp Parasitol* **79**: 250-259.
- Bendtsen, J., Nielsen, H., von Heijne, G., and Brunak, S. (2004) Improved prediction of signal peptides: SignalP 3.0. *J Mol Biol* **340**: 783-795.
- Benting, J., Mattei, D., and Lingelbach, K. (1994) Brefeldin A inhibits transport of the glycoporphin-binding protein from *Plasmodium falciparum* into the host erythrocyte. *Biochem J* **300 (Pt 3)**: 821-826.
- Bietz, S., Montilla, I., Külzer, S., Przyborski, J., and Lingelbach, K. (2009) Recruitment of human aquaporin 3 to internal membranes in the *Plasmodium falciparum* infected erythrocyte. *Mol Biochem Parasitol* **167**: 48-53.
- Blackman, M.J., Fujioka, H., Stafford, W.H.L., Sajid, M., Clough, B., Fleck, S.L., Aikawa, M., Grainger, M., and Hackett, F. (1998) A Subtilisin-like protein in secretory organelles of *Plasmodium falciparum* merozoites. *J. Biol. Chem.* **273**: 23398-23409.
- Blackman, M.J., and Bannister, L.H. (2001) Apical organelles of Apicomplexa: biology and isolation by subcellular fractionation. *Mol Biochem Parasitol* **117**: 11-25.
- Blackman, M. (2008) Malarial proteases and host cell egress: an 'emerging' cascade. *Cell Microbiol* **10**: 1925-1934.
- Blisnick, T., Morales Betoulle, M.E., Barale, J.-C., Uzureau, P., Berry, L., Desroses, S., Fujioka, H., Mattei, D., and Braun Breton, C. (2000) Pfsbp1, a Maurer's cleft *Plasmodium falciparum* protein, is associated with the erythrocyte skeleton. *Mol Biochem Parasitol* **111**: 107-121.
- Boddey, J., Moritz, R., Simpson, R., and Cowman, A. (2009) Role of the *Plasmodium* Export Element in trafficking parasite proteins to the infected erythrocyte. *Traffic* **10**: 285-299.
- Bozdech, Z., Llinás, M., Pulliam, B.L., Wong, E.D., Zhu, J., and DeRisi, J.L. (2003) The transcriptome of the intraerythrocytic developmental cycle of *Plasmodium falciparum*. *PLoS Biology* **1**: e5.
- Bracchi-Ricard, V., Moe, D., and Chakrabarti, D. (2005) Two *Plasmodium falciparum* ribonucleotide reductase small subunits, PfR2 and PfR4, interact

References

- with each other and are components of the in vivo enzyme complex. *J Mol Biol* **347**: 749-758.
- Camus, D., and Hadley, T.J. (1985) A *Plasmodium falciparum* antigen that binds to host erythrocytes and merozoites. *Science* **230**: 553-556.
- Carvalho, T.G., Thiberge, S., Sakamoto, H., and Menard, R. (2004) Conditional mutagenesis using site-specific recombination in *Plasmodium berghei*. *Proc Natl Acad Sci USA* **101**: 14931-14936.
- Chandramohanadas, R., Davis, P.H., Beiting, D.P., Harbut, M.B., Darling, C., Velmourougane, G., Lee, M.Y., Greer, P.A., Roos, D.S., and Greenbaum, D.C. (2009) Apicomplexan parasites co-opt host calpains to facilitate their escape from infected cells. *Science* **324**: 794-797.
- Chang, H.H., Falick, A.M., Carlton, P.M., Sedat, J.W., DeRisi, J.L., and Marletta, M.A. (2008) N-terminal processing of proteins exported by malaria parasites. *Mol Biochem Parasitol* **160**: 107-115.
- Charpian, S., and Przyborski, J. (2008) Protein transport across the parasitophorous vacuole of *Plasmodium falciparum*: into the great wide open. *Traffic* **9**: 157-165.
- Chen, F., Mackey, A.J., Stoeckert, C.J., Jr., and Roos, D.S. (2006) OrthoMCL-DB: querying a comprehensive multi-species collection of ortholog groups. *Nucl. Acids Res.* **34**: D363-368.
- Cooke, B.M., Lingelbach, K., Bannister, L.H., and Tilley, L. (2004) Protein trafficking in *Plasmodium falciparum*-infected red blood cells. *Trends Parasitol* **20**: 581-589.
- Cowman, A.F., and Crabb, B.S. (2005) Genetic manipulation of *Plasmodium falciparum*, I. W. Sherman (ed.). *Molecular approaches to malaria*. ASM Press, Washington, D.C.: 50-67.
- Cowman, A.F., and Crabb, B.S. (2006) Invasion of red blood cells by malaria parasites. *Cell* **124**: 755-766.
- Cox-Singh, J., and Singh, B. (2008) Knowlesi malaria: newly emergent and of public health importance? *Trends Parasitol* **24**: 406-410.
- Crabb, B.S., and Cowman, A.F. (1996) Characterization of promoters and stable transfection by homologous and nonhomologous recombination in *Plasmodium falciparum*. *Proc Natl Acad Sci USA* **93**: 7289 - 7294.
- Crabb, B.S., Cooke, B.M., Reeder, J.C., Waller, R.F., Caruana, S.R., Davern, K.M., Wickham, M.E., Brown, G.V., Coppel, R.L., and Cowman, A.F. (1997) Targeted gene disruption shows that knobs enable malaria-infected red cells to cytoadhere under physiological shear stress. *Cell* **89**: 287-296.
- Crabb, B.S., Rug, M., Gilberger, T.W., Thompson, J.K., Triglia, T., Maier, A.G., and Cowman, A.F. (2004) Transfection of the human malaria parasite *Plasmodium falciparum*. *Methods Mol Biol* **270**: 263-276.
- Culvenor, J.G., Day, K.P., and Anders, R.F. (1991) *Plasmodium falciparum* ring-infected erythrocyte surface antigen is released from merozoite dense granules after erythrocyte invasion. *Infect. Immun.* **59**: 1183-1187.
- de Koning-Ward, T.F., Fidock, D.A., Thathy, V., Menard, R., van Spaendonk, R.M.L., Waters, A.P., and Janse, C.J. (2000) The selectable marker human dihydrofolate reductase enables sequential genetic manipulation of the *Plasmodium berghei* genome. *Mol Biochem Parasitol* **106**: 199-212.
- de Koning-Ward, T.F., Waters, A.P., and Crabb, B.S. (2001) Puromycin-N-acetyltransferase as a selectable marker for use in *Plasmodium falciparum*. *Mol Biochem Parasitol* **117**: 155-160.

References

- Deitsch, K.W., and Wellems, T.E. (1996) Membrane modifications in erythrocytes parasitized by *Plasmodium falciparum*. *Mol Biochem Parasitol* **76**: 1-10.
- Delplace, P., Fortier, B., Tronchin, G., Dubremetz, J.F., and Vernes, A. (1987) Localization, biosynthesis, processing and isolation of a major 126 kDa antigen of the parasitophorous vacuole of *Plasmodium falciparum*. *Mol Biochem Parasitol* **23**: 193-201.
- Delplace, P., Bhatia, A., Cagnard, M., Camus, D., Colombet, G., Debrabant, A., Dubremetz, J.F., Dubreuil, N., Prensier, G., Fortier, B., and et al. (1988) Protein p126: a parasitophorous vacuole antigen associated with the release of *Plasmodium falciparum* merozoites. *Biol Cell* **64**: 215-221.
- Desai, S.A., and Rosenberg, R.L. (1997) Pore size of the malaria parasite's nutrient channel. *Proc Natl Acad Sci USA* **94**: 2045-2049.
- Dluzewski, A.R., Ling, I.T., Hopkins, J.M., Grainger, M., Margos, G., Mitchell, G.H., Holder, A.A., and Bannister, L.H. (2008) Formation of the food vacuole in *Plasmodium falciparum*: a potential role for the 19 kDa fragment of Merozoite Surface Protein 1 (MSP1¹⁹). *PLoS ONE* **3**: e3085.
- Duraisingh, M., Triglia, T., and Cowman, A. (2002) Negative selection of *Plasmodium falciparum* reveals targeted gene deletion by double crossover recombination. *Int J Parasitol.* **32**: 81-89.
- Duraisingh, M.T., Maier, A.G., Triglia, T., and Cowman, A.F. (2003) Erythrocyte-binding antigen 175 mediates invasion in *Plasmodium falciparum* utilizing sialic acid-dependent and -independent pathways. *Proc Natl Acad Sci USA* **100**: 4796-4801.
- Duraisingh, M.T., Triglia, T., Ralph, S.A., Rayner, J.C., Barnwell, J.W., McFadden, G.I., and Cowman, A.F. (2003) Phenotypic variation of *Plasmodium falciparum* merozoite proteins directs receptor targeting for invasion of human erythrocytes. *EMBO J* **22**: 1047-1057.
- Dvorak, J.A., Miller, L.H., Whitehouse, W.C., and Shiroishi, T. (1975) Invasion of erythrocytes by malaria merozoites. *Science* **187**: 748-750.
- Egan, T.J., Combrinck, J.M., Egan, J., Hearne, G.R., Marques, H.M., Ntenti, S., Sewell, B.T., Smith, P.J., Taylor, D., van Schalkwyk, D.A., and Walden, J.C. (2002) Fate of haem iron in the malaria parasite *Plasmodium falciparum*. *Biochem. J.* **365**: 343-347.
- Elford, B.C., Cowan, G.M., and Ferguson, D.J. (1995) Parasite-regulated membrane transport processes and metabolic control in malaria-infected erythrocytes. *Biochem. J.* **308**: 361-360.
- Elmendorf, H.G., and Haldar, K. (1993) Secretory transport in *Plasmodium*. *Parasitol Today* **9**: 98-102.
- Epp, C., Raskolnikov, D., and Deitsch, K. (2008) A regulatable transgene expression system for cultured *Plasmodium falciparum* parasites. *Malaria J* **7**: 86.
- Fidock, D.A., and Wellems, T.E. (1997) Transformation with human dihydrofolate reductase renders malaria parasites insensitive to WR99210 but does not affect the intrinsic activity of proguanil. *Proc Natl Acad Sci USA* **94**: 10931-10936.
- Florent, I., Charneau, S., and Grellier, P. (2004) *Plasmodium falciparum* genes differentially expressed during merozoite morphogenesis. *Mol Biochem Parasitol* **135**: 143-148.
- Francis, S.E., Sullivan, D.J., and Goldberg, a.D.E. (1997) Hemoglobin metabolism in the malaria parasite *Plasmodium falciparum*. *Annu Rev Microbiol* **51**: 97-123.
- Galinski, M., Dluzewski, A., and Barnwell, J. (2005) A mechanistic approach to merozoite invasion of red blood cells: merozoite biogenesis, rupture, and

References

- invasion of erythrocytes. In *Molecular approaches to malaria*. Sherman, I.W. (ed). Washington, D.C: ASM Press.
- Garcia, C.R.S., de Azevedo, M.F., Wunderlich, G., Budu, A., Young, J.A., Bannister, L., and Kwang, W.J. (2008) *Plasmodium* in the postgenomic era: new insights into the molecular cell biology of malaria parasites. *Int Rev Cell Mol Biol* **266**: 85-156.
- Gardner, M.J., Hall, N., Fung, E., White, O., Berriman, M., Hyman, R.W., Carlton, J.M., Pain, A., Nelson, K.E., Bowman, S., Paulsen, I.T., James, K., Eisen, J.A., Rutherford, K., Salzberg, S.L., Craig, A., Kyes, S., Chan, M.-S., Nene, V., Shallom, S.J., Suh, B., Peterson, J., Angiuoli, S., Pertea, M., Allen, J., Selengut, J., Haft, D., Mather, M.W., Vaidya, A.B., Martin, D.M.A., Fairlamb, A.H., Fraunholz, M.J., Roos, D.S., Ralph, S.A., McFadden, G.I., Cummings, L.M., Subramanian, G.M., Mungall, C., Venter, J.C., Carucci, D.J., Hoffman, S.L., Newbold, C., Davis, R.W., Fraser, C.M., and Barrell, B. (2002) Genome sequence of the human malaria parasite *Plasmodium falciparum*. *Nature* **419**: 498-511.
- Gasteiger, E., Hoogland, C., Gattiker, A., Duvaud, S., Wilkins, M.R., Appel, R.D., Bairoch, A. (2005) Protein identification and analysis tools on the ExPASy server. In *The Proteomics Protocols Handbook*. Walker, J.M. (ed). Totowa, NJ: Humana Press
- Gazarini, M.L., Thomas, A.P., Pozzan, T., and Garcia, C.R.S. (2003) Calcium signaling in a low calcium environment: how the intracellular malaria parasite solves the problem. *J. Cell Biol.* **161**: 103-110.
- Gehde, N., Hinrichs, C., Montilla, I., Charpian, S., Lingelbach, K., and Przyborski, J. (2009) Protein unfolding is an essential requirement for transport across the parasitophorous vacuolar membrane of *Plasmodium falciparum*. *Mol Microbiol* **71**: 613-628.
- Ginsburg, H., Krugliak, M., Eidelman, O., and Ioav Cabantchik, Z. (1983) New permeability pathways induced in membranes of *Plasmodium falciparum* infected erythrocytes. *Mol Biochem Parasitol* **8**: 177-190.
- Glushakova, S., Yin, D., Li, T., and Zimmerberg, J. (2005) Membrane transformation during malaria parasite release from human red blood cells. *Curr Biol* **15**: 1645-1650.
- Goldberg, D.E., Slater, A.F., Cerami, A., and Henderson, G.B. (1990) Hemoglobin degradation in the malaria parasite *Plasmodium falciparum*: an ordered process in a unique organelle. *Proc Natl Acad Sci USA* **87**: 2931-2935.
- Goonewardene, R., Daily, J., Kaslow, D., Sullivan, T.J., Duffy, P., Carter, R., Mendis, K., and Wirth, D. (1993) Transfection of the malaria parasite and expression of firefly luciferase. *Proc Natl Acad Sci USA* **90**: 5234-5236.
- Gowda, D.C., and Davidson, E.A. (1999) Protein glycosylation in the malaria parasite. *Parasitol Today* **15**: 147-152.
- Hakansson, S., Charron, A.J., and Sibley, L.D. (2001) *Toxoplasma* evacuoles: a two-step process of secretion and fusion forms the parasitophorous vacuole. *EMBO J* **20**: 3132-3144.
- Haldar, K., de Amorim, A.F., and Cross, G.A. (1989) Transport of fluorescent phospholipid analogues from the erythrocyte membrane to the parasite in *Plasmodium falciparum*-infected cells. *J. Cell Biol.* **108**: 2183-2192.
- Haldar, K., and Uyetake, L. (1992) The movement of fluorescent endocytic tracers in *Plasmodium falciparum* infected erythrocytes. *Mol Biochem Parasitol* **50**: 161-177.

References

- Hawkins, T., Luban, S., and Kihara, S. (2006) Enhanced automated function prediction using distantly related sequences and contextual association by PFP. *Protein Sci.* **15**: 1550-1556.
- Hawthorne, P.L., Trenholme, K.R., Skinner-Adams, T.S., Spielmann, T., Fischer, K., Dixon, M.W.A., Ortega, M.R., Anderson, K.L., Kemp, D.J., and Gardiner, D.L. (2004) A novel *Plasmodium falciparum* ring stage protein, REX, is located in Maurer's clefts. *Mol Biochem Parasitol* **136**: 181-189.
- Hay, S.I., Guerra, C.A., Gething, P.W., Patil, A.P., Tatem, A.J., Noor, A.M., Kabaria, C.W., Manh, B.H., Elyazar, I.R.F., Brooker, S., Smith, D.L., Moyeed, R.A., and Snow, R.W. (2009) A World Malaria Map: *Plasmodium falciparum* endemicity in 2007. *PLoS Med* **6**: e1000048.
- Helmby, H., Cavelier, L., Pettersson, U., and Wahlgren, M. (1993) Rosetting *Plasmodium falciparum*-infected erythrocytes express unique strain-specific antigens on their surface. *Infect Immun* **61**: 284-288.
- Hill, D.A., Pillai, A.D., Nawaz, F., Hayton, K., Doan, L., Lisk, G., and Desai, S.A. (2007) A blasticidin S-resistant *Plasmodium falciparum* mutant with a defective plasmodial surface anion channel. *Proc Natl Acad Sci USA* **104**: 1063-1068.
- Hiller, N.L., Akompong, T., Morrow, J.S., Holder, A.A., and Haldar, K. (2003) Identification of a stomatin orthologue in vacuoles induced in human erythrocytes by malaria parasites: a role for microbial raft proteins in apicomplexan vacuole biogenesis. *J. Biol. Chem.* **278**: 48413-48421.
- Hiller, N.L., Bhattacharjee, S., van Ooij, C., Liolios, K., Harrison, T., Lopez-Estrano, C., and Haldar, K. (2004) A host-targeting signal in virulence proteins reveals a secretome in malarial infection. *Science* **306**: 1934-1937.
- Hinterberg, K., and Scherf, A. (1994) PFGE: improved conditions for rapid and high-resolution separation of *Plasmodium falciparum* chromosomes. *Parasitol Today* **10**: 225.
- Holder, A.A., Guevara Patino, J.A., Uthapibull, C., Syed, S.E., Ling, I.T., Scott-Finnigan, T., and Blackman, M.J. (1999) Merozoite surface protein 1, immune evasion, and vaccines against asexual blood stage malaria. *Parassitologia* **41**: 409-414.
- Hulo, N., Bairoch, A., Bulliard, V., Cerutti, L., Cuche, B.A., de Castro, E., Lachaize, C., Langendijk-Genevaux, P.S., and Sigrist, C.J.A. (2008) The 20 years of PROSITE. *Nucl. Acids Res.* **36**: D245-249.
- Kadekoppala, M., Cheresh, P., Catron, D., Ji, D.D., Deitsch, K., Wellems, T.E., Seifert, H.S., and Haldar, K. (2001) Rapid recombination among transfected plasmids, chimeric episome formation and trans gene expression in *Plasmodium falciparum*. *Mol Biochem Parasitol* **112**: 211-218.
- Kadekoppala, M., O'Donnell, R.A., Grainger, M., Crabb, B.S., and Holder, A.A. (2008) Deletion of the *Plasmodium falciparum* merozoite surface protein 7 gene impairs parasite invasion of erythrocytes. *Eukaryot Cell* **7**: 2123-2132.
- Kilejian, A. (1979) Characterization of a protein correlated with the production of knob-like protrusions on membranes of erythrocytes infected with *Plasmodium falciparum*. *Proc Natl Acad Sci USA* **76**: 4650-4653.
- Kirk, K. (2001) Membrane transport in the malaria-infected erythrocyte. *Physiol. Rev.* **81**: 495-537.
- Kirk, K., and Saliba, K.J. (2007) Targeting nutrient uptake mechanisms in *Plasmodium*. *Curr Drug Targets* **8**: 75-88.

References

- Knapp, B., Hundt, E., Nau, U., and Küpper, H.A. (1989) Molecular cloning, genomic structure and localization in a blood stage antigen of *Plasmodium falciparum* characterized by a serine stretch. *Mol Biochem Parasitol* **32**: 73-83.
- Knapp, B., Nau, U., Hundt, E., and Küpper, H.A. (1991) A new blood stage antigen of *Plasmodium falciparum* highly homologous to the serine-stretch protein SERP. *Mol Biochem Parasitol* **44**: 1-13.
- Köhler, S., Delwiche, C.F., Denny, P.W., Tilney, L.G., Webster, P., Wilson, R.J.M., Palmer, J.D., and Roos, D.S. (1997) A plastid of probable green algal origin in Apicomplexan parasites. *Science* **275**: 1485-1489.
- Koussis, K., Withers-Martinez, C., Yeoh, S., Child, M., Hackett, F., Knuepfer, E., Juliano, L., Woehlbier, U., Bujard, H., and Blackman, M.J. (2009) A multifunctional serine protease primes the malaria parasite for red blood cell invasion. *EMBO J* **28**: 725-735.
- LaCount, D.J., Vignali, M., Chettier, R., Phansalkar, A., Bell, R., Hesselberth, J.R., Schoenfeld, L.W., Ota, I., Sahasrabudhe, S., Kurschner, C., Fields, S., and Hughes, R.E. (2005) A protein interaction network of the malaria parasite *Plasmodium falciparum*. *Nature* **438**: 103-107.
- Laemmli, U.K. (1970) Cleavage of structural proteins during the assembly of the head of bacteriophage T4. *Nature* **227**: 680-685.
- Lambros, C., and Vanderberg, J.P. (1979) Synchronization of *Plasmodium falciparum* erythrocytic stages in culture. *J Parasitol* **65**: 418-420.
- Langreth, S., Jensen, J., Reese, R., and Trager, W. (1978) Fine Structure of Human Malaria *In Vitro*. *J Eukaryot Microbiol* **25**: 443-452.
- Lanzer, M., Wickert, H., Krohne, G., Vincensini, L., and Braun Breton, C. (2006) Maurer's clefts: A novel multi-functional organelle in the cytoplasm of *Plasmodium falciparum*-infected erythrocytes. *Int J Parasitol* **36**: 23-36.
- Larkin, M.A., Blackshields, G., Brown, N.P., Chenna, R., McGettigan, P.A., McWilliam, H., Valentin, F., Wallace, I.M., Wilm, A., Lopez, R., Thompson, J.D., Gibson, T.J., and Higgins, D.G. (2007) Clustal W and Clustal X version 2.0. *Bioinformatics* **23**: 2947-2948.
- Le Roch, K.G., Zhou, Y., Blair, P.L., Grainger, M., Moch, J.K., Haynes, J.D., De la Vega, P., Holder, A.A., Batalov, S., Carucci, D.J., and Winzeler, E.A. (2003) Discovery of gene function by expression profiling of the malaria parasite life cycle. *Science* **301**: 1503-1508.
- Letunic, I., Doerks, T., and Bork, P. (2009) SMART 6: recent updates and new developments. *Nucl. Acids Res.* **37**: D229-232.
- Lew, V., Tiffert, T., and Ginsburg, H. (2003) Excess hemoglobin digestion and the osmotic stability of *Plasmodium falciparum*-infected red blood cells. *Blood* **101**: 4189-4194.
- Linding, R., Russell, R.B., Neduva, V., and Gibson, T.J. (2003) GlobPlot: exploring protein sequences for globularity and disorder. *Nucl. Acids Res.* **31**: 3701-3708.
- Lingelbach, K., and Joiner, K.A. (1998) The parasitophorous vacuole membrane surrounding *Plasmodium* and *Toxoplasma*: an unusual compartment in infected cells. *J Cell Sci* **111**: 1467-1475.
- Lingelbach, K., Kirk, K., Rogerson, S., Langhorne, J., Carucci, D., and Waters, A. (2004) Molecular approaches to malaria. *Mol Microbiol* **54**: 575-587.
- Lobo, C.-A., Fujioka, H., Aikawa, M., and Kumar, N. (1999) Disruption of the Pfg27 locus by homologous recombination leads to loss of the sexual phenotype in *P. falciparum*. *Mol Cell* **3**: 793-798.

References

- Luse, S.A., and Miller, L.H. (1971) *Plasmodium falciparum* malaria: ultrastructure of parasitized erythrocytes in cardiac vessels. *Am J Trop Med Hyg* **20**: 655-660.
- MacPherson, G.G., Warrell, M.J., White, N.J., Loareesuwan, S., and Warrell, D.A. (1985) Human cerebral malaria: a quantitative ultrastructural analysis of parasitized erythrocyte sequestration. *Am J Pathol* **119**: 385-401.
- Maier, A.G., Duraisingh, M.T., Reeder, J.C., Patel, S.S., Kazura, J.W., Zimmerman, P.A., and Cowman, A.F. (2003) *Plasmodium falciparum* erythrocyte invasion through glycophorin C and selection for Gerbich negativity in human populations. *Nat Med* **9**: 87-92.
- Maier, A.G., Braks, J.A., Waters, A.P., and Cowman, A.F. (2006) Negative selection using yeast cytosine deaminase/uracil phosphoribosyl transferase in *Plasmodium falciparum* for targeted gene deletion by double crossover recombination. *Mol Biochem Parasitol.* **150**: 118-121.
- Maier, A.G., Rug, M., O'Neill, M.T., Brown, M., Chakravorty, S., Szeszak, T., Chesson, J., Wu, Y., Hughes, K., Coppel, R.L., Newbold, C., Beeson, J.G., Craig, A., Crabb, B.S., and Cowman, A.F. (2008) Exported proteins required for virulence and rigidity of *Plasmodium falciparum*-infected human erythrocytes. *Cell* **134**: 48-61.
- Mamoun, C.B., Gluzman, I.Y., Goyard, S., Beverley, S.M., and Goldberg, D.E. (1999) A set of independent selectable markers for transfection of the human malaria parasite *Plasmodium falciparum*. *Proc Natl Acad Sci USA* **96**: 8716-8720.
- Margos, G., Bannister, L.H., Dluzewski, A.R., Hopkins, J., Williams, I.T., and Mitchell, G.H. (2004) Correlation of structural development and differential expression of invasion-related molecules in schizonts of *Plasmodium falciparum*. *Parasitology* **129**: 273-287.
- Marti, M., Good, R.T., Rug, M., Knuepfer, E., and Cowman, A.F. (2004) Targeting malaria virulence and remodeling proteins to the host erythrocyte. *Science* **306**: 1930-1933.
- McCoubrie, J.E., Miller, S.K., Sargeant, T., Good, R.T., Hodder, A.N., Speed, T.P., de Koning-Ward, T.F., and Crabb, B.S. (2007) Evidence for a common role for the serine-type *Plasmodium falciparum* serine repeat antigen proteases: implications for vaccine and drug design. *Infect. Immun.* **75**: 5565-5574.
- McFadden, G.I., Reith, M.E., Munholland, J., and Lang-Unnasch, N. (1996) Plastid in human parasites. *Nature* **381**: 482.
- Meissner, M., Krejany, E., Gilson, P.R., Koning-Ward, T.F., Soldati, D., and Crabb, B.S. (2005) Tetracycline analogue-regulated transgene expression in *Plasmodium falciparum* blood stages using *Toxoplasma gondii* transactivators. *Proc Natl Acad Sci USA* **102**: 2980 - 2985.
- Mercier, C., Adjogble, K.D.Z., Däubener, W., and Delauw, M.-F.-C. (2005) Dense granules: are they key organelles to help understand the parasitophorous vacuole of all apicomplexa parasites? *Int J Parasitol* **35**: 829-849.
- Militello, K., Refour, P., Comeaux, C., and Duraisingh, M. (2008) Antisense RNA and RNAi in protozoan parasites: Working hard or hardly working? *Mol Biochem Parasitol* **157**: 117-126.
- Miller, L.H., Baruch, D.I., Marsh, K., and Doumbo, O.K. (2002) The pathogenic basis of malaria. *Nature* **415**: 673-679.
- Miller, S.K., Good, R.T., Drew, D.R., Delorenzi, M., Sanders, P.R., Hodder, A.N., Speed, T.P., Cowman, A.F., de Koning-Ward, T.F., and Crabb, B.S. (2002) A subset of *Plasmodium falciparum* SERA genes are expressed and appear to

References

- play an important role in the erythrocytic cycle. *J. Biol. Chem.* **277**: 47524-47532.
- Mital, J., Meissner, M., Soldati, D., and Ward, G.E. (2005) Conditional expression of *Toxoplasma gondii* Apical Membrane Antigen-1 (TgAMA1) demonstrates that TgAMA1 plays a critical role in host cell invasion. *Mol. Biol. Cell* **16**: 4341-4349.
- Mitchell, G.H., and Bannister, L.H. (1988) Malaria parasite invasion: interactions with the red cell membrane. *Crit Rev Oncol Hematol* **8**: 225-310.
- Morahan, B.J., Wang, L., and Coppel, R.L. (2009) No TRAP, no invasion. *Trends Parasitol* **25**: 77-84.
- Morrisette, N.S., and Sibley, L.D. (2002) Cytoskeleton of apicomplexan parasites. *Microbiol. Mol. Biol. Rev.* **66**: 21-38.
- Murphy, S.C., Samuel, B.U., Harrison, T., Speicher, K.D., Speicher, D.W., Reid, M.E., Prohaska, R., Low, P.S., Tanner, M.J., Mohandas, N., and Haldar, K. (2004) Erythrocyte detergent-resistant membrane proteins: their characterization and selective uptake during malarial infection. *Blood* **103**: 1920-1928.
- Murphy, S.C., Fernandez-Pol, S., Chung, P.H., Prasanna Murthy, S.N., Milne, S.B., Salomao, M., Brown, H.A., Lomasney, J.W., Mohandas, N., and Haldar, K. (2007) Cytoplasmic remodeling of erythrocyte raft lipids during infection by the human malaria parasite *Plasmodium falciparum*. *Blood* **110**: 2132-2139.
- Nakamura, Y., Gojobori, T., and Ikemura, T. (2000) Codon usage tabulated from international DNA sequence databases: status for the year 2000. *Nucl. Acids Res.* **28**: 292-.
- Nkrumah, L.J., Muhle, R.A., Moura, P.A., Ghosh, P., Hatfull, G.F., Jacobs, W.R., and Fidock, D.A. (2006) Efficient site-specific integration in *Plasmodium falciparum* chromosomes mediated by mycobacteriophage Bxb1 integrase. *Nat Meth* **3**: 615-621.
- Nyalwidhe, J., Baumeister, S., Hibbs, A.R., Tawill, S., Papakrivov, J., Volker, U., and Lingelbach, K. (2002) A nonpermeant biotin derivative gains access to the parasitophorous vacuole in *Plasmodium falciparum*-infected erythrocytes permeabilized with streptolysin O. *J. Biol. Chem.* **277**: 40005-40011.
- Nyalwidhe, J., Maier, U., and Lingelbach, K. (2003) Intracellular parasitism: cell biological adaptations of parasitic protozoa to a life inside cells. *Zoology* **106**: 341-348.
- Nyalwidhe, J., and Lingelbach, K. (2006) Proteases and chaperones are the most abundant proteins in the parasitophorous vacuole of *Plasmodium falciparum*-infected erythrocytes. *Proteomics* **6**: 1563-1573.
- Obenauer, J.C., Cantley, L.C., and Yaffe, M.B. (2003) Scansite 2.0: proteome-wide prediction of cell signaling interactions using short sequence motifs. *Nucl. Acids Res.* **31**: 3635-3641.
- O'Donnell, R.A., Saul, A., Cowman, A.F., and Crabb, B.S. (2000) Functional conservation of the malaria vaccine antigen MSP-1₁₉ across distantly related *Plasmodium* species. *Nat Med* **6**: 91-95.
- O'Donnell, R.A., Preiser, P.R., Williamson, D.H., Moore, P.W., Cowman, A.F., and Crabb, B.S. (2001) An alteration in concatameric structure is associated with efficient segregation of plasmids in transfected *Plasmodium falciparum* parasites. *Nucl. Acids Res.* **29**: 716-724.
- O'Donnell, R.A., Freitas, L.H., Preiser, P.R., Williamson, D.H., Duraisingh, M., McElwain, T.F., Scherf, A., Cowman, A.F., and Crabb, B.S. (2002) A genetic

References

- screen for improved plasmid segregation reveals a role for Rep20 in the interaction of *Plasmodium falciparum* chromosomes. *EMBO J* **21**: 1231 - 1239.
- Parthasarathi, S., Varela-Echavarria, A., Ron, Y., Preston, B.D., and Dougherty, J.P. (1995) Genetic rearrangements occurring during a single cycle of murine leukemia virus vector replication: characterization and implications. *J. Virol.* **69**: 7991-8000.
- Pasvol, G., Wilson, R.J., Smalley, M.E., and Brown, J. (1978) Separation of viable schizont-infected red cells of *Plasmodium falciparum* from human blood. *Ann Trop Med Parasitol* **72**: 87-88.
- Petter, M., Haeggström, M., Khattab, A., Fernandez, V., Klinkert, M.-Q., and Wahlgren, M. (2007) Variant proteins of the *Plasmodium falciparum* RIFIN family show distinct subcellular localization and developmental expression patterns. *Mol Biochem Parasitol* **156**: 51-61.
- Plattner, F., and Soldati-Favre, D. (2008) Hijacking of host cellular functions by the apicomplexa. *Annu Rev Microbiol* **62**: 471-487.
- Pouvelle, B., Gormley, J.A., and Taraschi, T.F. (1994) Characterization of trafficking pathways and membrane genesis in malaria-infected erythrocytes. *Mol Biochem Parasitol* **66**: 83-96.
- Przyborski, J., Miller, S., Pfahler, J., Henrich, P., Rohrbach, P., Crabb, B., and Lanzer, M. (2005) Trafficking of STEVOR to the Maurer's clefts in *Plasmodium falciparum*-infected erythrocytes. *EMBO J* **24**: 2306 - 2317.
- Przyborski, J.M. (2008) The Maurer's clefts of *Plasmodium falciparum*: parasite-induced islands within an intracellular ocean. *Trends Parasitol* **24**: 285-288.
- Rajasekaran, S., Balla, S., Gradie, P., Gryk, M.R., Kadaveru, K., Kundeti, V., Maciejewski, M.W., Mi, T., Rubino, N., Vyas, J., and Schiller, M.R. (2009) Minomotif miner 2nd release: a database and web system for motif search. *Nucl. Acids Res.* **37**: D185-190.
- Roos, D.S., Sullivan, W.J., Striepen, B., Bohne, W., and Donald, R.G.K. (1997) Tagging genes and trapping promoters in *Toxoplasma gondii* by insertional mutagenesis. *Methods* **13**: 112-122.
- Rosario, V. (1981) Cloning of naturally occurring mixed infections of malaria parasites. *Science* **212**: 1037-1038.
- Rug, M., Prescott, S.W., Fernandez, K.M., Cooke, B.M., and Cowman, A.F. (2006) The role of KAHRP domains in knob formation and cytoadherence of *P. falciparum*-infected human erythrocytes. *Blood* **108**: 370-378.
- Sajid, M., Withers-Martinez, C., and Blackman, M.J. (2000) Maturation and specificity of *Plasmodium falciparum* subtilisin-like protease-1, a malaria merozoite subtilisin-like serine protease. *J. Biol. Chem.* **275**: 631-641.
- Sakamoto, H., Thiberge, S., Akerman, S., Janse, C.J., Carvalho, T.G., and Menard, R. (2005) Towards systematic identification of *Plasmodium* essential genes by transposon shuttle mutagenesis. *Nucl. Acids Res.* **33**: e174-.
- Sambrook, J., and Russell, D. (2001) *Molecular Cloning: A Laboratory Manual*: Cold Spring Harbor Laboratory Press.
- Sam-Yellowe, T.Y., Shio, H., and Perkins, M.E. (1988) Secretion of *Plasmodium falciparum* rhoptry protein into the plasma membrane of host erythrocytes. *J. Cell Biol.* **106**: 1507-1513.
- Sam-Yellowe, T.Y., Florens, L., Wang, T., Raine, J.D., Carucci, D.J., Sinden, R., and Yates, J.R. (2004) Proteome analysis of rhoptry-enriched fractions isolated from *Plasmodium* merozoites. *J Proteome Res.* **3**: 995-1001.

References

- Schultz, J.r., Milpetz, F., Bork, P., and Ponting, C.P. (1998) SMART, a simple modular architecture research tool: Identification of signaling domains. *Proc Natl Acad Sci USA* **95**: 5857-5864.
- Sidhu, A.B.S., Verdier-Pinard, D., and Fidock, D.A. (2002) Chloroquine resistance in *Plasmodium falciparum* malaria parasites conferred by *pfcr* mutations. *Science* **298**: 210-213.
- Smith, D.B., and Johnson, K.S. (1988) Single-step purification of polypeptides expressed in *Escherichia coli* as fusions with glutathione S-transferase. *Gene* **67**: 31-40.
- Soni, S., Dhawan, S., Rosen, K.M., Chafel, M., Chishti, A.H., and Hanspal, M. (2005) Characterization of events preceding the release of malaria parasite from the host red blood cell. *Blood Cells Mol Dis.* **35**: 201-211.
- Southern, E.M. (1975) Detection of specific sequences among DNA fragments separated by gel electrophoresis. *J Mol Biol* **98**: 503-517.
- Spielmann, T., and Beck, H.P. (2000) Analysis of stage-specific transcription in *Plasmodium falciparum* reveals a set of genes exclusively transcribed in ring stage parasites. *Mol Biochem Parasitol* **111**: 453-458.
- Spielmann, T., Hawthorne, P.L., Dixon, M.W.A., Hannemann, M., Klotz, K., Kemp, D.J., Klonis, N., Tilley, L., Trenholme, K.R., and Gardiner, D.L. (2006) A cluster of ring stage-specific genes linked to a locus implicated in cytoadherence in *Plasmodium falciparum* codes for PEXEL-negative and PEXEL-positive proteins exported into the host cell. *Mol. Biol. Cell* **17**: 3613-3624.
- Spycher, C., Klonis, N., Spielmann, T., Kump, E., Steiger, S., Tilley, L., and Beck, H.-P. (2003) MAHRP-1, a novel *Plasmodium falciparum* histidine-rich protein, binds ferriprotoporphyrin IX and localizes to the Maurer's clefts. *J. Biol. Chem.* **278**: 35373-35383.
- Sturm, A., Amino, R., van de Sand, C., Regen, T., Retzlaff, S., Rennenberg, A., Krueger, A., Pollok, J.-M., Menard, R., and Heussler, V.T. (2006) Manipulation of host hepatocytes by the malaria parasite for delivery into liver sinusoids. *Science* **313**: 1287-1290.
- Sturm, A., and Heussler, V. (2007) Live and let die: manipulation of host hepatocytes by exoerythrocytic *Plasmodium* parasites. *Med Microbiol Immunol* **196**: 127-133.
- Su, X.-z., Heatwole, V.M., Wertheimer, S.P., Guinet, F., Herrfeldt, J.A., Peterson, D.S., Ravetch, J.A., and Wellems, T.E. (1995) The large diverse gene family *var* encodes proteins involved in cytoadherence and antigenic variation of *Plasmodium falciparum*-infected erythrocytes. *Cell* **82**: 89-100.
- Sultan, A.A., Thathy, V., Frevert, U., Robson, K.J.H., Crisanti, A., Nussenzweig, V., Nussenzweig, R.S., and Ménard, R. (1997) TRAP is necessary for gliding motility and infectivity of *Plasmodium* sporozoites. *Cell* **90**: 511-522.
- Tilley, L., Sougrat, R., Lithgow, T., and Hanssen, E. (2008) The twists and turns of Maurer's cleft trafficking in *P. falciparum*-infected erythrocytes. *Traffic* **9**: 187-197.
- Trager, W., Rudzinska, M., and Bradbury, P. (1966) The fine structure of *Plasmodium falciparum* and its host erythrocytes in natural malarial infections in man. *Bulletin of the World Health Organization* **35**: 883-885.
- Trager, W., and Jensen, J.B. (1976) Human malaria parasites in continuous culture. *Science* **193**: 673-675.

References

- Triglia, T., Julie Healer Sonia R. Caruana Anthony N. Hodder Robin F. Anders Brendan S. Crabb Alan F. Cowman (2000) Apical membrane antigen 1 plays a central role in erythrocyte invasion by *Plasmodium* species. *Mol Microbiol* **38**: 706-718.
- Triglia, T., Duraisingh, M., Good, R., and Cowman, A. (2005) Reticulocyte-binding protein homologue 1 is required for sialic acid-dependent invasion into human erythrocytes by *Plasmodium falciparum*. *Mol Microbiol* **55**: 162-174.
- Valdes, J., Taylor, M.C., Cross, M.A., Ligtenberg, M.J., Rudenko, G., and Borst, P. (1996) The viral thymidine kinase gene as a tool for the study of mutagenesis in *Trypanosoma brucei*. *Nucl. Acids Res.* **24**: 1809-1815.
- van den Hoff, M.J., Moorman, A.F., and Lamers, W.H. (1992) Electroporation in 'intracellular' buffer increases cell survival. *Nucleic Acids Res* **20**: 2902.
- van Dijk, M.R., Waters, A.P., and Janse, C.J. (1995) Stable transfection of malaria parasite blood stages. *Science* **268**: 1358-1362.
- Varela-Echavarria, A., Prorock, C.M., Ron, Y., and Dougherty, J.P. (1993) High rate of genetic rearrangement during replication of a Moloney murine leukemia virus-based vector. *J. Virol.* **67**: 6357-6364.
- von Itzstein, M., Plebanski, M., Cooke, B.M., and Coppel, R.L. (2008) Hot, sweet and sticky: the glycobiology of *Plasmodium falciparum*. *Trends Parasitol* **24**: 210-218.
- Waller, R., and McFadden, G. (2005) The apicoplast: a review of the derived plastid of apicomplexan parasites. *Curr Issues Mol Biol.* **7**: 57-80.
- Walliker, D., Quakyi, I.A., Wellems, T.E., McCutchan, T.F., Szarfman, A., London, W.T., Corcoran, L.M., Burkot, T.R., and Carter, R. (1987) Genetic analysis of the human malaria parasite *Plasmodium falciparum*. *Science* **236**: 1661-1666.
- Wang, P., Wang, Q., Sims, P., and Hyde, J. (2002) Rapid positive selection of stable integrants following transfection of *Plasmodium falciparum*. *Mol Biochem Parasitol.* **123**: 1-10.
- Ward, G.E., Miller, L.H., and Dvorak, J.A. (1993) The origin of parasitophorous vacuole membrane lipids in malaria-infected erythrocytes. *J Cell Sci* **106**: 237-248.
- Waterkeyn, J.G., Wickham, M.E., Davern, K.M., Cooke, B.M., Coppel, R.L., Reeder, J.C., Culvenor, J.G., Waller, R.F., and Cowman, A.F. (2000) Targeted mutagenesis of *Plasmodium falciparum* erythrocyte membrane protein 3 (PfEMP3) disrupts cytoadherence of malaria-infected red blood cells. *EMBO J* **19**: 2813-2823.
- WHO (2008) World Malaria Report 2008. *Geneva, World Health Organization.*
- WHO (2008) Global burden of disease: 2004 update In *Geneva, World Health Organization.*
- Wickert, H., and Krohne, G. (2007) The complex morphology of Maurer's clefts: from discovery to three-dimensional reconstructions. *Trends Parasitol* **23**: 502-509.
- Wickham, M.E., Rug, M., Ralph, S.A., Klonis, N., McFadden, G.I., Tilley, L., and Cowman, A.F. (2001) Trafficking and assembly of the cytoadherence complex in *Plasmodium falciparum*-infected human erythrocytes. *EMBO J* **20**: 5636-5649.
- Wickham, M.E., Culvenor, J.G., and Cowman, A.F. (2003) Selective inhibition of a two-step egress of malaria parasites from the host erythrocyte. *J. Biol. Chem.* **278**: 37658-37663.

References

- Wilson, R.J.M., Denny, P.W., Preiser, P.R., Rangachari, K., Roberts, K., Roy, A., Whyte, A., Strath, M., Moore, D.J., Moore, P.W., and Williamson, D.H. (1996) Complete gene map of the plastid-like DNA of the malaria parasite *Plasmodium falciparum*. *J Mol Biol* **261**: 155-172.
- Winzeler, E.A. (2008) Malaria research in the post-genomic era. *Nature* **455**: 751-756.
- Wu, Y., Sifri, C.D., Lei, H.H., Su, X.Z., and Wellems, T.E. (1995) Transfection of *Plasmodium falciparum* within human red blood cells. *Proc Natl Acad Sci USA* **92**: 973-977.
- Wu, Y., Kirkman, L.A., and Wellems, T.E. (1996) Transformation of *Plasmodium falciparum* malaria parasites by homologous integration of plasmids that confer resistance to pyrimethamine. *Proc Natl Acad Sci USA* **93**: 1130-1134.
- Yeoh, S., O'Donnell, R.A., Koussis, K., Dluzewski, A.R., Ansell, K.H., Osborne, S.A., Hackett, F., Withers-Martinez, C., Mitchell, G.H., Bannister, L.H., Bryans, J.S., Kettleborough, C.A., and Blackman, M.J. (2007) Subcellular discharge of a serine protease mediates release of invasive malaria parasites from host erythrocytes. *Cell* **131**: 1072-1083.
- Zhou, Y., Young, J.A., Santosyan, A., Chen, K., Yan, S.F., and Winzeler, E.A. (2005) In silico gene function prediction using ontology-based pattern identification. *Bioinformatics* **21**: 1237-1245.

Summary

Summary

Malaria is one of the most lethal infectious diseases worldwide. Understanding the biology of the causative agent *Plasmodium* will lead to better control of the disease. The biogenesis and maintenance of the parasitophorous vacuole (PV) within the infected erythrocyte is an essential factor for parasite survival. The PV has been postulated to be involved in various pivotal functions, however little is known about the PV contents and their respective functions. Our group had previously provided the first PV's proteome research and have continuously exposed more members of this important compartment. The protein PfPV1 was a newly discovered PV localisation protein, encoded by the PF11_0302 gene. In order to address the function of this protein a gene knock-out strategy was applied. A search for the interacting proteins of PfPV1 was also carried out using the GST pull-down assay.

The first attempt to knock out the encoding gene was the double-crossover strategy in the presence of a negative selection. The knocked-out parasite was unable to obtain. However, the integration into the *PfPV1* locus did occur, evidenced by the presence of both endogenous and knock-out band in the specific southern blot hybridisation. The *PfPV1* gene was therefore assumed to be essential for in vitro growth, thus the targeting into the endogenous locus was accompanied by a duplication event for maintaining expression of the gene.

The assumption was further validated by the second knock-out strategy, using the complementing experiment. The result had been expected to be able to disrupt the endogenous gene locus through the knock-out vector while concomitantly expressing a copy of *PfPV1* under the control of a foreign promoter from an episomal plasmid, which should not recombine with the endogenous gene locus. However, the gene was still resistant to be disrupted. Various clones were isolated from the double transfected parasites. One of the clones has lost the episomal copy of the *PfPV1* gene and showed the same southern blot result as the single transfected parasite, indicating that the parasite needs to maintain the expression of the endogenous gene. Other clones, if keeping the episomal copy of the *PfPV1*, did not show the specific integration. The result strongly suggests that the *PfPV1* expression needs to be controlled by its endogenous promoter to be fully active.

Summary

The data has also proved for the first time that in some cases of the negative selection strategy, upon the integration, the *Plasmodium* parasite might rearrange the thymidine kinase encoding sequence in order to inactivate its activity, therefore prevent the lethal effect from converting ganciclovir to toxic metabolite.

In the GST pull-down assay, no interacting protein was obtained. However, the experiment was carried out with the cell extract from trophozoite-stage parasites, thus might not detect interactions at other stages.

In conclusion, the data suggest that PfPV1 is a conserved, unique protein with unknown but essential function during the intraerythrocytic cycle.

Zusammenfassung

Die Malaria ist noch immer eine der verheerendsten Infektionskrankheiten weltweit. Das Verständnis der Biologie des ihr zugrunde liegenden Pathogens, *Plasmodium falciparum* ist notwendig, um erfolgreich gegen diese Krankheit vorzugehen. Dabei ist die Genese und Aufrechterhaltung der parasitophoren Vakuole (PV) innerhalb des Erythrozyten ein essentieller Faktor für das Überleben des Parasiten. Obwohl diese grundlegende Bedeutung für den Parasiten bekannt ist, bleibt die genaue Zusammensetzung und die Funktion vieler Bestandteile der PV weiter ungeklärt. Unsere Gruppe hat dabei das erste Proteom dieses Kompartiments veröffentlicht und in der Vergangenheit weitere Komponenten desselben identifiziert. Pfpv1 ist eines dieser neu entdeckten Proteine. Um Informationen bezüglich der Funktion dieses Proteins gewinnen zu können, wurde in der vorliegenden Arbeit eine Knock-out Strategie gewählt. Zudem wurde versucht, Interaktionspartner von Pfpv1 mit Hilfe von GST Pull-Down Assays zu identifizieren.

Beim ersten Versuch des Knock-outs wurde eine Double-Crossover Strategie mit negativer Selektion verfolgt, wobei sich der erhaltene Knock-out Parasit nicht weiter kultivieren ließ. Die Integration in den Pfpv1- Locus war jedoch erfolgreich und so wurde bei der spezifischen Southern-Blot Hybridisierung sowohl eine endogene als auch eine Knock- Out Bande detektiert. Die Schlussfolgerung aus diesen Ergebnissen ist, dass Pfpv1 für das Überleben des Parasiten in-vitro essentiell ist, und dass im Zuge der Integration in den endogenen Locus eine Duplikation stattgefunden haben muss, welche die weitere Expression des Gens sichergestellt hat.

Die obige Annahme wurde durch die Ergebnisse der zweiten Knock-Out Strategie weiter bestätigt. Hierbei wurde versucht, das endogene Gen mit Hilfe eines Knock-Out Vektors zu zerstören, während gleichzeitig Pfpv1 unter der Kontrolle eines fremden Promotors von einem episomalen Plasmid exprimiert wird, welches nicht fähig ist mit dem endogenen Locus zu rekombinieren. Jedoch ließ sich auch mit Hilfe dieses Ansatzes das Pfpv1-Gen nicht zerstören. Die Analyse verschiedener Klone der doppelt transfizierten Parasiten zeigte folgende Ergebnisse. Bei einem der Klone war festzustellen, dass die episomale Kopie von Pfpv1 verloren gegangen war. Dieser Klon zeigte zu dem dasselbe Muster im Southern- Blot wie die einzel transfizierten

Summary

Parasiten. Dies geht konform mit der oben genannten Annahme, dass der Parasit zum Überleben auf die Expression des endogenen Gens angewiesen ist. Weitere Klone zeigten bei der Analyse, sofern sie die episomale Kopie behalten hatten, keine erfolgreiche Integration. Diese Ergebnisse weisen darauf hin, dass die erfolgreiche Expression von PfPV1 die Kontrolle des endogenen Promoters benötigt.

Die während dieser Arbeit generierten Daten zeigen zum ersten Mal, dass die negative Selektionsstrategie bei Integration dazu führen kann, dass bei *Plasmodium falciparum* die Thymidin-Kinase kodierende Sequenz dahingehend modifiziert wird, dass sie ihre Aktivität einbüßt und Ganciclovir nicht mehr in seine toxische Form überführt.

Bezüglich des GST pull down Assays gelang es nicht interagierende Proteine zu identifizieren. Möglicherweise finden Interaktionen mit PfPV1 jedoch in Entwicklungsstadien des Parasiten statt, die in dieser Arbeit nicht berücksichtigt wurden.

Zusammengefasst lassen sich die Ergebnisse dieser Arbeit so interpretieren, dass PfPV1 ein einzigartiges, konserviertes Protein mit essentieller, aber noch unbekannter Funktion darstellt.

Acknowledgement

No work of this scope can be accomplished without the support and cooperation of many people.

First and foremost, I am deeply indebted to my Supervisor, Professor Dr. Klaus Lingelbach for having accepted me to join his group and for his guidance and suggestions through out my PhD study.

I will always be indebted to Dr. Jude Przyborski for being such an excellent mentor. His expertise, enthusiasm and his suggestions has helped me all times, introduced me to many opportunities in malaria researches. I thank him for his guidance, constant advice and support without which the whole study would not be possible.

I wish to express my sincere gratitude and appreciation to my thesis committee members, Prof. Dr. Uwe Maier, Prof. Dr. Renkawitz Pohl and Prof. Dr. Erhard Bremer whose comments and suggestions were vital in shaping this dissertation.

I would like to make a grateful acknowledgement to Dr. Julius Nyalwidhe and Dr. Omid Azimzadeh for their endless support through out my PhD study, both in scientific and social discussion.

I am deeply grateful to the *International Max Planck Research School for Environmental, Cellular and Molecular Microbiology* for granting me the fellowship and for giving me great opportunities to attend conference and workshop all over the world, without their supporting the going seemed impossible. I am grateful to Susanne Rommel, Dr. Juliane Dörr and Christian Bengelsdorff for taking care of all of the official documents for my daily life in Marburg.

I also thank you all former and present members of the Lingelbach's lab, for their support, encouragement, and most of all, the fun time! My sincere thanks go to Simone Spork and Simone Külzer for their critical reading this dissertation, Nina Gehde for her constant care since my first day in Marburg; Markus Winterberg, Sven Bietz and Irine Bietz for the fun we have in the lab. I thank you Vera Sampels and Caroline Odelwald for their assistances in experiments of recombinant protein expression.

I wish to thank all friends from IMPRS who help me truly enjoy the life of an international student. Thank you all my friends in the tiny Vietnam community in Marburg, particular thanks to the family of anh Tuan – chi Hoa who have accepted me as a family member.

This work is one of the ways I would like to express my deepest gratitude to my parents and my sister, for their love, encouragement and support through out my life.

Last but not least, Anh Tuan, thank you for always being there, understanding and supporting me, giving me the confidence to finish the work. Thank you, my dear husband.

Curriculum Vitae

Personal data **Trang Chu**
29.03.1978
Vietnam

Education

- 9/2005 – 10/2009 PhD
Faculty of Biology, Philipps University Marburg
Germany
Title of dissertation: “A genetic analysis to elucidate the function of the *Plasmodium falciparum* parasitophorous vacuole protein, PfPV1”
- 9/2002 – 9/2004 Master of Science,
School of Medicine, Sungkyunkwan University
South Korea
Title of thesis: “Crystal structure of guamerin, an elastase inhibitor, in complex with proteases and their application in setting up elastase specific inhibitor”
- 9/1996 – 9/2000 Bachelor of Science,
School of Biology, University of Sciences – HoChiMinh city
Vietnam
Title of thesis “Simultaneous detection of *Escherichia coli* ETEC, *Salmonella sp* and *Vibrio cholerae* in food sample by multiplex PCR”

Publications

1. Spork S, Hiss JA, Mandel K, Sommer M, Kooij TW, **Chu TT**, Schneider G, Maier UG, Przyborski JM. An unusual ERAD-like complex is targeted to the apicoplast of *Plasmodium falciparum*. *Euk. Cell*, **2009**, 8, 1134 – 1145.
2. Kim H*, **Chu TT***, Kim DY, Kim DR, Nguyen CM, Choi J, Lee JR, Hahn MJ, Kim KK. The crystal structure of Guamerin in complex with chymotrypsin and the development of an elastase-specific inhibitor. *J. Mol. Biol*, **2008**, 376, 184-192 (* authors contributed equally to this work).
3. Kim DR, Kim DY, **Chu TT**, Jung KH, Kim KK. Crystallization and preliminary X-ray crystallographic study of the leech protease inhibitor guamerin and its complex with bovine pancreatic chymotrypsin. *Biochim. et Biophys. Acta*, **2004**, 1699, 285 – 287.

Erklärung

ich versichere, dass ich meine Dissertation

“A genetic analysis to elucidate the function of the *Plasmodium falciparum* parasitophorous vacuole protein, PfPV1.”

selbständig, ohne unerlaubte Hilfe angefertigt und mich dabei keiner anderen als der von mir ausdrücklich bezeichneten Quellen und Hilfen bedient habe.

Die Dissertation wurde in der jetzigen oder einer ähnlichen Form noch bei keiner anderen Hochschule eingereicht und hat noch keinen sonstigen Prüfungszwecken gedient.

Ort/ Datum

Unterschrift (Vor- und Zuname)